

**STUDIES ON PHYSICO-CHEMICAL  
BEHAVIOUR OF WATER SOLUBLE  
SYNTHETIC POLYMERS**

THESIS SUBMITTED FOR THE DEGREE OF  
DOCTOR OF PHILOSOPHY (SCIENCE) OF THE  
UNIVERSITY OF NORTH BENGAL

2006

By

GOUTAM BIT, M.Sc.  
DEPARTMENT OF CHEMISTRY  
UNIVERSITY OF NORTH BENGAL  
SILIGURI, DARJEELING – 734013  
INDIA



547.8427

B624 S

189153

09 JAN 2007

SPRING-2011 |

## Acknowledgement

---

*I take this opportunity to express my heartfelt gratitude to my supervisor, Prof. S.K. Saha, Department of Chemistry, North Bengal University for his wise guidance and incessant encouragement throughout the entire period of work.*

*I thankfully acknowledge the award of study leave by the Department of Higher and Technical Education, Government of Mizoram for completion of this work and appreciate the authorities of North Bengal University for extending laboratory facilities.*

*The cooperation and help from the teachers, officers, research scholars and other staff of the Department of Chemistry, North Bengal University is thankfully acknowledged.*

*I am specially thankful to S. K. Das, A. Chakraborty, B. Debnath, S. Chakraborty and M. Jha of this laboratory for their good gesture and generous help.*

*I extend my sincere thanks and gratitude to V. Suakbuanga, Principal; Dr. P. K. Sarkar, Head, Dept. of Physics; C. Laldawngliana, Lecturer and Zirsangliana Paite, Lecturer, Government Champhai College for their kind cooperation.*

*I express my best regards to my parents and other elders of my family for their ceaseless blessings and inspiration.*

*Finally, I would like to thank my wife for her constant support under all circumstances.*

University of North Bengal

Date 08.03.06

  
Goutam Bit

# Contents

---

<b>Chapter 1 : Introduction</b>	1-15
1.1 Vermiculite	3-6
1.2 Clay catalyzed polymerization	6-9
1.3 Polymer solvent interaction	9-12
1.4 References	12-15
<b>Chapter 2: Scope and Object</b>	16-20
<b>Chapter 3: Experimental</b>	21-25.
3.1 Materials	21-22
3.2 Polymerization	22-23
3.3 Viscosity measurements	23-24
3.4 Potentiometric and conductometric measurements	24
3.5 Elemental Analysis	24
3.6 Measurements of surface tension	24-25
3.7 Sorption of TU and AM onto vermiculite	25
3.8 References	25
<b>Chapter 4: Studies on redox polymerization of acrylamide on aqueous vermiculite media</b>	26-61
4.A Studies on aqueous polymerization of acrylamide by Ce (IV)-TU redox couple on vermiculite surface	26-41
4.A.1 Introduction and review of previous works	26-32
4.A.2 Results and discussion	32-41
4.B Studies on copolymerization of acrylamide with N-tert butyl acrylamide by Fe (III)-TU redox couple on vermiculite surface	42-50
4.B.1 Introduction and review of previous works	42-45
4.B.2 Results and discussion	45-50

4.C	General discussion	51-54
4.D	References	54-61
<b>Chapter 5: Studies on solution properties of hydrolyzed and unhydrolyzed polyacrylamide in water-N, N dimethyl formamide mixtures</b>		62-94
5.A	Studies on solution properties of polyacrylamide in water-N, N dimethyl formamide mixtures	62-76
5.A.1	Introduction and review of previous works	62-69
5.A.2	Results and discussion	69-76
5.B	Studies on solution properties of hydrolyzed polyacrylamide in water-N, N dimethyl formamide mixtures	77-85
5.B.1	Introduction and review of previous works	77-78
5.B.2	Results and discussion	78-85
5.B.3	Application of Huggins equation below the overlap concentrations	85-88
5.C	References	88-94
<b>Chapter 6: Studies on dilute solution behaviour of progressively hydrolyzed polyacrylamide in aqueous solution.</b>		95-109
6.1	Introduction and review of previous works	95-98
6.2	Results and discussion	99-107
6.3	References	107-109
<b>Chapter 7: Studies on solution properties of polymer-nonionic surfactant mixed system</b>		110-126
7.1	Introduction and review of previous works	110-112
7.2	Results and discussion	113-124
7.3	References	125-126
<b>Chapter 8: Summary and conclusion</b>		127-135
<b>List of Publications</b>		136

**CHAPTER 1**  
**INTRODUCTION**

## INTRODUCTION

Water-soluble polymers are those, which can either dissolve or swell in water to form either solution or hydrogel. The key to water solubility of water-soluble polymers lies in positioning sufficient number of hydrophilic functional groups along the backbone or side chains of polymers.<sup>1</sup> Some of the major functional groups that possess sufficient polarity, charge or hydrogen bonding capability for hydration are  $-\text{COOH}$ ,  $-\text{COO}^- \text{M}^+$ ,  $-\text{CONH}_2$ ,  $-\text{SO}_3^- \text{M}^+$ ,  $-\text{SO}_3\text{H}$ ,  $-\text{NH}_2\text{OH}$ ,  $-\text{NH}_2$ ,  $-\text{SH}$ ,  $-\text{NHR}$ , and  $-\text{N}^+ \text{R}_3^- \text{X}^-$ , where M, R and X stand for metal, alkyl and halogen respectively.

These functional groups not only impart solubility but also bring many useful properties like chelating, dispersing, absorption, flocculation, thickening, drag reduction etc. to the polymers. Water-soluble polymers may be used as materials (e.g. super absorbent, soluble packaging, soft contact lens etc.), but most applications arise from their properties in solution, especially from their ability to modify the rheology of an aqueous medium and to adsorb from solution onto particles or surfaces. Moreover, some of these groups can further react to form other kinds of functional groups. The water-soluble polymers, therefore, find extensive applications in areas including water treatment, cosmetics, personal care product, pharmaceutical, oil recovery, pulp and paper production, mineral processing, agriculture etc.

Water-soluble polymers can be divided into three categories, viz., naturally occurring polymers (e.g. polypeptides, albumin, gelatin, agar, etc.), semi synthetic polymers (e.g. cellular ethers and starch derivatives) and synthetic water-soluble polymers. Among these, synthetic water-soluble polymers have experienced the most rapid development and represent a major business with estimated world market around \$6 billion per year. Its diversity and quantity far exceeds those of the natural and semi-synthetic water-soluble polymers and receives greater interest with the development of the petrochemical industry. Some important examples of synthetic water-soluble polymers are listed below:

*Nonionic:* polyacrylamide, polyvinyl alcohol, polyvinyl pyrrolidone,

*Anionic:* polyacrylic acid, polyphosphoric acid, polystyrenesulphonic acid,

*Cationic:* polyvinylamine, polydimethyldiallyl ammonium chloride, poly (4-vinyl-N-alkyl-pyridinium) salts.

Water-soluble polymers are commonly synthesized from water-soluble monomers, e.g.: acrylic acid (AA) and its sodium salt, acrylamide (AM), hydroxyethyl methacrylate (HEMA), hydroxyethyl acrylate (HEA), vinylpyrrolidone (VP) and quaternary ammonium salts like, dimethyldiallyl ammonium chloride (DMDAAC) etc. Various processes including aqueous solution polymerization, inverse suspension polymerization and inverse emulsion polymerization are generally applied for commercial synthesis. Solution polymerization is commonly used in the synthesis of linear, low molecular weight water-soluble polymers. In the solution polymerization process, the water-soluble monomers are polymerized in a homogenous aqueous solution in the presence of free-radical initiators mostly by redox couples. The polymerization is a very exothermic reaction ( $\Delta H=55-95$  kJ/mol) in the solution process. As the conversion of the monomer and molecular weight of the polymer increase, the viscosity of the system increases sharply; this makes heat removal very difficult. This could cause explosive polymerization and is detrimental to the production. Therefore, in such a process the monomer content in the solution must be controlled. Linear, high molecule weight, polyacrylamide-based polymers are often commercially synthesized through inverse emulsion (W/O, 0.05-1  $\mu\text{m}$ ) polymerization<sup>2-7</sup>, whereas the production of lightly crosslinked polyacrylic acid based super absorbent polymers are generally manufactured by inverse suspension (W/O, 0.05-2 mm) polymerization. In both cases the water and monomer mixture (i.e. water phase) is emulsified/suspended in an aliphatic or aromatic hydrocarbon phase (i.e. oil phase), where the size of the particles strongly depends on the chemical and physical properties of the emulsifiers or dispersing agents used. The existence of the oil phase overcomes some of the problems associated in solution process, since it lowers solution viscosities and can dissipate the heat of polymerization. Moreover, it is also an attractive method because the oil phase permits relatively higher monomer content. However, the biggest disadvantage in these processes is the separation and/or recycling of the oil phase after the polymerization, which drives up the cost and causes environmental pollution. A clean, low cost process with good productivity is highly desired in the industry. Usually, redox polymerization of acrylamide in aqueous medium yields polymer having not so high molecular weights primarily because of fast termination process via transfer of electron to the oxidant of the

redox couple (e.g. metal ions at higher oxidation state) from the growing polymer chain. However, it has been shown recently that if the polymerization is carried out in a constrained space of a reactor (e.g. interlayer space of a clay mineral) such that the growing polymer chain may not be able to transfer the electrons to the metal ions, high molecular weight polymers are formed.<sup>8</sup> The effect of microenvironment of a phyllosilicate in the polymerization process is not usually confined to delayed termination only; it also affects the mechanism of formation and sometimes the structure of the polymer. The role of charged groups on factors that govern the efficiency of polyacrylamide (PAM) in its use as discussed above especially its recent application as water soluble viscofier and displacement fluid in secondary oil recovery in the salt rich waters, a complete molecular characterization is required. In the case of charged PAM the relative dissociation of the ionic groups and the distribution and alignment of the charged dipoles along the chain are expected to play a decisive role on the final state of conformation of the polymer chain. The effect of hydrodynamic field on the viscosity of partially hydrolyzed PAM has been discussed in the literature. The effect of various salt ions on the characteristic of polyelectrolyte in the aqueous solution and the site-binding interaction of salt ions with the polymer is also important.

## **1.1 VERMICULITE**

Vermiculite occurs in nature in the form of macroscopic crystals. Vermiculites, the geological name given to a group of hydrated laminar minerals, aluminium iron magnesium silicates, are similar in appearance to mica. Biotite and phlogopite are common parent minerals of vermiculite and mixed-layer mica/vermiculite (hydrobiotite or hydrophlogopite). Due to its structural features, vermiculite clays play an important role in many natural processes and industrial applications. These include oil and gas production,<sup>9</sup> and the removal of organic contaminants from water etc.<sup>10-12</sup> Recently, these clays have also been used to produce new nanoporous materials.<sup>13</sup> Vermiculite crystals are constituted of stacking negatively charged sheets, which are held together by charge balancing interlayer counter ions.<sup>14</sup> The sizeable interlayer spacing of the clay plays an important role in the transport processes of natural and contaminant species in the soil. Modeling of clay minerals is therefore of significant interest for understanding the underlying physico-chemical processes in these phenomena, particularly clay swelling and the behavior of metallic ions and organic

compounds in the interlamellar space. This behavior may well depend on the dynamics of the clay structure that is generally probed by the methods of vibrational spectroscopy.

## CHEMICAL COMPOSITION & STRUCTURE

Vermiculite is a trioctahedral 2:1 layered silicate. Its empirical formula is:  $Mg_{1.8}Fe^{2+}_{0.9}Al_{4.3}SiO_{10}(OH)_2 \cdot 4(H_2O)$

The negatively charged layer of its structure is formed from a sheet of edge-connected  $XO_6$  octahedra, where X is an octahedral atom (Mg, Al, Fe), which are symmetrically bound to two sheets of corner-connected  $TO_4$  tetrahedra, where T is a tetrahedral atom (Si, Al), forming six-membered silicate rings.<sup>15</sup> The vermiculite structure, which is shown in Fig.1.1, contains three types of oxygen atoms. Oxygen atoms of the first type ( $O_I$ ) link two Si atoms and are located at the corners of the  $SiO_4$  tetrahedra. Oxygen atoms of the second type ( $O_{II}$ ) are tetra-coordinated oxygen bound to a silicon atom and three magnesium atoms. Oxygen atoms of the third type ( $O_{III}$ ) are tetra-coordinated oxygen coordinated to one hydrogen atom and three magnesium atoms. The external surfaces of the layer are built from oxygen of the first kind ( $O_I$ ). The structure of vermiculite has a monoclinic unit cell and the unit cell is characterized by the following values of the lattice parameters:  $a = 5.33 \text{ \AA}$ ,  $b = 9.18 \text{ \AA}$ ,  $c = 28.90 \text{ \AA}$ , and  $\beta = 97^\circ$  (ref. 15). The interlamellar spaces are large enough (Fig.1.1) to accommodate both inorganic and organic counter ions compensating the eventual charge of the layer. The amount of isomorphous substitution in vermiculite, however, is greater than in montmorillonite and much of this occurs in tetrahedral sheet but as Walker has pointed out, it seems probable that highly charged members of smectite group grade into the low-charged vermiculites. Only in the fully hydrated phase ( $d(001) = 1.48 \text{ nm}$ ) are all the available sites occupied by water molecules. As dehydration progresses, some of the unbound water are removed before the bound water. The interlayer expansion and collapse of vermiculite layers are influenced by the nature of the exchangeable cation as well as by that of the interlayer liquid.<sup>16</sup> In this respect and its ability to form complexes with organic compound vermiculite bear a striking resemblance to montmorillonite.<sup>17-19</sup> However, Mg-saturated vermiculite fails to expand beyond a basal spacing of  $\sim 1.45 \text{ nm}$  with glycerol whereas all Mg montmorillonite appear to give double layer complex with glycerol ( $d(001) \sim 1.78 \text{ nm}$ ). Weiss has reported that the basal spacing of vermiculite containing n-alkyl

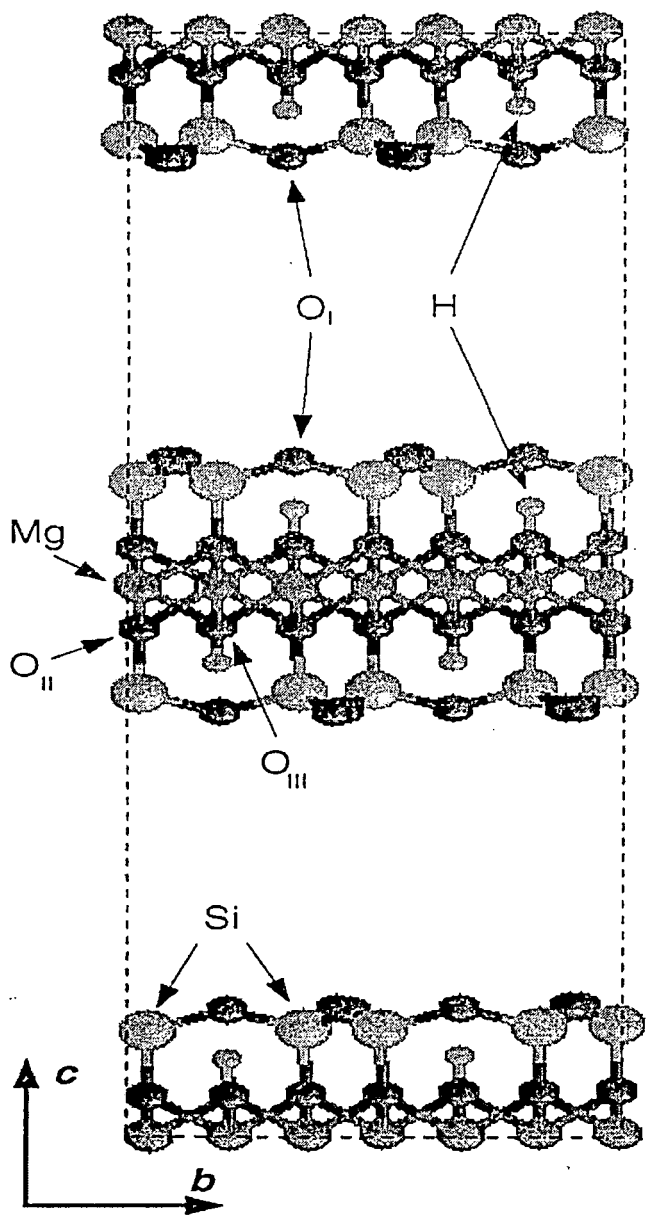


Figure 1.1. The layered structure of vermiculite.

ammonium ions of increasing chain length ( $C_5$  to  $C_{12}$ ) increases in a stepwise fashion.<sup>20</sup> This behavior was thought to arise from the fact that on passing from an odd to next even number of carbon atoms the interlayer distance increases by 0.20-0.21 nm, but that on passing from an even to next higher odd number of carbon atoms – there is virtually no increase in this distance. Walker and co-workers demonstrated the presence of two distinct types of interlayer water in vermiculite crystal.<sup>23,26</sup> The existence of both types of water in vermiculite has since been substantiated by IR spectroscopy. Howard and coworkers observed that montmorillonite intercalated two layers of ethylene glycol or glycerol from their respective vapor phase whereas vermiculite did not yield regular double layer complexes with either ethylene glycol or glycerol, irrespective of the saturated cation and the pre-exposure to water vapor.<sup>21</sup> Rather, a series of complexes formed with basal spacing of about 1.36, 1.40, 1.43, 1.50, and 1.53 nm; two or more complexes may be present in the sample. Brindley has drawn the attention to the fact that about 1/6 of the diagonal sites are associated with monovalent cations in montmorillonite and with divalent cation in vermiculite.<sup>22</sup> In a double layer complex of extended amine molecules, 5/6 of the total sites are therefore available on each oxygen surface. This means that the amount of organic molecules, which can accommodate in a complex of this type far exceeds that which is present in the corresponding one-layer complex. With vermiculite, interlayer swelling is usually less pronounced, probably because the silicate layers are more strongly held compared to montmorillonite. The amide molecules tend to link to the cation by means of water bridges. Some vermiculite samples, however, may expand to a basal spacing of 6.3 nm after prolonged immersion in liquid N-ethylacetamide. This behavior is reminiscent of that shown by n-butyl ammonium-vermiculite in water producing large interlayer separation. Extensive crystalline swelling of this type is attributed to the operation of osmotic repulsive forces giving rise to the formation of diffuse double layers when vermiculite crystals are immersed in strong amino acid solutions.<sup>23,24</sup> The effect of adsorbent charge and the kind of exchangeable cation present on the adsorption and retention of diquat and paraquat by 2:1 type layer silicates have been investigated by Weaver.<sup>25</sup> Maximum uptake by montmorillonite was close to the exchange capacity of the sample, being little influenced by nature of the saturating organic cations. On the other hand vermiculite adsorbed appreciably less than its exchange capacity and the extent of adsorption depended on the saturating organic cation decreasing in the

order  $\text{Na}^+ > \text{Ca}^{+2} > \text{Mg}^{+2}$ . Vermiculite can also intercalate various amino acids. The relative lack of experimental data on vermiculite-amino acid complexes is perhaps explained by the fact that the interlayer sorption of the organic species is usually less readily achieved with vermiculite than with montmorillonite because of greater charge and hence greater electrostatic attraction between the vermiculite layers. Extensive interlayer expansion can occur in vermiculite complexes with amino acid cations.<sup>26</sup> Thus single crystal of vermiculite of which the inorganic cations initially present have been replaced by ornithine, lysine, and  $\gamma$ -amino butyric acid cations, swell in the respective amino acid solutions, when its concentration is below a critical value. Following Norrish, this type of swelling is initiated by the hydration of the interlayer amino acid cation, which dissociate from the clay surface.<sup>27</sup> This is followed by the development of diffuse double layer on interlayer surfaces so that subsequent interlayer expansion is controlled by osmotic repulsive interactions.

## 1.2 CLAY CATALYZED POLYMERIZATION

Clay is the key inorganic substance with applications ranging from pollution prevention and remediation to enhanced oil recovery, the treatment of petroleum liquids to the manufacture of cosmetics and pharmaceuticals to the synthesis of polymer nanocomposite materials. An understanding of clay-organic interactions and the effects of these interactions on the structure of clay complexes is a key issue for future development in all of these applications. Synthetic and naturally occurring clay minerals due to their favorable structures, are used in a number of widely diversified roles in the chemical industry as catalyst for cracking or depolymerization,<sup>28</sup> alkylation,<sup>29</sup> isomerization<sup>30</sup> polymerization<sup>31</sup> etc. In 1960's and earlier clay initiated polymerizations of vinyl monomers emphasized on the use of dry clay minerals and non-polar solvents.<sup>16,32,33</sup> Although the carbocationic polymerizations of vinyl monomers have been investigated extensively with Lewis acid such as  $\text{AlCl}_3$ ,  $\text{TiCl}_4$ ,  $\text{Et}_2\text{O}$ ,  $\text{BCl}_3$ , alkyl aluminiums etc.<sup>34-40</sup> the first report on such polymerization of styrene with acid clays<sup>32</sup> came in 1964. Almost 100% yield of polystyrene of molecular weights 500-2000 was achieved. The catalytic activity of the clay has been shown to be due to active protons associated with tetrahedral (due to dehydration of mineral) aluminium.<sup>41,42</sup> The formation of carbonium ion following surface adsorption of olefins on acid sites caused subsequent polymerization. Proton accepting contaminants such as water, amines etc., being preferentially adsorbed

over styrene suppressed the polymerization. Styrene polymerized on the surface of homoionic clays.<sup>43</sup> It is argued that an electron transfer from adsorbed styrene to the aluminium produces radical cations, which dimerize rapidly. Both radical cation and dimers are involved in the initiation step but the propagation being cationic. Using activated clay minerals, however, styrene did not polymerize in the presence of ethanol, dioxane, ethyl acetate and methyl methacrylate (MMA) within 30 minutes of the reaction. All these data lead to postulate that the active sites are the octahedral aluminium at the crystal edges. The aluminium acts as electron acceptors. Matsumoto, Sakai and Arihara preferred the concept of Brønsted acidity rather than Lewis acidity to be responsible for the initiation of the polymerization of styrene by montmorillonite, a smectite clay mineral.<sup>44</sup> The inconsistency of their experiments, however, is in the reduction of polymer yield in the presence of trityl chloride, which selectively adsorbs on Lewis acid sites. They argued in favor of the Brønsted acidity on the ground that the replacement of exchangeable hydrogen ions by sodium or ammonium ions almost completely inhibited the polymerization. On reacidifying the mineral, however, the activity to polymerize styrene was restored. Since the degree of polymerization increased with the dielectric constant of the medium and was almost independent of the initial concentration, cationic mechanism for the initiation process was favored.<sup>45</sup> This would apply equally well to the propagating process and therefore, the initiation by a radical ion mechanism cannot be ruled out.<sup>43</sup> The possibility of proton transfer to monomer leading to decreased average degree of polymerization, as in conventional cationic mechanism, has also been discussed.<sup>41</sup> The work of Matsumoto and co-workers along with Solomon and Rosser lead one to the conclusion that acidity of the clay cannot be solely ascribed to either Brønsted acidity or Lewis acidity.<sup>43,44</sup> It is understood that dry mineral surface is very acidic due to the polarization of residual water molecules by the exchangeable cations. Such acidity is influenced by the solvent as evident from the blue colorations of aqueous benzidine in the presence of oxidized montmorillonite<sup>43,46</sup>. Solomon and Rosser failed to find evidence of styrene interacting with the clay mineral which lead them to assume that styrene is either incapable of moving into the interlayer space or capable of doing so with difficulty. Blumstein and co-worker have studied the polymerization of MMA and methyl acrylate in montmorillonite interlayer induced by  $\gamma$ -radiation.<sup>47-50</sup> The interlayer polymer was difficult to isolate by the usual solvent extraction and could only be isolated by treating the clay polymer complex with

hydrofluoric acid, which damaged most polymers.<sup>51</sup> Glavati and co-workers found that the polymerization of acrylonitrile/montmorillonite complex by  $\gamma$ -radiation produced stereospecific polymers.<sup>51</sup>

Thermal polymerization of a number of vinyl monomers could be induced by montmorillonite/2-2 azobis-isobutyramidine (AIBA) system if AIBA was previously introduced to the clay mineral.<sup>52</sup> The cationic form of AIBA goes to the exchange sites in montmorillonite to form AIBA-clay complex, which decomposes thermally to generate free radicals. The complex has initiating efficiency. The rate of polymerization with AIBA-montmorillonite complex initiator is greater than for AIBA alone.<sup>53</sup> It has been proposed that free radicals remain attached to the adjacent planes of AIBA-montmorillonite dispersed in water and on heating these planes move away from each other allowing more water to penetrate. The influence of aluminosilicates and magnesium silicates on the free radical polymerization of MMA has been studied in terms of termination reaction and supported by studies of the reaction of stable free radicals with the minerals. In the absence of clay mineral the yield of polymethylmethacrylate (PMMA) was 3.68% (mol. wt.  $1.36 \times 10^6$ ) whereas with montmorillonite the yield was 0.68% (mol. wt.  $3.05 \times 10^6$ ). That the decreased amount of polymer in presence of mineral is not due to depolymerization has been established by heating PMMA with montmorillonite and determining the viscosity average molecular weight,  $M_v$ , before and after treatment. In a recent ESR study to assess the state of iron in montmorillonite, signals in the weak field at 'g' values of 7.6, 4.2 and 3.9 were assigned to Fe (III) ions in the octahedral layer of the mineral. The intensities of the wide bands of the spectra remain unchanged when the cations were altered as the exchanging sites. This indicated that the montmorillonite had particularly no iron in the ion exchangeable positions. Studies on structural properties of the polymers from clay catalyzed polymerizations of vinyl monomers have been made by several workers. Blumstein and co-workers studied the dilute solution properties of the polymers prepared in the presence of clay minerals which differed significantly from those obtained using conventional free radical technique and suggested that the interlayer PMMA developed a two-dimensional sheet structure in the presence of a cross linking agent during the polymerization.<sup>47-50</sup> Analyzing the NMR data they concluded that PMMA probably consisted predominantly of isotactic sequences. Small-scale stereo-regularity of this kind could be ascribed to the orientation induced in the intercalated monomer by ion dipole and the ester carbonyl

group of the monomer. Earlier, Glavati and co-workers obtained oriented stereo regular polyacrylonitrile and polyacrylic acid using similar procedures.<sup>51</sup> It has been reported that the influence of clay minerals on polymerization reactions extends beyond direct action on monomers.<sup>53-54</sup> The minerals may also modify the chemical compounds used as polymerization initiators. It has been observed that clay minerals could affect both the rate and the rate of decomposition of initiators. Uskov and co-workers reported that polyvinylchloride (PVC) or a vinyl chloride copolymer modified by latex of butylacrylate-methylmethacrylate copolymer, butadiene-styrene copolymer, PMMA or a similar polymer was prepared by adding the latex to the reactor during the suspension polymerization.<sup>55</sup> The addition was made after 30-95% conversion of monomers. If inorganic compounds such as silica, montmorillonite or a calcium phosphate were added before or during the polymerization, the polymer with satisfactory particle size separated out from the aqueous suspension. Recently, Talapatra, Saha and co-workers reported that bentonite in conjunction with alcohols or thiols effectively initiate aqueous polymerization of vinyl monomers on the surface of the minerals.<sup>56-60</sup> A granular soil amendment was formulated from acrylamide polymers, silicic acid or silicate and once or more of phosphates, nitrates and sulfates or free form of urea, guanidine, dicyandiamide and amidinothiourea.<sup>61</sup> The product markedly improved aggregation of clay containing soils. T. Ono and co-workers, however, polymerized MMA in H<sub>2</sub>O containing phyllosilicates in presence water and azo initiators.<sup>62</sup>

### **1.3 POLYMER-SOLVENT INTERACTION**

In view of the wide range of use of water-soluble synthetic polymers, the understanding of the role of polar groups on different factors, which govern the efficiency of their use, is important. Attempts at describing solvent, temperature and molecular weight dependence on the conformational characteristics of the polymer have stimulated the development of many fundamental models for polymer structure and dynamics. One of the outstanding problems involves providing a description of the degree to which solvent penetrates through the polymer coils as the chain dimension swell with increased excluded volume interactions. The theory of polymer solution dynamics is associated with establishing the relation between the macroscopic hydrodynamic properties of polymer solution and molecular structure of the polymer and the solvent. The increase in molecular dimension from monomer to

oligomer, oligomer to usual length polymer and from the later to the pleistomer is accompanied by the appearance of new properties.<sup>63</sup> Many present and possible industrial applications of high molecular weight polymers arise from the unusual properties they induce to their solutions. The study of their solution properties is prerequisite for the development of this modern domain.

In the treatment of properties of very dilute polymer solutions it is convenient to represent the molecule as a statistical distribution of the chain elements or segments about the center of gravity.<sup>64</sup> For a random chain devoid of intramolecular interactions between segments mean square distance between the ends of polymer chain is proportional to the number of segments in the chain and hence to the molecular weight. This is true regardless of steric restrictions due to interaction between neighboring segments and other restrictions on rotations about bonds of the chain, provided that the chain possesses a degree of flexibility and that it is sufficiently long. Interactions between remotely connected segments separated by many intervening segments along the chain may be considered to alter the linear dimension of the polymer chain. Interactions between remotely connected segments of the given chain arise as consequences of the finite volume of each segments from which all other segments are excluded, and of the net energy of interactions between segments which happen to be in contact. In thermodynamic terms, this implies that the entropy change is important when a macromolecule dissolves. There may also be significant enthalpy change on account of the interaction of the solvent with large number of component monomer units in the polymer. There are both entropic (excluded volume) and enthalpic (attraction and repulsion) contribution to the non-ideality of the polymer solution and for most polymer-solvent system there is a unique temperature where their effects cancel. This temperature is called theta temperature and at this temperature the osmotic virial coefficient is zero. The cancellation of the effects at this temperature means the solutions then behaves ideally even though the concentration is not low and it's thermodynamic and structural properties are easier to describe.<sup>65,66</sup> Systematic studies arising from the coupling of different experimental techniques are required for elucidation of diverse theoretical experimental aspects. The most important parameters characterizing macromolecular chain in dilute solution are the molecular weight, mean square radius of gyration and intrinsic viscosity. Their determination for high molecular weight polymers, on the basis of different theoretical approximations, opens a large area for discussing various

aspects such as influence of molecular weight and solvent power on concentration domain, theta condition and the chain flexibility in the perturbed and unperturbed states. A long chain hydrocarbon molecule in a solution takes on somewhat kinked or curled shape, intermediate between tightly rolled up mass and the rigid linear configuration. Presumably all possible degrees of curling are represented owing to internal Brownian movement of the flexible chains but the configuration of intermediate extension predominate statistically. If a continuous energetically indifferent solvent surrounds the long chain molecule, the weight factor for particular configuration is determined only by internal parameters - potential energy for restricted rotation and prohibition of segment interpenetration. The mean value of any internal property in such an indifferent solvent might be called unbiased statistical mean for the property. If the solvent is energetically unfavorable, so that dissolving of the high polymer is an endothermic process, the polymer segments will attract each other in solution and squeeze out the solvent between them. Other conditions being equal, a given high polymeric material made up of flexible molecules will exhibit a high intrinsic viscosity in an energetically favorable solvent and low intrinsic viscosity in an energetically unfavorable solvent. This is of course hold only in very dilute system. At higher concentrations energetically unfavorable solvent will favour polymer-polymer contact and hence lead to danger of gelation while an energetically favorable solvent will stand at higher concentration of the polymer and yet give a stable solution. If a good solvent is mixed with a precipitating agent, the resulting mixture may be expected to be less favorable to long chain molecule than in a pure solvent. There should also be close connection between intrinsic viscosity and intramolecular agglomeration. Exactly the same solvent characteristic, which determines the mean geometrical property of isolated long chain molecule, should determine the amount of association of different solute molecules into aggregate. When a nonsolvent is added to a high polymer solution the point at which precipitate begins represent a certain agglomeration tendency for chain segment of different molecules. To a first approximation, therefore, it should represent a certain definite mean value for any shape dependent internal property. The solvent composition, which is critical from the standpoint of solubility, should correspond to certain intrinsic viscosity no matter what the solvent and what the nonsolvent be.<sup>67</sup> All these should be more pronounced for the polymer molecules of high flexibility than for the rigid chains. In a poor solvent the effective molecular shape is more compact and curled

than the unbiased statistical mean. An increase in temperature should increase the relative importance of entropic factor over the energetic factor. In such a solvent increase in temperature should result in an increase in intrinsic viscosity. In a very good solvent, energetic weighting factor favors the most extended configuration of the polymer.

#### 1.4 REFERENCES

1. C.L. McCormick, "Water-Soluble Polymers" ACS Symposium Series, **467**,2(1991).
2. J.W. Vanderhoff and R.M. Wiley, US Pat. **3284**,393, 3(1966).
3. D.L. Visioli, M.S. El-Aasser and J.W. Vanderhoff, *Polym. Mater. Sci. Eng.*, **51**, 258 (1984).
4. C. Graillat, C. Pichot, A. Guyot and M.S. ElAasser, *J. Polym. Sci., Part A: Polym. Chem.*, **24**(3), 427(1986).
5. V. Glukhikh, C. Graillat and C. Pichot, *J. Polym. Sci., Part A : Polym. Chem.*, **25**(4), 1127 (1987).
6. F.A. Adamsky and E.J. Beckman, *Macromolecules*, **27**(1), 312(1994).
7. V. Juranicova, S. Kawamoto, K. Fujimoto, H. Kawaguchi and J. Barton, *J. Angew. Makromol. Chem.*, **258**, 27(1998).
8. P. Bera and S.K. Saha, *Macromol. Rapid Commun.* **18**, 261(1997).
9. S. Karaborni, B. Smit, W. Heidug, J. Urai and E. Oort, *Science*, **271**, 1102 (1996).
10. S.A. Boyd, J. F. Lee and M. Mortland, *Nature (London)*, **333**, 345(1988).
11. G.D. Williams, N.T. Skipper, M.V. Smalley, A.K. Soper and S.M. King, *Faraday Discuss. Chem. Soc.*, **104**, 295(1996).
12. L.S. Kajita, *Clays Clay Miner.*, **45**, 609(1997).
13. R. Dhamodharan, J.D. Jeyaprakash, S. Samuel and M.K. Rajeswari, *J. Appl. Polym. Sci.*, **82**, 555(2001).

14. A.C.D. Newman, in *Chemistry of Clay and Clay Minerals*, Mineralogical Society, London, 1987.
15. A. Mathieson and G. F. Walker, *Am. Mineral*, **39**,231(1954).
16. J.A. Bittles, A.K. Chaughuri and S.W. Benson, *J. Polym. Sci.*,A-2,1221(1964).
17. W.D. Johns, W.D and R.T. Tetenhorst, *Am.Mineralogist*.**44**, 894(1959)
18. G.W. Brindley, K. Wiewiora and A. Wiewiora, *Am. Mineralogist*, **54**,1635(1969).
19. A. Amil, and D.M.C. Macewan, *Kolloid Z.*, **155**, 134(1957).
20. A. Weiss, *Angew. Chem. Int. Edit. Engl.*, **2**,134(1963).
21. M. Harward, D.D. Carstea, and A.H. Sayegh. *Clays Clay Minerals*, **16**, 437 (1969).
22. G.W. Brindley, *Clay Minerals*, **6**,91 (1965).
23. G.F. Walker and W.G. Garrett, *Nature*, **191**,1389(1961).
24. I. Barshad, *Soil Sci. Soc. Am.Proc.***16**: 176(1952).
25. C.E. Weaver, *Am. Mineralogist*, **43**,839(1958).
26. G.F. Walker and W.G. Garrett, *Nature*,**191**,1389(1961).
27. K. Norrish, *Disc. Faraday Soc*, **18**,120(1954)
28. C. Kemball and J.J. Rooney, *Proc. Roy. Soc., Japan*, **52**, 43(1949).
29. S. Mohil , Oil Co., INC., Brit.Pat.896, 864(1962).
30. Y. Suehiro, M. Kuwabara and V. Ayukawa, *J. Chem. Soc., Japan*, **52**, 43 (1949).
31. F.E. Shephard, J.J. Rooney and C. Kemball, *J.Catalysis*, **1**,379(1962).
32. H.Z. Friendlander, *J. Polym. Sci.*, **C-4**, 1291(1964).
33. D.H. Solomon, J.D. Swift and A.J. Murphy, *J. Macromol. Sci.*, **A5 (3)**, 587 (1971).
34. P.H. Flesch, *Cationic Polymerization and Related Complexes*, Academic Press, New York (1953).
35. D.C. Pepper, *Trans Faraday Soc.*, **45**, 3979(1949).

36. D.C. Pepper, *Trans Faraday Soc.*, **45**, 404(1949).
37. D.C. Pepper and M.J. Hayes, *Proc. Chem.Soc.*,228(1958).
38. A.G. Evans and G.W. Meadows, *Trans. Faraday Soc.* **46**, 327(1950).
39. G.F. Endres and C.G. Overberger, *J. Am. Chem. Soc.* **77**, 2201(1955).
  
40. J.P. Kenedy, *Cationic Polymerization of Olifins. : A Critical Inventory*, Wiley-Interscience, (1975).
41. J.A. Britles, A.K. Choudhuri and S.W. Benson, *J.Polym.Sci.*, **A-2**,1847(1964).
42. J.A. Britles, A.K. Choudhuri and S.W. Benson, *J.Polym.Sci*, **A-2**, 3203(1964).
43. D.H. Solomon and M.J. Rosser, *J. Polym. Sci.* **9**, 1261(1965).
44. T. Matsumoto, I. Sakai and M. Arihara, *Chem. High Polymers (Japan)*, **26**, 378 (1969).
45. M.M. Mortland, *Trans. 9th Intern. Cong Soil Sci. Adelaide*, **1**,691(1968).
46. W. Bodenheimer, L. Heller and S. Yariv, *Internat. Clay Conf., Jerusalem*, **1**, 251 (1966).
47. A. Blumstein, *J. Polym Sci.*, **A-3**, 2653(1965).
48. A. Blumstein and F.W. Bilmeyer, *J. Polym. Sci.***A-4**, 465(1966).
49. A. Blumstein and R.Blumstein, *Polymer Letters*, **5**, 69(1967).
50. A. Blumstein, S.L. Malhotra and A.C. Waterson, *A.C.S., Polymer Reprints*, **167** April (1968).
51. O.L. Glavati, L.S. Polak and V.I. Shchexin, *Neftekhimiya*,**3**, 905(1963).
52. H.G.G. Dekking, *J.Appl.Polym.Sci.*, **9**,1641(1965).
53. H.G.G. Dekking, *J.Appl.Polym.Sci.*, **11**,23(1967).
54. D.H. Solomon and B.C. Loft, *J.Appl.Polym.Sci.*, **12**, 1253 (1968).
55. I.A.Uskov, Yu.G.tarasenco, V.P.Solomko, *Vysokomolekhul. Soedin*, **6** 1768 (1964).
56. S. Talapatra, S.K. Saha, S.K. Chakroborti and S.C. Guhaniyogi, *Polym. Bull.*,

- 10, 21 (1983).
57. S. Talapatra, S.C. Guhaniyogi, and S.K. Chakraborti, *J. Macromol. Sci. Chem.*, **A22 (11)**, 1611 (1985).
  58. J. Bhattacharya, S.K. Chakraborti, S. Talapatra, S.K. Saha and S.C. Guhaniyogi, *J. Polym. Sci., Part-A : Polymer Chemistry*, **27**, 3977 (1989).
  59. J. Bhattacharya, S.K. Saha and S.C. Guhaniyogi, *J. Polym. Sci, Part-A : Polymer Chemistry*, **28**, 2249 (1990).
  60. S.K. Saha and D.J. Greenslade, *Bulletin of Chemical Society of Japan*, **65**, 2720 (1992).
  61. Jpn. Patent, 58, 28, 313, June 15, 1983, Nilto Chemical Industry Co. Ltd.
  62. T. Ono, T. Takahashi, M. Konno and T. Mikawa, *Ken Kyu Kiyomiyagi, Kagyo Koto Senmon Gakko*, **18,57**(1982).
  63. C.I. Simionescu, B.C. Simionescu and S. Ioan. *J. Macromol. Sci. Chem.*, **A22**, 765 (1985).
  64. P. Debye and I.M. Krieger (unpublished) have shown that the average distribution of each segment about the centre of gravity is exactly Gaussian for random chain unperturbed by intramolecular interactions.
  65. P.J. Flory and T.G. Fox, *J Am Chem Soc*, **73** : 1904 and 1915 (1951).
  66. H. Kurata, W.H. Stockmayer and A. Roig, *J Chem Phys*, **33(1)**, 151(1960).
  67. P.J. Flory, *Principles of Polymer Chemistry*, Cornell University Press, Ithaca, N.W., Chap. XIV, (1953).

**CHAPTER 2**  
**SCOPE AND OBJECT**

## **SCOPE AND OBJECT OF THE PRESENT WORK**

In recent years, scientists and engineers working on environmental and industrial problems have renewed their interest in water-soluble synthetic polymers because of their very broad range of applications. Important classes of these materials are the acrylamide-based polymers, which are widely used as flocculants, adhesives, rheology control agents, paper manufacturing, mining, and oil well stimulation etc. During the past decades, many patents have described the synthesis of homo and copolymers of acrylamide with special properties considering its versatile application in numerous fields in industries and also as water-soluble viscofier and displacement fluids in enhanced oil recovery. Anionic polyelectrolyte such as poly acrylamide-co-sodium acrylate (partially hydrolyzed polyacrylamide) is also used in a variety of water-soluble applications viz., in flocculation and as mobility control agent in enhanced oil recovery. But the critical limitation of polyelectrolytes including those derived from hydrolyzed homo-polyacrylamide is the loss of viscosity in presence of mono and /or multivalent electrolytes. Very high molecular weight polyacrylamide has been found to be exceptionally effective flocculants. Redox initiated polymerization of acrylamide is one of the most common technique applied for aqueous polymerization because of the simplicity of the technique as well as high yield and reaction rates. However, one difficulty of such a technique is the fast termination by oxidant of the redox couple. Recently a novel technique has been applied to control the linear termination process and to increase the chain growth of acrylamide polymer where the potential electron acceptor (e.g. metal ions) was loaded in the interlayer space of a smectite clay viz, montmorillonite prior to polymerization reaction starts. This ensures the slow termination rate due to inability of a growing polymer chain to transfer to the oxidant trapped inside the layered space. As a result, high molecular weight polymer was formed. The efficiency of the technique lies in the fact that the monomer and the components of redox systems (including the organic activator) could intercalate between the layers of the phyllosilicates, but the growing polymer chain after achieving a certain critical length comes out of the layered space and continue to grow in the bulk solutions. The growing chain is unable to transfer electron to the acceptor (viz, metal ions) embedded in the constrained space. Vermiculite is another important smectite of the

phyllosilicate group, which may also be efficient in this respect since the basal spacing of vermiculite is even less than that of montmorillonite. Further, industrially clay minerals are used as fillers and reinforcers in polymer systems such as elastomers, polyethylene, polyvinyl chloride and other thermoplastics. All things being equal the efficiency of a filler in improving the physico-chemical properties of a polymer system is primarily determined by the degree of its dispersion in the polymer matrix. The most effective way of achieving such compatibility is to graft a suitable polymer on to the filler surface and/or to encapsulate the mineral particles with polymer layer. Indeed, clay minerals, specially those of phyllosilicates (e.g. vermiculite) themselves, are known to catalyze a variety of organic reactions including those lead to polymer formation. Moreover, research on intercalation chemistry of phyllosilicates is gaining momentum rapidly to transform these abundant materials into new classes of selective heterogeneous catalysts. Interestingly, when metallic cations are adsorbed in vermiculite, they are also trapped between interlayer spaces at the negatively charged sites of the minerals like montmorillonite (Detail discussion is in Chapter 1).

Therefore, one of the objectives of the present investigation is to perform the polymerization reaction of acrylamide monomer onto the vermiculite surface by a redox initiators viz., Ce (IV)/Thiourea system involving the trapped metal ions with a view to enhance the chain growth of the polymer. Moreover, copolymers of acrylamide have also shown a number of properties leading themselves to a variety of industrial applications and the growing importance are related to their use as water-soluble viscofier and displacement fluid in enhanced oil recovery. With a view to prepare copolymers with large hydrodynamic volume and molecular weight attempts have been made to prepare poly (acrylamide-co-N-tert-butyl acrylamide) on the vermiculite surface. In an attempt to examine the scope of the technique, another redox couple viz., Fe (III)/ TU system will also be tested. However, one important objective of the above study is also to prepare polymers of desired molecular weight by selective application of the technique in order to carry on further studies on solution properties of polymers as mentioned below.

According to hydrodynamics, the specific viscosity of a Newtonian liquid containing a small amount of dissolved material should depend in the first approximation only upon the volume concentration and the shapes of the suspended particles. The unperturbed dimension (UD) of a given polymer in a solvent does not



depend on the nature of the solvent, as long as the solvent has no influence on the rotation of the chain segments. This is true in many cases, especially for nonpolar polymer-solvent pairs, but in the cases of polar polymer - polar solvents systems, the unperturbed dimension vary considerably with the nature of the solvent. Most of the polymeric materials are soluble only in a limited number of primary solvents, but they could be made soluble in all proportions in mixtures consisting of two or more solvents, which may be individually poor solvent for the polymers. Several mixtures of nonsolvents are also known which produce good solvent systems or at least increase the solvency power of primary solvents. Many present and possible industrial applications of high molecular weight polymer arise from unusual properties they induce to their solutions. The study of their solution property is a prerequisite for the development of this modern domain. The characterization of very high molecular weight polymers raises a number of problems. Therefore, systematic studies arising from the coupling of different experimental techniques are required for the elucidation of diverse theoretical and experimental aspects. The most important parameters characterizing macromolecular chains in dilute solution are the molecular weight, the mean square radius of gyration and the intrinsic viscosity. Their determination for very high molecular weight polymers opens a large area for discussing, on the basis of different theoretical approximations. The area of discussion includes such subjects as influence of molecular weight and solvent power on concentration domain, theta condition and unperturbed dimensions, chain flexibility in perturbed and unperturbed state, the type of interaction (short range and long range), the conformational characteristics including the transition phenomena influenced by temperature and solvent.

Polyelectrolyte finds a widening field of applications based on their specific properties. In recent years the study of polyelectrolytes has been stimulated by the use of newly available experimental techniques and the introduction of new theoretical concepts. Solutions of polyelectrolyte exhibit a behavior that may differ considerably from that of either uncharged macromolecules or low-molar-mass electrolytes. The origin of this specificity lies in the combination of properties derived from those of long-chain molecules with properties that results from charge-charge interactions. Physical properties of polyelectrolyte solutions have been studied for long time, but several of them have not yet found a satisfactory theoretical explanation. In many cases a qualitative understanding is available but a quantitative

interpretation is still lacking. Such a study is of interest from both industrial as well as academic points of view. Recently the interest is mainly focused on the relationship between the structure/charge density and the state of conformation. Although the solution behaviour of the polyelectrolyte homopolymers has been well studied the structure property relationship in charged co and ter polymers is yet to be fully investigated. The development of the dual charge on the same chain is expected to produce interesting effects on the final state of its conformation. Polyelectrolyte solution has been much more extensively studied in aqueous solution than in nonaqueous solution and in aqueous-organic mixtures.

In view of the above a detail study of solution properties of nonionic (unhydrolyzed) and anionic (hydrolyzed) polyacrylamide in water and water-organic (N, N dimethyl formamide) mixtures has been carried out. It is well established that the introduction of ionic groups in a polymer results in its expansion in aqueous solution. The use of aqueous polymer solutions in secondary oil recovery has been the subject of great interest as has already been mentioned. It is reported that (G. Muller, J.P. Laine, J.C. Fenyo, J. Pol. Sc., Polymer Chem. Ed.,17,1979,659) more oil is recoverable by the addition of only small quantity of polymers to injection water. The choice of polymer to be added to injection water must take into consideration a number of parameters, viz., the pH of the reservoir and the nature and concentration of salts. The effectiveness of the polymers is related to their molecular weight, the absence of branched chains and solubility in water. The enhanced recovery seems to be a consequence of molecular expansion that results from electrostatic repulsion between the charges carried by the polymer chains. To understand the role of charged groups on factors that govern the efficiency of PAM in the above use especially in the salt rich waters, complete molecular characterization is required. In the case of charged PAM the relative dissociation of the ionic groups and the distribution and alignment of the charged dipoles along the chain are expected to play a decisive role on the final state of conformation of the polymer chain. In addition, the synergism in properties of surfactants and polymers in aqueous solutions has been the focus of intensive fundamental applied research. Attention to this area of research is driven by numerous industrial applications of water borne fluids incorporating mixtures of both polymers and surfactants. These include detergents, cosmetics, paints and coating, photographic films, food and pharmaceutical products. The surfactant provides emulsion property and the

polymers impart colloidal and special rheological features. When surfactants are employed in practice they are almost without exception mixed with various substances either unintentionally or for improving their performances. This is also true for polymers in solution. When a surfactant and a polymer are mixed together in aqueous solutions, often significant changes in properties of the individual species appear. These may arise because both the polymer and the surfactant belong to the group of substances whose solution property shows marked deviation from regularities. Thus polymer surfactant interactions are not only a diverse industrial interest but also stimulate academic investigations. The practical importance of polymer-surfactant systems has led to a significant experimental effort to study their behaviour.

Keeping the above in view the behaviour and properties of hydrolyzed PAM as a function of the factors which are known to effect the expansion of polyelectrolyte molecules i.e., the degree of ionization, polymer concentration and the concentration of added salt have been investigated. PAM is of interest because it is possible to obtain high molecular weight samples that are easily soluble in water. Moreover, the controlled hydrolysis of PAM samples yield polymers of various charge densities. Because its effectiveness is related to the state of extension of dissolved chains, hydrolysis is a powerful means of increasing viscosities and because the electrostatic repulsion that govern the extension are sensitive to the added salt, hydrolysis is an important chemical variable. The object of the work, therefore, is two fold (1) to study ionomeric and polyelectrolytic characteristics of weakly and strongly hydrolyzed PAM in aqueous solution in terms of their solution properties and (2) effect of the charges on polymer chain vis-à-vis screening by added electrolyte and to show how the polyelectrolyte behaves like a neutral polymer in presence of sufficient amount of salt.

**CHAPTER 3**  
**EXPERIMENTAL**

## EXPERIMENTAL

### 3.1 MATERIALS

Acrylamide (AM, reagent grade, Fluka) was purified by recrystallisation from methanol (two times) and dried in vacuum oven at 45° C for two days. Thiourea (TU, E.Merck) was used after recrystallising twice from distilled water (m.p.180°C). N-tertiary butylacrylamide (N-t BAM) (reagent grade, Fluka) was used as received. Triton-X100 (octylphenoxy polyethoxyethanol) was purchased from Fluka (Switzerland) and used without further purification. N, N dimethyl formamide (Merck, India) used for the present study, was stored over P<sub>2</sub>O<sub>5</sub> for nearly 10 hours and distilled before use. Low carboxyl content polyacrylamide (LPAM; molecular weight 2.0X10<sup>5</sup>), and high carboxyl content polyacrylamide (HPAM; molecular weight 2.0X10<sup>5</sup>) were purchased from Across Organics (USA) and were used as received. High molecular weight polymers (viscosity average molecular weight 8.9x10<sup>6</sup>, A-type, NPAM) were purchased from Across Organics (USA). Double distilled water has been used throughout.

An aqueous suspension of 25 liter was prepared by stirring continuously 100 gms of the vermiculite (Aldrich) mineral in double distilled water. The suspension was maintained at pH 8.0 by adding NaOH solution. After every 24 hours, 10 cm layer of the suspension (from the top) was siphoned out and each time the original volume was restored by adding water. This process gives sample having particle size less than 2 micron<sup>1</sup>. The clay suspension was collected after acidification with HCl to pH nearly 4 and allowing settling at the bottom of the container or by centrifugation. This coagulated clay was washed repeatedly with double distilled water and centrifuged. Free iron oxide was removed by dithionate-citrate method. Organic matters were removed by gently heating at 80° C with 30 % (v/v) H<sub>2</sub>O<sub>2</sub> (Merck). H<sup>+</sup>-Vermiculite (HV) was prepared by shaking the stock minerals (3% w/w) in presence of 0.2 (M) HCl for about 6 hours followed by repeated centrifugation (20,000 rpm) and washing with doubled distilled water <sup>2</sup>. The cation exchange capacity (CEC) of vermiculite was determined by potentiometric titration with standard KOH solution under nitrogen atmosphere and found to be 1.50 meq.g<sup>-1</sup>. Ce (IV)-vermiculite (CeV) was prepared by shaking HV suspension (3%w/v) in presences of 0.3 (M) cerric ammonium nitrate

$(\text{NH}_4)_2[\text{Ce}(\text{NO}_3)_6]$  (reagent grade) at pH 2.5 for 6 h. followed by purification by repeated centrifugation and washing with doubled distilled water until the test of Ce (IV) ion in the supernatant liquid was negative. A separate adsorption experiment of Ce(IV) onto  $\text{H}^+$ -vermiculite (HV) showed that maximum exchange capacity of Ce(IV) ion onto the mineral was same ( $1.50 \text{ meq.g}^{-1}$ ) as above. The colloid content of clay minerals in each case was determined by evaporating a known volume of suspension to complete dryness. The suspensions were stored at  $5\text{-}10^\circ\text{C}$  temperatures.

The water content of vermiculite sample was measured following the method described by Marinsky and coworkers and found to be  $10 \text{ ml.g}^{-1}$  (ref.3).

The commercial grade nitrogen was passed through a series of bubblers containing Fiesser's solution.<sup>4</sup> The oxygen free nitrogen was dried by passing through two bubblers containing concentrated sulphuric acid dried.

### **3.2 POLYMERIZATION**

Measured quantities of acrylamide (AM) were taken in well-stoppered Pyrex bottles and polymerization reaction was carried out in dark to avoid any photo-initiated polymerization. Required amount of TU solution were added to the bottles and the mixtures were purged with purified nitrogen for 30 minutes at the experimental temperature. Required amount of dilute HCl solution was added drop wise to maintain pH of the reaction mixture. Polymerization reaction was started by adding deaerated CeV solution to the mixture. The reactions were carried out for desired time with intermittent shaking. Polymerization reactions were stopped by lowering the temperature with chilled water placing the reaction vessel in an ice bath after different time interval to determine degree of conversion as a function of polymerization time. The freezed reaction mixtures were then centrifuged to remove the clay mineral. The polymer was precipitated out by adding excess of acetone (Merck), washed repeatedly with acetone and dried in vacuum at  $40^\circ\text{C}$  for 48 hours. Four series of copolymers of acrylamide with *N*-t BAM at various concentrations but with a total monomer concentration of  $0.42 \text{ M}$  were conducted in aqueous solution at  $50^\circ\text{C}$  using Fe (III)-TU redox system in which Fe [III] ions were preloaded in the interlayer space of vermiculite clay mineral. Required amounts of AM and *N*-t BAM (dissolved in miceller pseudo-phase of nonionic surfactant, Triton-X 100(R) because *N*-tert butyl acrylamide is insoluble in water) were taken in a well stopperd Pyrex

bottle. Appropriate amount of TU solutions were added to the bottles and the mixtures were purged with purified nitrogen gas for thirty minutes at the experimental temperature. Dilute HCl was used to adjust pH, which was necessary to ensure the formation of adequate amount of amido-sulphenyl primary radicals to initiate the copolymerization reaction.<sup>5</sup> In another set of bottles, known amount of aqueous FeV suspension was degassed and finally added to the former bottles under nitrogen atmosphere to initiate the polymerization reactions. After different time intervals the reaction stopped by lowering the temperature with chilled water placing the reaction vessel in an ice bath. FeV suspensions were separated by centrifugation of the reaction mixture at 20,000 rpm. Low molecular weight polymers (viscosity average molecular weight  $2.3 \times 10^5$ , C-type) were prepared via redox polymerization of 0.4M acrylamide monomer initiated by Fe (III)/TU redox system at 50°C and pH 1.98 ( $1.5 \times 10^{-3}$  M FeCl<sub>3</sub> and 0.04 M TU). To obtain medium molecular weight polymers (viscosity average molecular weight  $1.6 \times 10^6$ , B-type) 0.4M monomer and 0.06M TU in aqueous suspension of ferric vermiculite (Fe(III)-V) were used at 60°C temperature and at pH=1.98.

The reaction mixtures were centrifuged (20,000 r.p.m.) to remove clay vermiculite after the completion of the reaction. The polymer was precipitated out by adding excess of acetone to the supernatants, washed repeatedly with acetone and dried at 40°C for 48 hours under vacuum. The centrifuged clay mineral was also washed and dried at 60°C for 48 hours under vacuum. The dried samples of polymer as well as mineral weighed to determine the polymer yield and non-extractable polymers in the clay minerals respectively.

### **3.3 VISCOSITY MEASUREMENTS**

Two types of viscometers were used to measure the relative viscosities of the polymer solutions. One is Ubbelohde type suspended level viscometer and another is modified Ostwald type viscometer. First one was used to measure viscosities of polymer solutions prepared in the mixtures of solvents and the later one was used to measure the relative viscosities at various shear rates ranging from few tens per second to few thousands per second for polymer solutions prepared in aqueous solutions in presence and in the absence of added salt. In both cases viscometers were placed in thermostated water bath at appropriate temperature, controlled within the range of  $\pm 0.1^\circ\text{C}$  and a digital stopwatch with accuracy  $\pm 0.1$  sec measured the

flow time. Solvent flow times were larger than 120 seconds so that the kinetic energy corrections are not necessary<sup>6</sup>. Required quantities of dry polymer were dissolved in 0.2(M), 0.1(M), 0.05(M), 0.025(M), and 0.0125(M) aqueous NaCl solutions to study the effects of salt on solution viscosity. Care was taken to avoid excessive shear during dissolution of the polymer. The dissolution process was generally complete within 1-2 days. These solutions were further diluted to the required concentrations. Desired pH of the solutions was adjusted by using dilute HCl or NaOH solutions. Viscosities were measured after 15 days of completion of dissolution to avoid the effect of aging. The molecular weight of the synthesized polymers was determined by viscosity measurement in aqueous 0.1 (M) NaCl solutions at 30°C using a suspended level Ubbelohde Viscometer and a Mark-Houwink relationship.<sup>7,8</sup>

$$[\eta] = 9.33 \times 10^{-3} M^{-0.75} \text{ cm}^3 / \text{g}.$$

1

### **3.4 POTENTIOMETRIC AND CONDUCTOMETRIC MEASUREMENTS**

Measurements of pH were made using Systronics (pH system 361, India) pH-mV meter. The meter was standardized using two-point calibration method. Conductance measurements were carried out on Systronics conductivity meter-306 using a dip type cell with a cell constant 1.15 cm<sup>-1</sup>. The cell was calibrated by standard KCl solutions. The measurements were made in a container maintained at desired temperature.

### **3.5 ELEMENTAL ANALYSIS**

For the determination of copolymer composition elemental analysis for carbon and nitrogen of AM-*N*-t BAM copolymers were conducted by CDRI, Lucknow, India. The copolymer compositions were calculated based on C/N weight % ratios because of the variability of absolute values due to the hygroscopic nature of the copolymer. Elemental analysis was conducted at polymer conversion levels, low and high, to assess drift in the copolymer.

### **3.6 MEASUREMENT OF SURFACE TENSION**

Surface tension of TritonX-100 solutions and solutions of polymer surfactants mixtures were measured using the ring method with a Kruss balance (Germany) at four different temperatures (20<sup>o</sup>,30<sup>o</sup>,40<sup>o</sup>,50<sup>o</sup>C). The ring was cleaned between two measurements of surface tension. The solutions were thermostated by circulating

water at desired temperature. Sets of measurements were made by adding small aliquots of concentrated surfactant solutions at constant polymer concentration. Each measurement took 20-40 minutes to reach the equilibrium.

### 3.7 SORPTION OF TU AND AM ONTO VERMICULITE

10ml portion of a 0.5% suspension of clay was placed in a number of Pyrex bottles and different amounts of either thiourea or acrylamide were added followed by pH adjustment at 2.0 by dilute HCl solution. The total volume of the suspension was made upto 15 ml in each case by adding the requisite amount of water and was shaken at 30°C for 4 hours to attain equilibrium. The supernatant solutions were then centrifuged (20,000 r.p.m.) and analyzed. The electronic absorption spectra were recorded with double beam UV-VIS spectrophotometer (Shimadzu, model-240, Japan) at 235 nm and 195 nm for TU or AM respectively. The temperature was maintained within  $\pm 0.1^\circ\text{C}$ . Double distilled water was used as solvent.

### 3.8 REFERENCES

1. M.L. Jackson, Soil Chemical Analysis, Prentice Hall of India (P) Ltd. New Delhi, 168
2. S. Talapatra, S.C. Guhaniyogi, and S.K. Chakraborti, *J. Macromol. Sci Chem.*, **A22 (11)**,1611(1985).
3. J.A. Marinsky, F.G. Lin and K.S. Chung, *J. Phys.Chem.* **87**, 3139 (1983).
4. B.S. Ruruiss, A.J. Haknorfod, V. Rogers, P.W.G. Smith and A.R. Tatchell, Vogel Text Book of Practical Organic Chemistry.
5. R.E. Grim, Clay Mineralogy, Academic Press Inc. London (1964).
6. S. Ajitkumar, D. Prasadkumar, S. Kansara and N.K. Patel, *J. Eur. Polym.* **32**, 149 (1995).
7. J.Bhattacharya, S.K. Chakraborti, S. Talapatra, S.K. Saha and S.C. Guhaniyogi, *J. Polym. Sci., Part- A: Polymer Chemistry*, **27**, 3977(1989).
8. J. Bhattacharya, S.K. Saha and S.C. Guhaniyogi, *J. Polym. Sci, Part A: Polymer Chemistry*, **28**, 2249(1990).

## CHAPTER 4

# STUDIES ON REDOX POLYMERIZATION OF ACRYLAMIDE IN AQUEOUS – VERMICULITE MEDIA

# **SECTION A: AQUEOUS POLYMERIZATION OF ACRYLAMIDE BY Ce (IV) - TU REDOX COUPLE ON VERMICULITE SURFACE**

## **4 A 1 INTRODUCTION AND REVIEW OF PREVIOUS WORKS**

The synthesis of the water-soluble polymers is generally commercially implemented by various processes including aqueous solution polymerization, inverse suspension polymerization and inverse emulsion polymerization, which are initiated by either thermal initiators or redox couple initiators. Polymerization of vinyl monomers in aqueous media may be classified into four different categories.

1. Solution polymerization  
(Both monomer and polymer are soluble in water).
2. Precipitation polymerization  
(Monomer is soluble in water but polymer is not soluble in water).
3. Emulsion polymerization  
(Both monomer and polymer are insoluble in water. Monomer is emulsified by emulsifiers in water).
4. Suspension polymerization  
(Both monomer and polymer are insoluble in water. Monomer is dispersed as droplets by suspension stabilizer in water).

The solvent acts as diluents and aids in the transfer of the heat of polymerization. The solvent also allows easier stirring, since the viscosity of the reaction mixture is decreased. On the other hand, the presence of solvent may create new difficulties; chain transfer to solvent and/or to the solute may occur. Acrylamide, vinyl acetate, acrylonitrile and ester of acrylic acid etc. are polymerized in solution. When water is used as solvent, there are some advantages over organic solvents. Water is a cheap, clean and environmental friendly solvent and chain transfer to the solvent is not possible. However, for homogenous polymerization process it is limited to only water-soluble polymers and monomers. Each of the

above processes has its associated disadvantages, however, which limits its practical use in the manufacturing of the water-soluble polymers.

Among all of the water-soluble polymers, poly acrylic acid and polyacrylamide based water-soluble polymers are used in a wide range of products because of their high performance and low cost. Ability of clay minerals to intercalate various molecules and their catalytic properties are long known. The clay-polymer interaction has found many and varied applications.<sup>1</sup> Smectite clays like montmorillonite, vermiculite etc. have been shown to catalyze the polymerization of some unsaturated organic compounds and yet to inhibit polymer formation from other structurally related monomers such as methylmethacrylate.<sup>2</sup> This behavior is believed to be due to electron accepting or electron donating sites on the clay minerals. Over last couple of decades, the use of thiourea (TU) and N-substituted TU as redox components for the initiation of aqueous vinyl polymerization has been examined<sup>3</sup>. These experiments applied various oxidants, viz, metallic salts, organic and inorganic peroxides, persulphate, permanganate to name a few. The special features of these systems are a very short induction period, low activation energy and low temperature required. Redox polymerization of acrylamide is one of the most common techniques applied for aqueous polymerization because of the simplicity of the technique as well as high yield and reaction rates. Water-soluble polymers are synthesized via free radical polymerization mechanism. Solution polymerization is commonly used in the synthesis of linear, low molecular weight water-soluble polymers. Polyacrylamide and its copolymer with dimethyldiallyl ammonium chloride (DMDAAC), which is used as cationic flocculent are polymerized in solution.<sup>4-6</sup> In order to synthesize the high molecular weight polyacrylic acid, polyacrylamide and their copolymers, inverse suspension/emulsion processes are also used. In the solution process, the water-soluble monomers are polymerized in a homogenous aqueous solution in the presence of free-radical initiators mostly redox couples. Acrylamide is readily polymerized in aqueous solution at elevated temperatures with free radical initiators. Several workers have reported polymerization of acrylamide in aqueous solution with different free radical initiators.<sup>7-35</sup> Gnansundaram and co-workers observed that for the initiator, bis [2-[(2-hydroxy-ethylamino) ethoxy] copper (II) at pH 1.8, the polymerization rate was first order with respect to acrylamide monomer and 0.5 with respect to catalyst<sup>9</sup>. Faster polymerization and high molecular weight polymers were obtained using 2, 2'-azobis [2-(N, N'-ethylenamidino)] propane initiator than those

obtained using  $K_2S_2O_8$ -Mohr's salt initiating system.<sup>10</sup> The rate of polymerization of acrylamide by peroxydiphosphate in  $H_2S_2O_4$  was decreased when the temperature was raised from  $30^0$  to  $50^0C$  but increased above that temperature, which was independent of pH.<sup>11</sup> Kinetics of polymerization in aqueous acetic acid (AcOH) using  $Pb(OAc)_4$  as initiator was studied by Balakrishnan who found that polymerization rate was first order with respect to AM.<sup>16</sup> The propagation and termination reaction of the  $K_2S_2O_8$  initiated polymerization of AM in water were not influenced by anionic emulsifier Dowfax 2 Al.<sup>17</sup> The induction of polymerization was affected by manganous salts while the polymerization rate and the polymer molecular weight was not affected to a detectable degree, as was observed by Xuanchi.<sup>18</sup> Using trigol and polyethylene glycol initiators, it was found that the yield and the molecular weight of the polymer decreased with chain length of substituted AM.<sup>20</sup> Cvetkovska and coworkers explained the kinetic model by the formation of a monomer-initiator complex and inhibiting effect of the Mn (II) acetylacetonate formed by the reduction of Mn (III) acetylacetonate.<sup>21</sup> The polymerization rate of AM in  $H_2S_2O_4$  or AcOH by Co (III) system showed similar mechanism to follow as that of  $Pb(OAc)_4$  initiator in AcOH.<sup>22</sup> Vaskova and co-workers found that in mixtures of water and aliphatic alcohols, in the presence and absence of an inhibitor, the rate of polymerization and molecular weight were reduced depending upon the length and character of the aliphatic chain.<sup>23</sup> Liu and co-workers observed that the polymerization rate was dependent on the catalyst concentration and pH of the solution.<sup>24,26</sup> Takahashi and co-workers found that the average molecular weight of polymer was  $(1 - 7) \times 10^4$  when (2, 2'- bipyridine) cobalt (II) complex was used as initiator. Bhanu and coworkers observed that co-ordinately unsaturated Co (II) complexes significantly inhibited the thermal polymerization of AM but they imparted a significant induction period during AIBN (azobisisobutyronitrile) initiated polymerization of AM.<sup>31</sup> High molecular weight polyacrylamide could be obtained by using heptanes as the organic phase,  $K_2S_2O_8$  as catalyst and sorbitol-s-20 system as the emulsifier.<sup>33</sup> The author also reported that the polymer molecular weight increased with the concentration of AM and the emulsifier and also by decreasing catalyst concentration. Redox catalyst systems were frequently employed for polymerization at comparatively lower temperatures. Bajpai, Misra, Behari and co-workers investigated the polymerization of AM initiated by  $KMnO_4$ / various amino acids and unsaturated acids redox couples.<sup>34-46</sup> A value of  $KMnO_4$  catalyst exponent of unity in the rate equation

confirmed a unimolecular chain termination process by redox system.<sup>34,40</sup> However, a bimolecular chain termination was observed by other redox systems.<sup>37,39,42-44</sup> The rate of polymerization was first order for the monomer in all the above systems. Bajpai and co-workers suggested that polymer molecular weight was directly proportional to initial monomer concentration and inversely proportional to the rate of initiation. With the increase in temperature, the molecular weight of polymer was decreased in most of the cases. The effects of various additives (alcohols, neutral salts, complexing agents) on the polymerization rate were also investigated. A number of workers studied the mechanism and kinetics of aqueous polymerization of AM in acidic medium initiated by Ce (IV)/ reductant couples.<sup>47-65</sup> The rate of polymerization was first order in monomer and half order with respect to Ce (IV) ion concentration in cases where initiator was either Ce (IV) / thioglycolic acid or Ce (IV)/ L-cysteine.<sup>50,51</sup> In the polymerization of AM initiated by Ce (IV) / thiourea in water, the polymerization rate is governed by the relation  $R_p = k_p [AM]^{1.20} [Ce (IV)]^{0.5} [TU]^{0.5}$ , where  $R_p$  is the initial rate of polymerization. Presence of alkyl phenyl carbonate or alkyl-4-tolyl-carbonate increased the polymerization rate of AM initiated by Ce (IV) in H<sub>2</sub>O-MeCN and H<sub>2</sub>O-HCONH<sub>2</sub> and decreased the activation energy of polymerization compared to system where Ce (IV) used alone. The rate of polymerization was derived as  $R_p = k_p [AM]^{1.5} [Ce]^{0.39} [\text{alkyl phenyl carbonate}]$ . The overall rate of polymerization was faster and activation energy was lower with Ce (IV)/p-acetotoluidide system compared to Mn (III)/ p-acetotoluidide.<sup>60</sup> Different workers studied the effects of various aliphatic diamines on vinyl polymerization using persulfate as initiator.<sup>66-76</sup> They suggested that the promoting activities of diamines on vinyl polymerization were of the order: t-diamine > s-diamine > p-diamine. In a reversible redox initiating system involving metals and porphyrin, the aqueous polymerization rate depended on the types of metal ion (e.g. Ce(IV), Cu (II), Ti (IV), Mn (II)) in the porphyrin complex, polymerization temperature and concentration of AM.<sup>68</sup> The presence of carboxylic acids had promoted and enhanced the polymerization rate of AM initiated by Mn (OAc)<sub>4</sub> (Ref.70). Kurenkov and co-workers observed that higher molecular weight polymers could be obtained with higher conversions using K<sub>2</sub>S<sub>2</sub>O<sub>8</sub> / Na<sub>2</sub>S<sub>2</sub>O<sub>3</sub> redox system during adiabatic polymerization of AM in comparison to the K<sub>2</sub>S<sub>2</sub>O<sub>8</sub>/Na<sub>2</sub>S<sub>2</sub>O<sub>3</sub>-CuSO<sub>4</sub> system.<sup>71-73</sup> Molecular weight of the polymer was increased with increasing monomer concentration but decreasing catalyst concentration. Akopyan and co-workers obtained polymers having molecular weight of 8.0x10<sup>5</sup> at

25°C by three component catalyst system comprising of  $K_2S_2O_8$ , triethanolamine and amino acetic acid.<sup>74</sup> The overall polymerization rate was increased in presence of Cu (II) ions for the polymerization initiated by persulfate - (dimethylamino) ethylmethacrylate-Cu(II) catalyst. Kurenkov and co-workers demonstrated an increase in molecular weight with an increase in concentration of the monomer and a decrease in concentration of the initiating system ( $K_2S_2O_8$ / sodium metabisulfate-copper sulfate)<sup>75</sup>. Several workers examined the polymerization kinetics, mechanism, polymer molecular weight and effect of additives for various redox polymerizations involving chelate complexes.<sup>21,77-97</sup> For radical polymerization of acrylamide initiated by Mn (III) - acetylacetonate in aqueous solution of pH 2.0, Cvetkovska explained the deviation of the kinetics from the conventional kinetic model via the formation of monomer-initiator complex.<sup>21</sup> Smith obtained polymers having molecular weight as high as  $4.0 \times 10^6$  by Fe (II) / hydro peroxide redox initiator at the temperature range between -20°C and +40°C<sup>78</sup>. Wu and He obtained polyacrylamide having molecular weight of  $10^7$  at room temperature by  $NaHSO_3$ -O-  $MnSO_4$  catalyst.<sup>79</sup> They also pointed out that the presence of  $MnSO_4$  would only affect the catalytic activity of the system but it did not involve in chain propagation or termination. Electrochemical study of the redox initiating systems, Ce (IV)-EDTA/  $N_2H_4$ - $H_2O_2$  and Ce (IV)-EDTA/ $NH_2OH$ - $H_2O_2$ , in alkaline aqueous media (pH=9-11) showed that the former redox system was more effective than the later. Lenka and Nayak observed that the polymerisation rate was decreased with increasing thiosulfate concentration and was first order with respect to AM during aqueous polymerization of AM initiated by potassium peroxydiphosphate / Na-thiosulfate redox system.<sup>86</sup> The kinetics was examined for the thermal polymerization of AM in the presence of  $CCl_4$  and a bis amino acid chelate of Cu (II) with glutamic acid, serine or valine by Namasivayan and Natarajan.<sup>88</sup> The activation energy of polymerization reaction decreased from 78.24 to 18.83 kJ/ mole on addition of 1.0 ppm Fe during the polymerization by  $H_2O_2$  /  $NH_2OH$ -HCl redox couple.<sup>89</sup> From this observation, it was concluded that the predominant reaction appeared to be Fe catalyzed decomposition of the peroxide in presence of small amount of  $NH_2OH$ -HCl. Sur and Choi found that the reaction rate in presence of  $CoCl_2$  and N, N-dimethylaniline was proportional to  $[AM]^{1.08}$  and  $[Co (II)]^{0.53}$  indicating bimolecular termination process to be involved.<sup>94,97</sup> The rate of polymerization and the maximum yield decreased when the temperature was raised above 40°C. Chshmarityan and Beileryan observed that the polymerization of AM in

aqueous solution initiated by  $K_2S_2O_8$ -Ag (aminoacetate) chelate system was first order in monomer and 0.5 order in initiator.<sup>99</sup> Some researchers investigated a series of sulfur-containing compounds as electron donors in photo induced free-radical (ethionine, methionine, Gly-Met, Met-Gly and methioninemethyl ester) polymerization, in conjunction with 4-carboxybenzophenone (CB) as sensitizer.<sup>100</sup> The results were compared with the nonsulfur-containing compounds, alanine and triethanolamine. The best initiation yields are observed for the system CB-(phenylthio) acetic acid. The kinetic and mechanistic features of potassium ditelluratoargentate (III) (DTA) initiated aqueous polymerization of acrylamide (AM) have been investigated in an alkaline medium by Yanghai and co-workers.<sup>101</sup> The polymerization behavior as a function of  $[AM]$ ,  $[DTA]$ , pH as well as temperature, have been studied. The overall rate of polymerization has been determined from gravimetry. The rate has been found to bear 1.68 and 0.76 dependence on  $[AM]$  and  $[DTA]$  respectively. The overall activation energy of AM polymerization is measured as 33.6kJ/mol.

In view of the use of acrylamide in various applications including that as displacement fluid in secondary oil recovery, high molecular weight polyacrylamide with large hydrodynamic volume is essential. Recently it has been shown that linear termination process is controlled in aqueous redox polymerization of acrylamide, by loading metal ions of Fe (III) – TU systems in the interlayer space of montmorillonite and thereby high molecular weight polymer is formed. Vermiculite being the similar smectite to montmorillonite may also provide potential microenvironment for aqueous acrylamide polymerization to high degree. In this section of the present chapter, attempts have therefore been made to examine the catalytic activity of clay mineral (viz., vermiculite) in the aqueous polymerization process of water-soluble polymers and to prepare polymers having high molecular weight with high rate of formation under ordinary condition. Vermiculite microenvironment seems to have a dramatic effect on the polymerization of acrylamide by Ce (IV)/TU combination in aqueous medium. A detail study concerning the kinetic and mechanistic aspects has been made for the aqueous polymerization of acrylamide with ceric vermiculite (CeV)/thiourea (TU) initiating system. Spectroscopy and other analytical data have been taken into consideration to determine the pathways involved in the reaction. Another objective of the present study is to prepare high molecular weight polymers for subsequent studies on solution properties in aqueous and aqueous –organic

mixtures, which has been presented in chapter 5 of the thesis.

## 4 A 2 RESULTS AND DISCUSSION

Polymerization mechanism and kinetics both are affected to a great extent due to the occurrence of the reaction in the mineral microenvironment. Tables 4.1-4.4 show the data pertaining to the initial rate of polymerization ( $R_p$ ), polymer yield ( $X_L$ ), intrinsic viscosity  $[\eta]$ , as well as molecular weight ( $M_v$ ) and the amount of non-extractable polymer formed as functions of the concentration of Ce (IV), TU, AM and the temperature. The molecular weights of the polymer are moderately high and ranged from  $2.39 \times 10^5$  to  $2.17 \times 10^6$ . The initial rate of polymerization,  $R_p$ 's obtained are ranged between  $(0.79-7.13) \times 10^{-4} \text{ mol.L}^{-1}.\text{s}^{-1}$  depending on various reaction parameters. The rate of polymerization  $R_p$ , polymer yield ( $X_L$ ), intrinsic viscosity  $[\eta]$ , and molecular weight  $M_v$  increased with increasing monomer concentration ( $0.2-1.0 \text{ mol. L}^{-1}$ ) for a fixed TU and CeV concentrations. No reaction took place at or below the monomer concentration of  $0.2 \text{ mol. L}^{-1}$ . The percent conversion of monomer has been plotted as a function of time of reaction at different TU, AM and Ce (IV) concentrations and shown in figures 4.1-4.3. Induction period was around 10 minutes at  $60^\circ\text{C}$ . However, the induction period is found to be different at different temperatures (e.g., 40 minutes at  $45^\circ\text{C}$  and 0 at  $70^\circ\text{C}$ ). The  $R_p$  increases from  $1.70 \times 10^{-4}$  to  $3.89 \times 10^{-4} \text{ mol. L}^{-1}.\text{s}^{-1}$  when TU concentration is increased from  $0.04$  to  $0.10 \text{ mol. L}^{-1}$ .

**Table 4 .1 Polymerization of AM in aqueous medium in presence of 0.04M TU and  $1.50 \times 10^{-3} \text{ M}$  ceric vermiculite and various concentrations of AM at  $60^\circ\text{C}$ (pH=1.98).**

AM $\text{mol.L}^{-1}$	$R_p \times 10^4$ $\text{mol. L}^{-1}.\text{s}^{-1}$	$X_L$	$[\eta]$ $\text{ml.g}^{-1}$	$M_v \times 10^{-5}$	Non- extractable PAM (wt%)
0.2	-	-	-	-	-
0.4	1.69	58	132	3.41	0.05
0.6	2.52	83	323	11.48	0.14
0.8	5.54	92	423	16.17	0.25
1.0	7.13	98	528	21.72	0.21

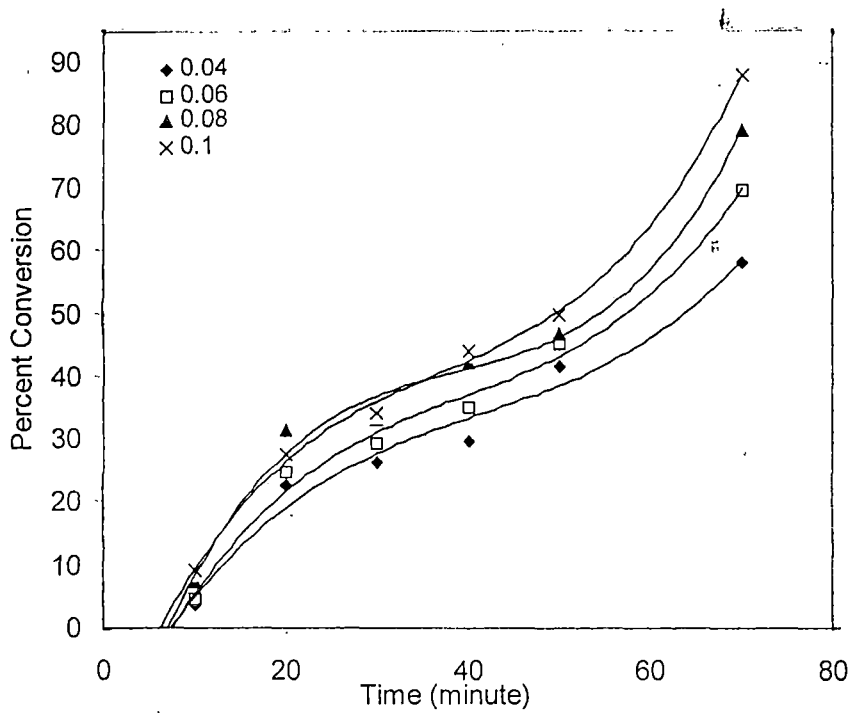


Figure:4.1: Time-conversion plots for the aqueous polymerization of AM at 60°C with Ce<sup>IV</sup>/TU: [AM]=0.4M; intercalated Ce(IV)=1.50mmol/lit and various conc.(M) of TU.

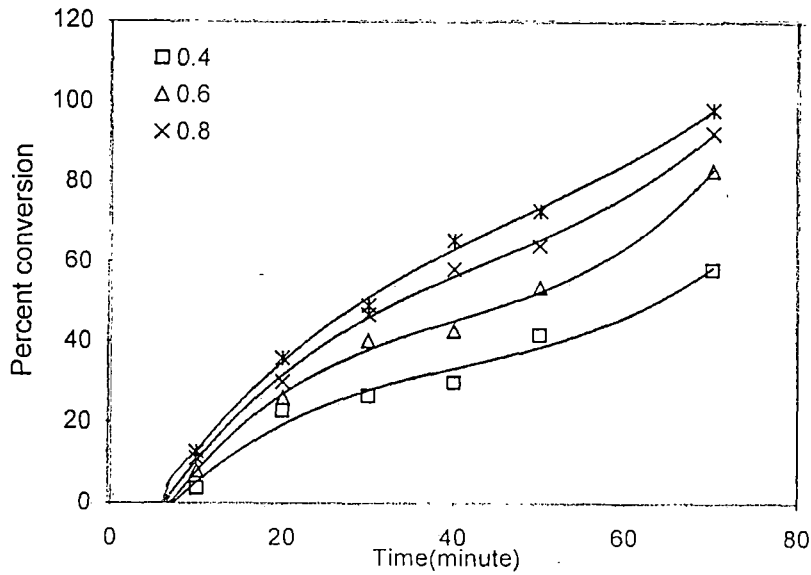


Figure:4.2: Time-conversion plots for the aqueous polymerization of AM at 60°C with Ce<sup>IV</sup>/TU: [TU]=0.04M; Ce(IV)=1.50mmol/lit and various concentrations (M) of AM.

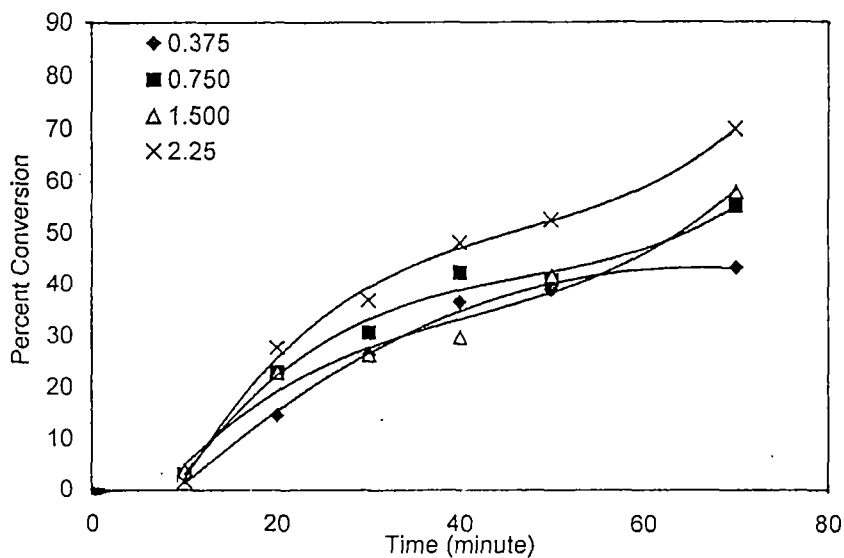


Figure:4.3 : Time-conversion plots for the aqueous polymerization of AM at 60°C with CeV/TU:[AM]=0.4M; [TU]=0.04M and various conc.(mmol/lit) of intercalated Ce(IV).

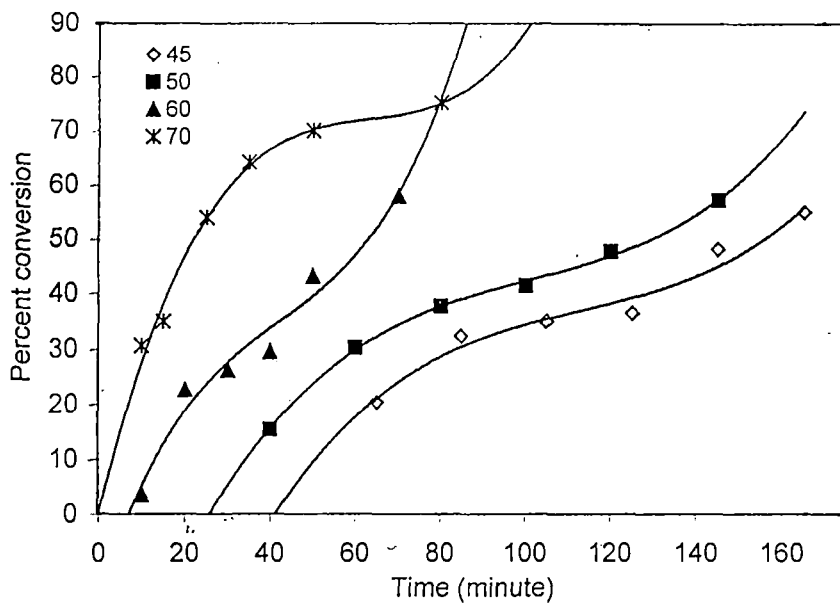


Figure:4.4: Time-conversion plots for the aqueous polymerization of AM at 70°C, 60°C, 50°C, 45°C; [AM]=0.4M; [TU]=0.04M; [CeV]=1.50 mmol/lit.

**Table 4.2 Polymerization of AM (0.4M) in aqueous medium in presence of  $1.50 \times 10^{-3}$  M ceric vermiculite at  $60^\circ\text{C}$  and various concentrations of TU (pH=1.98).**

TU Mol.L <sup>-1</sup>	R <sub>p</sub> X10 <sup>4</sup> mol. L <sup>-1</sup> S <sup>-1</sup>	X <sub>L</sub>	[η] ml.g <sup>-1</sup>	M <sub>v</sub> X10 <sup>-5</sup>	Non- extractable PAM (wt%)
0.04	1.698	58	132	3.41	0.08
0.06	2.902	69	118	2.95	0.34
0.08	3.055	79	156	4.27	0.31
0.10	3.890	88	144	3.84	0.28

**Table 4.3 Polymerization of AM (0.4M) in aqueous medium in presence of 0.04M TU at  $60^\circ\text{C}$  and various concentrations of ceric vermiculite (pH=1.98).**

CeV mmolL <sup>-1</sup>	R <sub>p</sub> X10 <sup>4</sup> mol. L <sup>-1</sup> S <sup>-1</sup>	X <sub>L</sub>	[η] ml.g <sup>-1</sup>	M <sub>v</sub> X10 <sup>-5</sup>	Non- extractable PAM (wt%)
0.375(0.008 <sup>f</sup> )	1.698	43	129	3.32	0.21
0.750(0.016 <sup>f</sup> )	3.24	55	115	2.85	0.26
1.500(0.031 <sup>f</sup> )	3.639	58	132	3.41	0.30
2.250(0.047 <sup>f</sup> )	4.144	70	101	2.39	0.33

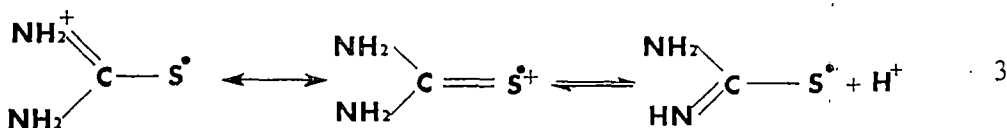
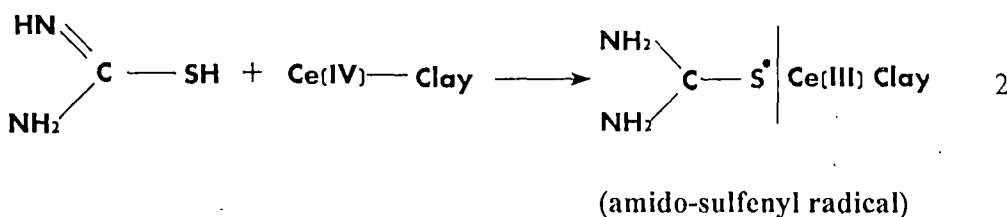
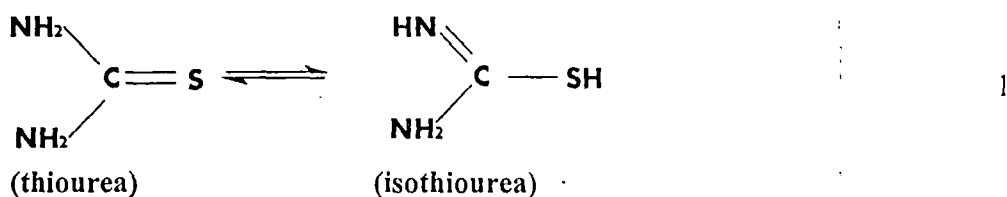
<sup>f</sup> moles of interlayer Ce(IV) in 1000ml of vermiculite gel phase).

**Table 4.4 Polymerization of AM (0.4M) in aqueous medium in presence of 0.04M TU and  $1.50 \times 10^{-3}$  M ceric vermiculite at various temperatures (pH=1.98)**

Temperature in °C	R <sub>p</sub> X10 <sup>4</sup> mol. L <sup>-1</sup> S <sup>-1</sup>	X <sub>L</sub>	[η] ml.g <sup>-1</sup>	M <sub>v</sub> X10 <sup>-5</sup>	Non- extractable PAM (wt%)
45	0.79	37	252	8.11	0.15
50	1.20	46	223	6.89	0.11
60	1.99	58	132	3.41	0.11
65	3.09	89	134	3.48	0.17
70	5.88	99	123	3.11	0.08

Hence on increasing the concentration of catalyst more TU is oxidized to generate relatively more isothiocarbamido radicals (shown below). Consequently the number of propagating polymer chains and hence the rate of polymerization increases. At the concentration of TU lower than 0.04 mol. L<sup>-1</sup> the polymer yield was too little to be

detected. At such a low concentration of TU, concentration of initiating species is too small to initiate the polymerization. The  $M_v$  of the polymer reached its maximum value ( $4.27 \times 10^5$ ) at  $0.08 \text{ mol. L}^{-1}$  of TU,  $0.4 \text{ M}$  AM and  $1.50 \text{ mmol. L}^{-1}$  CeV at  $60^\circ \text{ C}$  and a minimum value of  $2.95 \times 10^5$  at  $0.06 \text{ mol. L}^{-1}$  TU concentrations. Initially  $R_p$  increases rapidly with increasing the concentration of Ce (IV) (keeping all other variables viz. concentration of AM, TU and temperature constant) but at higher concentration of Ce (IV) the rate of increment is slow. Aqueous polymerization of AM is also dependent significantly on the pH of the solution. Previous report showed that low-moisture content clay minerals promote the spontaneous cationic polymerization. Both Bronsted and Lewis acidity have been involved in the cationic polymerization initiated by dry clay minerals. The acidity of the clay increases on drying.<sup>102-104</sup> In the present study, the reaction is carried out in aqueous medium and the surface acidity is as compared to the dry mineral. Above pH 2.10, no significant polymerization takes place. The metal ion Ce (IV) in the interlayer space of vermiculite reacted with isothiurea, the tautomeric form of thiourea, generating amido-sulfenyl radical to initiate polymerization. At low pH the tautomeric equilibrium of TU in aqueous solution is shifted towards isothiocarbamido form facilitating the formation of primary radical. Moreover, the protonated form of the amido-sulfenyl radical at low pH is more stable than the radical itself and consequently the dimerization process is less favorable.<sup>105</sup>



## EFFECT OF TEMPERATURE

The effect of temperature on the rate of polymerization of acrylamide was investigated over the range of 45° – 70°C. The higher the temperature faster is the rate of polymerization and higher the polymer yield. On the other hand, higher the temperature lower is the molecular weight of the polyacrylamide formed. Temperature dependence of polymerization rate is illustrated in figure 4.4. The plot of the logarithm of empirical rate constant  $R_p$  against the reciprocal of the absolute temperature (figure 4.5) yields the value of activation energy of the reaction as 29.29 kJ/mol. The value of activation energy of the present acrylamide polymerization system is usually found to be around 83.68 kJ/mol in aqueous medium.<sup>106</sup> Thus, it is seen that polymerization mechanisms is affected to a great extent due to the occurrence of the reaction in the mineral microenvironment.

## <sup>1</sup>H AND <sup>13</sup>C NMR SPECTRA OF PAM

<sup>1</sup>H and <sup>13</sup>C NMR spectra of polyacrylamide samples obtained from the polymerization on vermiculite surface by CeV/TU initiator are shown in figure 4.6a. <sup>1</sup>H and <sup>13</sup>C NMR spectra of polyacrylamide is not usually an well resolved spectrum and no special feature is apparent in the present spectrum except that of overlapping of a sharp line with chemical shift of 2.12 ppm near the –CHCONH<sub>2</sub> position. This line in all probability represents the hydrogen from the isothiocabamido end groups of thiourea terminated PAM. The expanded <sup>13</sup>C spectra (figure 4.6b) showed methylene, methane and carbonyl carbons of head-to-tail polymer of acrylamide. The carbonyl carbon (180.2 ppm) splitting was small. The methine resonance (42.2 – 43.5) is a triplet, which further split, showing pentade sensitivity. The low field and high field triplet peaks may be assigned to rr (syndiotactic) and mm (isotactic) sequences respectively. The central peak corresponds to heterotactic sequences (mr+rm). The methylene carbon lines (34 - 37.4) also fall into three well-separated groups with 20 lines required by hexad sensitivity resolved. It seems apparent from the <sup>13</sup>C spectra that Bernoulli statistics is followed and steregularity has not been observed. Both <sup>1</sup>H and <sup>13</sup>C nmr spectra of polyacrylamide are similar to those obtained in presence of montmorillonite microenvironment. However, the polymer trapped inside the interlayer spaces of vermiculite, which could not be extracted by

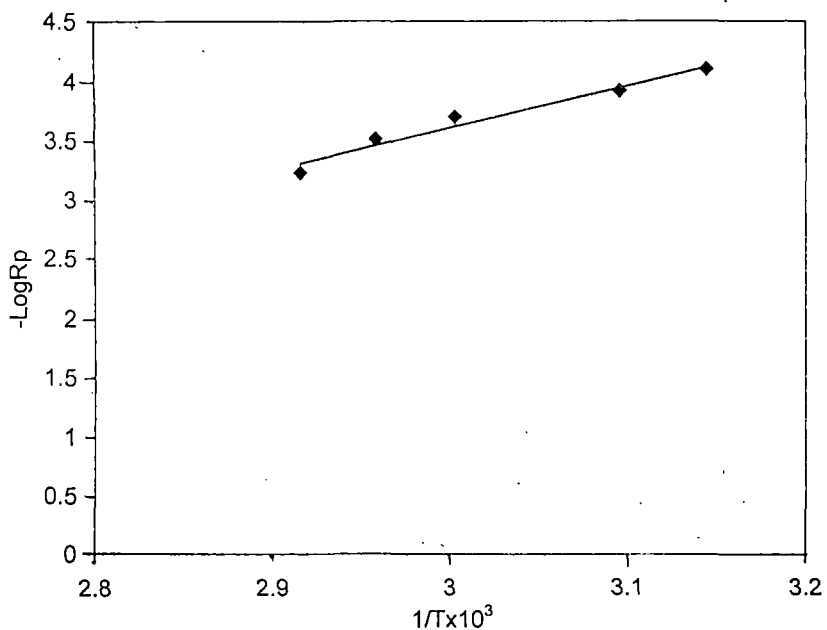


Figure:4.5:Plot of  $-\text{Log}R_p$  vs.  $1/T$  for aqueous polymerization of AM with CeV/TU.  $[\text{AM}] = 0.4\text{M}$ ,  $[\text{TU}] = 0.04\text{M}$ ,  $[\text{Ce(IV)}] = 1.50 \times 10^{-3}\text{M}$ .

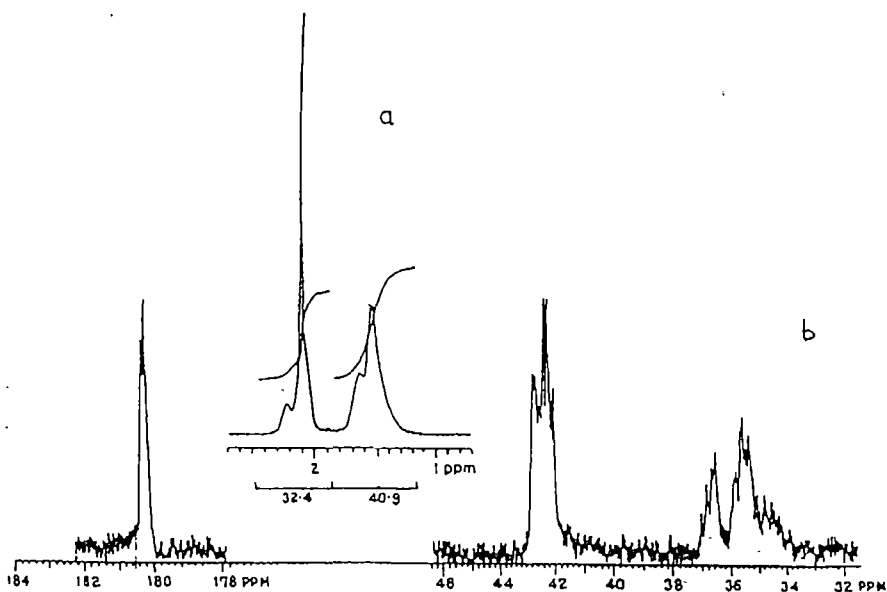


Figure:4.6.  $^1\text{H}$  and  $^{13}\text{C}$  nmr spectra of thiourea terminated polyacrylamide on vermiculite surface, (a)  $^1\text{H}$  nmr spectrum, (b)  $^{13}\text{C}$  nmr spectrum.

washing with water may have such possibility of showing stereoregularity. Attempts are being made to extract these polymers in mild condition for further study.

## KINETICS AND MECHANISM

A plot of  $\log R_p$  versus  $\log [AM]$  is linear with a slope of 1.86 (Figure 4.7). Therefore, the rate law almost follows the second order kinetics with respect to the monomer concentration, which is deviated from the homogeneous aqueous medium reaction condition.<sup>105</sup> The significant changes due to the occurrences of the reaction on the vermiculite surface indicates that the polymerization mechanism is greatly affected by mineral microenvironment. Figure 4.8 shows that with the increase of CeV concentration the initial rate of polymerization increases linearly and the slope of the plot of  $R_p$  vs. logarithm  $[AM]$  is almost 0.47, which indicates that the rate of polymerization is approximately 0.5 order with respect to metal ion oxidant. Unlike montmorillonite phase reaction, acrylamide polymerization initiated by CeV / TU system shows identical value of metal exponent of 0.5 for the initial rate in both the cases i.e., whether the reaction propagates in the bulk phase or in the vermiculite gel phase (in the later case, metal ion concentration in vermiculite gel was varied by adding calculated amount of HV in the reaction mixture; the water content of vermiculite sample was found to be  $10\text{ml.g}^{-1}$ ). This shows that the well-dispersed vermiculite in aqueous medium behaves like a homogeneous single phase. Although the polymerization reaction is initiated and progress to some extent inside the layered space, the polymer chain after achieving a certain length (depending upon vermiculite particle size) inside the layered space continue to grow in aqueous solution. This is also supported by the fact that vigorous stirring of the reaction mixture stops polymerization to take place in vermiculite catalyzed acrylamide polymerization reaction. Generally, the rate of polymerization decreases with the increase of metal ion concentration in homogeneous polymerization involving metal ion/TU redox system.<sup>105</sup> The use of vermiculite medium controls the linear termination rate and the rate of reaction increases with the increase of metal ion concentration. Figure 4.9 shows that the rate of polymerization varies with the variation of TU concentration under constant monomer concentration of  $0.4\text{ mol. L}^{-1}$  at  $\text{pH}=1.98$ . Metal ion concentration also remains fixed at  $1.5 \times 10^{-3}\text{ mol.L}^{-1}$ . The relationship of polymerization rate with TU concentration was obtained from the slope of  $\log R_p$  versus  $\log [TU]$  plot. The thiourea exponent is observed as 0.85, which is

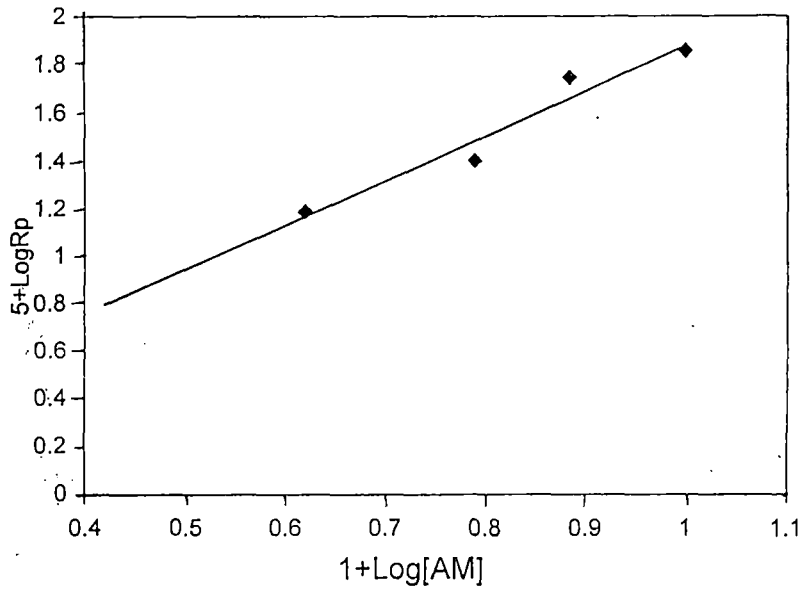


Figure:4.7: Logarithmic plot of  $R_p$  vs.  $[AM]$  for aqueous polymerization of AM with CeV/TU.  
 $[TU]=0.04M, Ce(IV)=1.50 \times 10^{-3}M$  at  $60^\circ C$

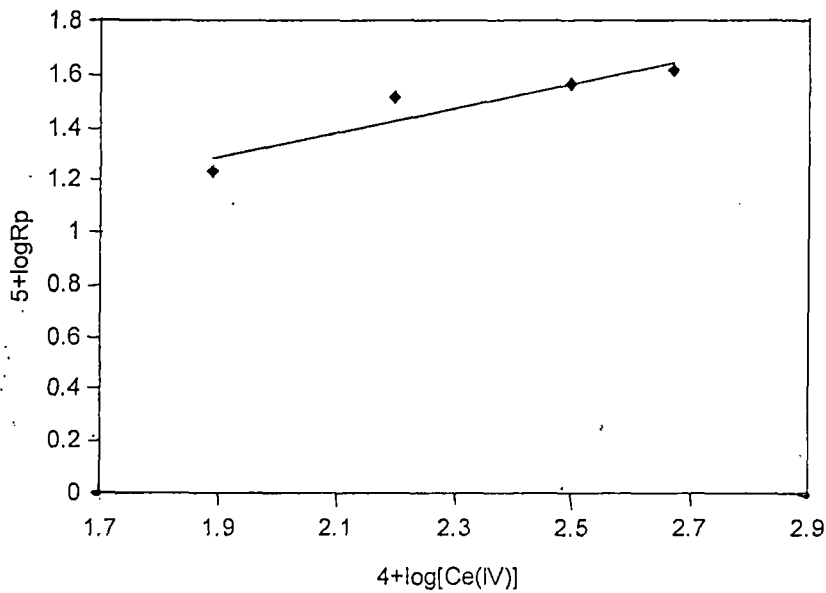


Figure:4.8: Logarithmic plot of  $R_p$  vs.  $[Ce(IV)]$  for aqueous polymerization of AM with CeV/TU.  $[AM]=0.4M,$   
 $[TU]=0.04M$  at  $60^\circ C$ .

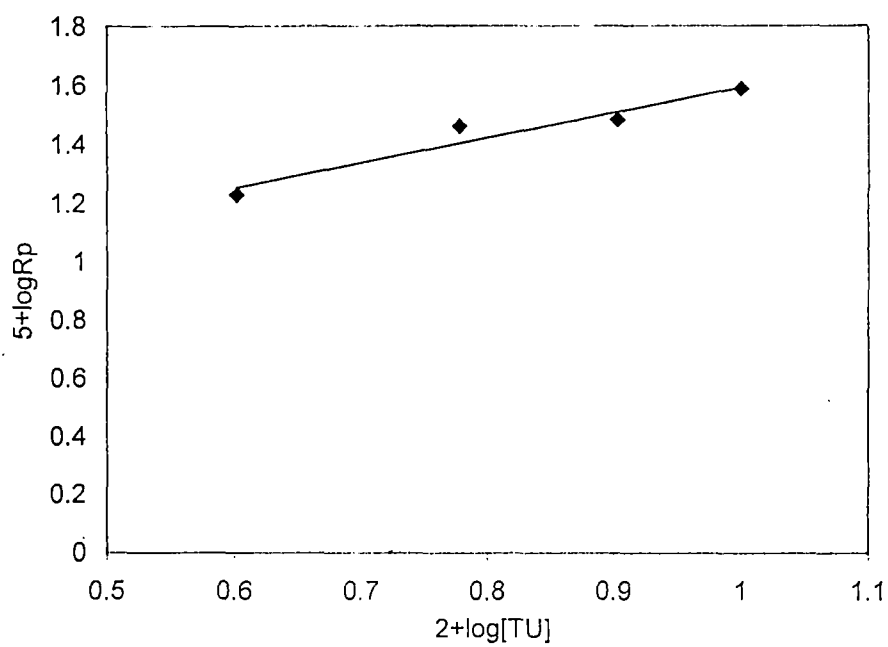


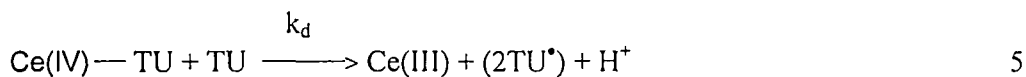
Figure:4.9:Logarithmic plot of  $R_p$  vs.  $[TU]$  for aqueous polymerization of AM with  $[AM]=0.4M$ ,  $[Ce(IV)]=1.50 \times 10^{-3}M$  at  $60^\circ C$ .

deviated from homogeneous polymerization reaction in which second order kinetics with respect to [TU] has been reported to follow.<sup>106</sup> Ce (IV)-TU is an effective initiator for the aqueous polymerization of acrylamide. The polymers formed by this system should carry with TU at the terminal. To rationalize the above findings and to predict the possible mechanism of the above polymerization reactions following assumptions are made.<sup>144</sup>

1. Intercalated TU reacts with Ce (IV) ions of the vermiculite layered spaces to form reactive isothiocarbamido primary radical via an intermediate complex. The decomposition of the complex is the rate-determining step.
2. In the constrained interlayer space of vermiculite the monomer molecules remains as pair either through hemi salt formation where two amide molecules share a proton by means of symmetrical hydrogen bond or /and through weak coordination to the exchanged cations.
3. Cage effect (which suggests that when the initiator decomposes into two radicals, there is a formation of a potential barrier by the surrounding solvent molecules which prevent their immediate recombination) is prominent in the vermiculite phase reactions in which the solvent molecules in the constrained space form a potential barrier such that reactive isothiocarbamido radical cannot diffuse out from the wall of the barrier and favors their recombination.
4. Since initiation of polymerization taken place in the interlayer space of vermiculite, the linear termination of growing polymer chain by Ce (IV) ions is restricted due to the presence of metal ions in the layered space.

Various steps of reactions are shown below:

Initiation :

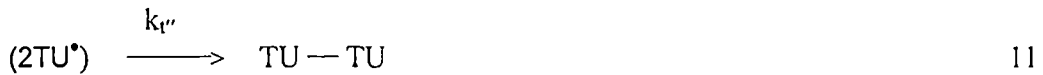




Propagation:



Termination:



$$-d/dt[Ce(IV)] = \{k_d K [Ce(IV)] [TU]^2\} / (1 + K [TU]) \quad 12$$

(Caged species are enclosed in brackets). Using the equation (4) and (5) the consumption rate of Ce (IV) concentration is given in equation 12. Now, assuming that the rate of formation of TU radicals is exactly equal to the rate of disappearing intercalated Ce (IV) ions, we obtain, (considering the steady state of TU radical).

$$\{k_d K [Ce(IV)] [TU]^2\} / (1 + K [TU]) = k_i K^1 [TU^\bullet] [M]^2 + \frac{k_t' [TU^\bullet] [Ce(IV)]}{1 + K [TU]} + k_t'' [TU^\bullet] \quad 13$$

( $K^1 = [M_2H^+] / [M]^2$ ) is the apparent protonation constant at a fixed pH ( or a formation constant)

$$[\text{TU}^\bullet] = \frac{k_d K [\text{Ce(IV)}] [\text{TU}]^2}{\{k_i K^1 [\text{M}]^2 + (k_r [\text{Ce(IV)}] + k_{tr}) / (1 + K [\text{TU}])\} \{1 + K [\text{TU}]\}} \quad 14$$

Again considering the steady state of  $M_n^\bullet$  radical

$$k_i K^1 [\text{TU}^\bullet] [\text{M}]^2 = k_t [M_n^\bullet]^2 \quad 15$$

$$[\text{TU}^\bullet] = (k_t [M_n^\bullet]^2) / (k_i K^1 [\text{M}]^2) \quad 16$$

Equating RHS of equation (14) and (16)

$$[M_n^\bullet]^2 = \frac{\{(k_i K^1 K k_d) [\text{Ce(IV)}] [\text{TU}]^2 [\text{M}]^2\}}{\{k_i (k_i K^1 [\text{M}]^2 + k_i K^1 K [\text{M}]^2 [\text{TU}] + k_r [\text{Ce(IV)}] + k_{tr} (1 + K [\text{TU}]))\}} \quad 17$$

$$[M_n^\bullet] = \frac{\{(k_i K^1 K k_d)^{1/2} [\text{Ce(IV)}]^{1/2} [\text{TU}] [\text{M}]\}}{k_t^{1/2} \{(k_i K^1 [\text{M}]^2 + k_i K^1 K [\text{M}]^2 [\text{TU}] + k_r [\text{Ce(IV)}] + k_{tr} (1 + K [\text{TU}]))^{1/2}} \quad 18$$

$$R_p = \frac{\{k_p (k_i K^1 K k_d)^{1/2} [\text{Ce(IV)}]^{1/2} [\text{TU}] [\text{M}]^2\}}{k_t^{1/2} \{(k_i K^1 [\text{M}]^2 + k_i K^1 K [\text{M}]^2 [\text{TU}] + k_r [\text{Ce(IV)}] + k_{tr} (1 + K [\text{TU}]))^{1/2}} \quad 19$$

$$R_p = k_p [M_n^*] [M] \quad 20$$

$$R_p = \frac{k_p \{(k_i K^1 K k_d)^{1/2} [Ce(IV)]^{1/2} [TU] [M]^2\}}{k_t^{1/2} \{k_i K^1 [M]^2 + k_i K^1 K [M]^2 [TU] + k_{t'} [Ce(IV)] + k_{t''} (1 + K [TU])\}^{1/2}} \quad 21$$

If the oxidative termination (step – 10) is assumed to be insignificant in comparison with the dimerization rate of caged radicals, equation (21) reduces to:

$$R_p = \frac{\{k_p (k_i K^1 K k_d)^{1/2} [Ce(IV)]^{1/2} [TU] [M]^2\}}{k_t^{1/2} \{k_i K^1 [M]^2 [TU] + k_i K^1 K [M]^2 + k_{t''} (1 + K [TU])\}^{1/2}} \quad 22$$

The interpretation of high kinetic order of the monomer finally hinges on the dominance of a reaction between caged radicals and those of monomers with the radical at the cage wall. Although the concentration of the monomer and TU in solution phase were fixed mostly at 0.40 mol. L<sup>-1</sup> and 0.04 mol. L<sup>-1</sup> respectively, the concentration of intercalated species must be much lower, specially due to the presence of water molecules in the interlayer spaces. Thus, the concentrations, [M] and [TU], in the vermiculite gel phase should be

$$[M] = L_0^a \theta_m = (L_0^a K_m^a [M]_s) / (1 + K_{TU}^a [TU]_s + K_m^a [M]_s) \quad 23$$

$$[TU] = L_0^a \theta_m = (L_0^a K_{TU}^a [TU]_s) / (1 + K_{TU}^a [TU]_s + K_m^a [M]_s) \quad 24$$

(subscript s denotes solution)

( $L_0^a$  and  $\theta$  are the total active sites in unit mass of vermiculite and the fraction of total sites occupied by such species respectively;  $K_m^a$  and  $K_{TU}^a$  are the selectivity coefficients).

The denominators of equations (23) and (24) are nearly unity. By appropriate substitution of  $[M]$  and  $[TU]$  in equation (22) and considering the dominance of the last term of the denominator over others, the equation becomes

$$R_p = \frac{k_p(k_d k_i K K^1 / k_t k_{t'})^{1/2} K_{TU}^a (K_m^a)^2 (L_0^a)^3 [Ce(IV)]^{1/2} [TU]_s [M]_s^2}{(1 + K L_0^a K_{TU}^a [TU]_s)^{1/2}} \quad 25$$

(Values of  $K_m^a$  (or  $K_{TU}^a$ ),  $L_0^a$  and  $K$  are of the order of  $10^{-2}$ ,  $2 \text{ m.mol.g}^{-1}$  and  $2 \text{ L.mol}^{-1}$  respectively <sup>107</sup>. Small values of above parameters including that of  $K^1$  ensure that terms involving quadratic and higher concentration terms are very small in the present conditions. <sup>108, 109</sup>

Further inspection of equation (25) shows that the value of  $K L_0^a K_{TU}^a [TU]_s$  in the denominator varies from  $10^{-5}$  to  $10^{-6}$  for the variation of aqueous TU concentration from 0.05 to 0.005  $\text{mol.L}^{-1}$ . This implies that the rate equation under the present condition is reduced to

$$R_p = k_p(k_d k_i K K^1 / k_t k_{t'})^{1/2} K_{TU}^a (K_m^a)^{1/2} (L_0^a)^3 [Ce(IV)]^{1/2} [TU]_s [M]_s^2 \quad 26$$

Reviewing the above result, it is found that equation (26) could satisfactorily account for the present behaviour of the Ce(IV)/TU initiated acrylamide polymerization exhibited in the aqueous vermiculite layered spaces.

## SECTION-B

# STUDIES ON COPOLYMERIZATION OF ACRYLAMIDE WITH N-tert BUTYL ACRYLAMIDE BY Fe (III)/TU REDOX COUPLE ON VERMICULITE SURFACE

### 4 B 1 INTRODUCTION AND REVIEW OF PREVIOUS WORKS

Copolymers of AM have shown a number of properties lending themselves to a variety of applications. Of growing importance are those related to use as water-soluble viscofier and displacement fluids in enhanced oil recovery.<sup>110-115</sup> Two of the critical limitations of polyelectrolyte are, however, loss of viscosity in the presence of mono or multivalent electrolytes and the ion binding to the porous reservoir rock substrates. Copolymers of AM and acrylate can be synthesized by several methods including those of solution<sup>116-117</sup> and emulsion<sup>118-121</sup> polymerizations. The physical properties of the polymers in some cases are independent of the method of preparation. The copolymers of AM with sodium acrylate in aqueous ammonium persulfate solution was conducted at 70°C for 60 minute producing a honey like copolymer which had molecular weight  $1.25 \times 10^6$  as reported by Soltez and co-workers.<sup>116</sup> Cationic free radical copolymers of AM with dimethylaminoethyl methacrylate and dimethylaminoethyl acrylate had been prepared by Baade and Hunkeler.<sup>117</sup> With azocyano valeric acid and  $K_2S_2O_8$  at 45°-60°C, Lafuma and Durand have found that during random copolymer formation of AM and quaternary ammonium acrylate monomer, the cleavage of the ester function occurred in mild alkaline medium with a simultaneous inter-chain reaction resulting in imide group formation.<sup>117</sup> Lavrov and co-workers reported that copolymerization of 2-hydroxy ethyl methacrylate with AM in aqueous solution in the presence of  $(NH_4)_2S_2O_8$  / ascorbic acid redox catalyst proceeded without the gel effect characteristic of bulk polymerization.<sup>119</sup> The reactivity ratio of the dimethylamino ethyl methacrylate methyl chloride salt with AM at 54°C was 1.54 and 0.30 respectively when redox azo compounds were used as catalyst.<sup>120</sup> The molecular weight of copolymers of auxin-containing monomers with AM was determined to be in the range of  $(5.5 - 18.0 \times 10^4)$  when a 4-pyrrolidinopyridine and dicyclohexyl carbodiimide catalysts were used.<sup>121</sup> For AM-sodium acrylate copolymer, prepared in aqueous solution at room

temperature and at pH 7.4 - 12.1, the reactivity ratios were 0.9 - 1.18 and 0.32 - 0.48 respectively.<sup>122</sup> McCormick and Salazar reported that the increasing randomness in the copolymers of AM with Na-3-acrylamido-3-methylbutanoate is observed if prepared in NaCl solution rather than in distilled water. The polyelectrolyte had inherent hydrogen bonding capacity and pseudo plasticity and exhibited large dimension in aqueous solution.<sup>125</sup> In inverse microemulsion polymerization of AM with methylacrylate initiated with AIBN by Viscera was a typical "dead-end" polymerization.<sup>128</sup> In inverse emulsion polymerization method, incorporation of high hydrophile-lyophile balance co-emulsifier in addition to oil-in-water type main emulsifier increased the rate of polymerization significantly. Srinivasula and co-workers investigated free radical copolymerization of AM with butylacrylamide or isopropyl methacrylate in the presence of AIBN in DMF at 60°C.<sup>129,130</sup> The chemical structure of random copolymers of AM with Na-2-sulfoethylmethacrylate in dextran were determined by McCormick in order to gain a more complete understanding of the structure property relations and performance under simulated field conditions encountered in enhanced oil recovery.<sup>131</sup> The synthesis and characterization of copolymers of AM with N-alkylacrylamide were investigated by McCormick and co-workers in aqueous solution utilizing Na-dodecylsulfate as a surfactant and  $K_2S_2O_8$  as the initiator.<sup>132</sup> A remarkable increase in apparent viscosity was observed at low mol fractions of N-alkylacrylamide in the copolymer at a critical concentration, which is a function of alkyl chain length in the monomer and copolymer molecular weight. The viscosity behaviour is interpreted in terms of a concentration dependent model involving interchain hydrophobic association in aqueous solution.<sup>132</sup> The copolymer microstructures and reactivity ratios of copolymers of AM with N- (1, 1-dimethyl-3-oxo-butyl) N- (n-propyl) acrylamide were studied by McCormick and Blackmon and the value of  $r_1r_2$  determined to be 2.20 (ref.133). The copolymer of AM with N- (1,1-dimethyl-3-oxo-butyl)- acrylamide yielded a  $r_1r_2$  value of 0.75 and the copolymer of AM with N, N-dimethyl acrylamide provided  $r_1r_2$  value of 0.86 as reported by McCormick and Chen.<sup>134</sup> Monoazeotropic and non-ideal copolymers were prepared during copolymerization of methylmethacrylate with AM, N-methylacrylamide and N, N-dimethylacrylamide in 1,4 dioxane solution at 65°C using AIBN as initiator.<sup>135</sup> Low molecular weight water-soluble copolymers of AM with itaconic acid; methacrylic acid and acrylic acid were prepared in the presence of  $K_2S_2O_8$  and thioglycerine by Sumi and co-workers.<sup>136</sup> Thomas had prepared granular copolymers of ethylacrylate and

acrylonitrile with dispersed bentonite when monomer and comonomer were dissolved in ethanol and heated under reflux condition with benzoyl peroxide for six hours.<sup>137</sup> Bhattacharya and coworkers studied the copolymerization of <sup>1</sup>H and <sup>13</sup>C NMR spectra of polyacrylamide with acrylonitrile and methacrylonitrile in the presence of HM/ TU redox couple.<sup>138</sup> Ktritskaya and Ponomarev studied the possibility for initiating AM and acrylic acid polymerization in acidic solutions in contact with metal surfaces of Mg and Al<sup>139</sup>. They observed the maximum rate of polymerization to be 2 wt% / min and established the occurrence of quadratic termination of growing chains. Rakshit and co-workers synthesized homopolymers and co-polymer of AM and acrylic acid by free radical solution polymerization technique.<sup>140</sup> Feed ratios of the monomers and acrylic acids were 85:15, 65:35, and 50:50(w/w) respectively. Hydrogen peroxide, potassium persulphate and benzoyl peroxide were used as initiators. The reactivity ratios of AM and acrylic acid are 0.427 and 0.945 respectively. Ebril and Uyan synthesized copolymers of itaconic acid and acrylamide.<sup>141</sup> Homopolymers of itaconic acid (IA) and its copolymers with acrylamide (IA-AM) were synthesized using either ceric ammonium nitrate (NH<sub>4</sub>)<sub>2</sub>Ce(NO<sub>3</sub>)<sub>6</sub> in combination with nitrilotriacetic acid (NTA) or potassium persulphate at pH 1 as initiators. The chain structures of the resulting products have been studied by FTIR spectroscopy. It is concluded from a comparison of spectroscopic results with gravimetric and viscometric data that the depressions in the yields and viscosity numbers in the case of Ce(IV)–NTA redox pair result from interactions between the constituents of the redox initiator and IA. Spectra of the insoluble and pale yellow precipitates, which are formed during the first 4 hrs of the reaction after the addition of Ce(IV) solution to the NTA and NTA–IA homogeneous solutions also indicate the presence of various oxidation products. Furthermore, it is observed that H-bonded homopolymer complex obtained from PAM–IA blends, prepared from aqueous solutions containing equal unit moles of each polymer, contain both ordered and defective structures. The graft copolymerization of methylmethacrylate (MMA) onto starch with potassium ditelluratocuprate(III) (DTC)/starch redox system as initiator was studied in alkaline medium by Yinghai and coworkers.<sup>142</sup> The grafting parameters have been determined as a function of temperature, ratio of monomer to starch, initiator concentration, and pH. The structure of the graft copolymers was confirmed by (FTIR), X-ray diffraction, and scanning electron microscope (SEM). It was found that the DTC-starch system is an efficient redox initiator for this graft

copolymerization. A reaction mechanism is proposed to explain the formation of radicals and the initiation. Kurenkov and coworkers studied the kinetics of copolymerization of acrylamide with magnesium-, calcium-, and strontium- 2-acrylamido-2-methylpropanesulfonates in aqueous solutions in the presence of potassium persulphate-sodium hydrosulfite initiating redox system at pH 9 and 50°C (ref. 143). Importance of the study lie in the fact that at least one of the above copolymers has already shown some promises by not losing its solution viscosities in the presence of added electrolytes.<sup>144,145</sup>

In the present work attempts have been made to prepare water soluble copolymers of AM with N-t-butyl acrylamide (N-t-BAM) on the vermiculite surface by interlayer trapped Fe (III) ions in the presence of TU. Objective of the present study is two fold. (1) To examine whether the copolymerization reaction could be initiated in the interlayer space of vermiculite with a different metal (viz., Fe(III)) / TU system. (2) To prepare copolymers with high molecular weight and large hydrodynamic volume. The success in copolymerization would result in relatively pure copolymer without subsequent solvent extractions. Moreover, the microenvironment of the clay mineral may control the structure and physico-chemical property of the copolymer. Present part of this chapter deals with the studies on copolymerization of AM with N-t-BAM and including microstructures and reactivity ratios of the copolymers.

## **4 B 2 RESULTS AND DISCUSSION**

High molecular weight water soluble copolymers of AM with N-t-butyl acrylamide are formed on the vermiculite surface by a redox initiating system involving trapped Fe (III) and TU in the interlayer space of the mineral. Intrinsic viscosities of copolymers are ranged from 123.43 to 259.40 mlg<sup>-1</sup>. The study of copolymerization involves the calculation of reactivity ratios of the monomers. Present investigation involves the copolymer of AM with n-tert BAM, which have been chosen because the position occupied by methyl group in the monomer is similar the vinyl carbon atom. The copolymerization reaction proceeds efficiently in presence of a surfactant, Triton X-100(R). The monomer conversion increases with decreasing AM :N -tert BAM ratios. FeV/TU initiating system also provides high conversion of the monomers (table 4.8).

## REACTIVITY RATIO

The variation in the feed ratio and the resultant copolymer composition (table-4.5) determined by elemental analysis were used to evaluate reactivity ratios for the AM-N-t BAM copolymer.

The Fineman-Ross and the Kelen-Tüdös method were used to determine the monomer reactivity ratios at low conversion polymerization condition.<sup>146,147</sup> The reactivity ratios  $r_1$  and  $r_2$  for the monomer pair  $M_1$  and  $M_2$  can be determined by

$$F \frac{(f-1)}{f} = r_1 \left( \frac{F^2}{f} \right) - r_2 \quad 27$$

where  $f = d(M_1) / d(M_2)$ ,  $F = (M_1) / (M_2)$ .

The reactivity ratios  $r_1$  is determined from the slope and  $r_2$  from the intercept in the Fineman-Ross plot. However, it is well known that in Fineman-Ross analysis, values of reactivity ratio are dependent on the indexing of the monomers.

The Kelen-Tüdös approach is used to determine the reactivity ratios for the same monomer pairs according to

$$v = r_1 \xi - r_2 (1 - \xi) / \alpha \quad 28$$

Where  $v = G / (\alpha + H)$  and  $\xi = H / (\alpha + H)$

The transformed variable G and H are given by

$$G = \frac{\{[M_1] / [M_2]\} \{d [M_1] / (d [M_2] - 1)\}}{d [M_1] / (d [M_2])} \quad 29$$

$$H = \frac{\{[M_1] / [M_2]\}^2}{d [M_1] / (d [M_2])} \quad 30$$

The parameter  $\alpha$  was calculated by taking the square root of the product of the lowest and the highest values of H for the copolymerization series. The values of  $r_1$  and  $r_2$  determined from Fineman-Ross (fig-4.10) and Kelen-Tüdös (fig-4.11) plot for the polymerization of AM with N-t-BAM on vermiculite surface are shown in table-4.6. The observed data indicate that the copolymerization follow the conventional

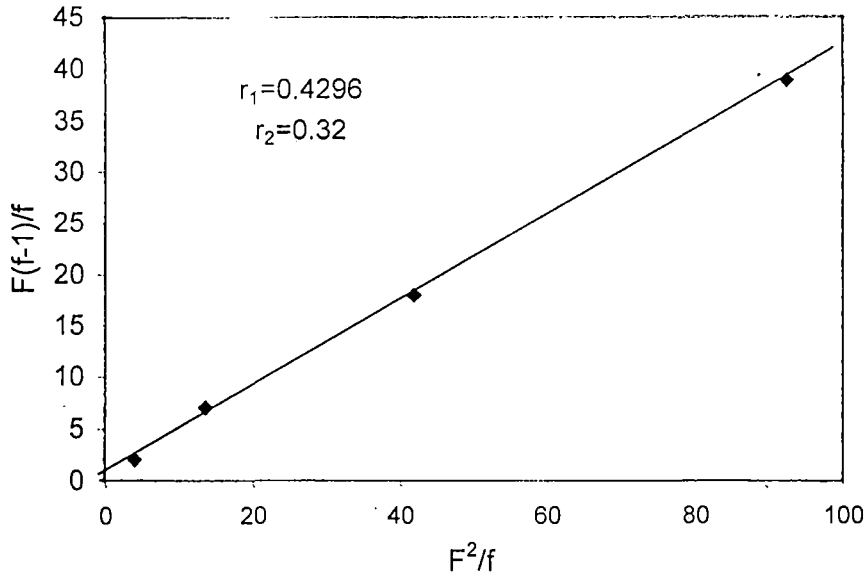


Figure 4.10: Determination of reactivity ratio for copolymerization of AM with N-t BAM by Fineman-Ross method.

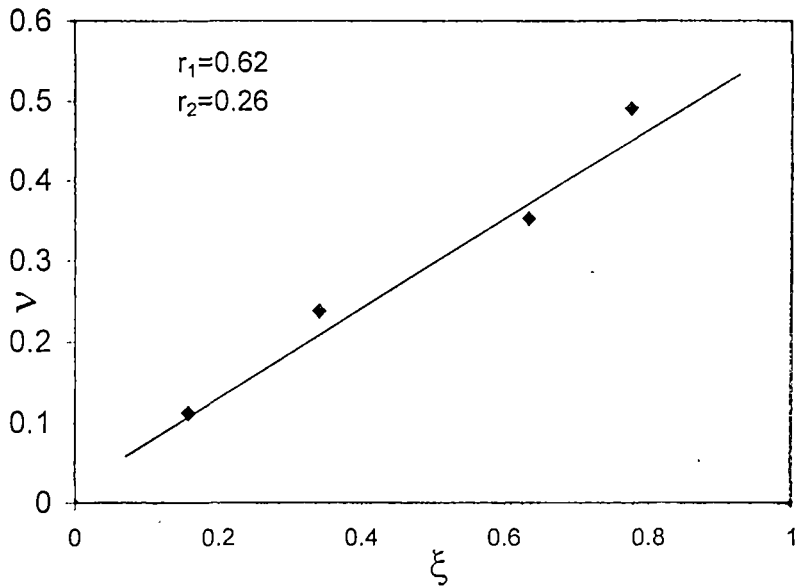


Figure 4.11: Determination of reactivity ratio for copolymerization of AM with N-t BAM by Kelen-Tüdös method.

copolymerization kinetics under a prerequisite that the reactivity of a polymer radical is only determined by the terminal monomer unit.<sup>38</sup>

**Table 4.5** Reaction parameters for the copolymerization of AM with varying amount of N-t-BAM in distilled water in presence of 0.04M TU and 0.1 % (w/v) FeV at 50°C (pH=1.98) in the presence of surfactant Triton X-100 (R).

[AM]mol. L <sup>-1</sup>	[N-t-BAM]mol. L <sup>-1</sup>	$\frac{[AM]}{[N-t-BAM]}$	Conversion (%) after 4.5 hrs.
0.40	0.01	41.0	58.1
0.40	0.02	20.0	69.1
0.40	0.03	13.3	66.4
0.40	0.04	10.0	57.2

**Table 4.6** Reactivity ratios for copolymerization of AM ( $r_1$ ) with N-t-BAM ( $r_2$ )  
<sup>a</sup> $M_1=AM, M_2=N-t-BAM$ ; <sup>b</sup> $M_1 = N-t-BAM, M_2 =AM$

Method	$r_1$	$r_2$
Fineman-Ross <sup>a</sup>	0.429±0.0	0.32 ± 0.0
Fineman-Ross <sup>b</sup>	1.56±0.01	0.44±0.01
Kelen-Tüdös	0.62 ± 0.0	0.26± 0.00

Values of  $r_1$  and  $r_2$  have been found to be 0.43 and 0.32 respectively for Fineman-Ross method and 0.62 and 0.26 for Kelen-Tüdös method. On reversing the indices of the monomer, the values of the reactivity ratios changes from 0.43 to 1.56 ( $r_1$ ) and 0.32 to 0.44 ( $r_2$ ). However, Bera and coworkers have found the value of  $r_1 = 1.50$  and  $r_2 = 0.46$  for AM-N-t-BAM copolymers obtained by free radical polymerizations using montmorillonite clay suspension.<sup>148</sup> (Considering Kelen-Tüdös method). Fig.4.12 shows the changes of co-polymer composition as a function of feed composition in which co-polymer compositions were determined from the experimentally determined reactivity ratios. The AM-DAAM co-polymers with  $r_1r_2 = 0.12$  and the AM-N-t BAM co-polymer with  $r_1r_2 = 0.16$  exhibit an opposite tendency towards alternation. Experimental points on the figures are, however, restricted up to 80 mole % of AM in the feed for AM-N-t BAM co-polymers because no copolymers were formed below that value.

## COPOLYMER MICROSTRUCTURE

The microstructures of the AM-*N*-t-BAM copolymer are expected to be important in determining the solution properties of copolymer. As mentioned earlier, the observed data follow the conventional copolymerization equation and the adherence of the data to this equation is an important point in establishing the validity of the statistical micro structural analysis. Thus the calculation of the statistical distribution of monomer sequence,  $M_1-M_1$ ,  $M_2-M_2$ , and  $M_1-M_2$  may be performed utilizing equation 31 to 33 (ref.150).

$$X = \frac{\phi_1 - 2\phi_1(1-\phi_1)}{\{1 + [(2\phi_1 - 1)^2 + 4r_1r_2\phi_1(1-\phi_1)]\}^{1/2}} \quad 31$$

$$Y = \frac{(1-\phi_1) - 2\phi_1(1-\phi_1)}{\{1 + [(2\phi_1 - 1)^2 + 4r_1r_2\phi_1(1-\phi_1)]\}^{1/2}} \quad 32$$

$$Z = \frac{4\phi_1(1-\phi_1)}{\{1 + [(2\phi_1 - 1)^2 + 4r_1r_2\phi_1(1-\phi_1)]\}^{1/2}} \quad 33$$

The mole fraction of  $M_1-M_1$ ,  $M_2-M_2$ , and  $M_1-M_2$  sequences in the copolymer are designated by X, Y and Z respectively.  $\phi_1$  represents the mole fraction of  $M_1$  in the copolymer, and  $r_1$  and  $r_2$  are the reactivity ratios for the monomer pairs. Mean square lengths,  $\mu_1$  and  $\mu_2$ , can be calculated utilizing equation (34) and (35)<sup>150</sup>

$$\mu_1 = 1 + r_1 \cdot [M_1] / [M_2] \quad 34$$

$$\mu_2 = 1 + r_2 \cdot [M_2] / [M_1] \quad 35$$

The structural data for the co-polymers of AM-*N*-t-BAM are presented in table 4.7 (Kelen-Tüdös values of reactivity ratios were used for the calculation). For the AM-*N*-t-BAM co-polymers  $\mu_{AM}$  vary between 18.61 and 2.83 at molar ratio of 94.79/5.21 to 81.99/18.01 respectively. For those molar ratio compositions the values of  $\mu_{N-t-BAM}$  were 1.01 and 1.075 respectively.

## EFFECT OF FEED COMPOSITION

The effects of feed composition on molecular weight (viscosity average) were studied for AM - *N*-t-BAM co-polymer shown in table-4.8. Figure 4.13 illustrates the effects of feed composition on the intrinsic viscosity for each copolymer series. It is interesting to note that in a copolymerization involving acrylamide, the molecular weight gradually decreases with increasing monomer content and this may be

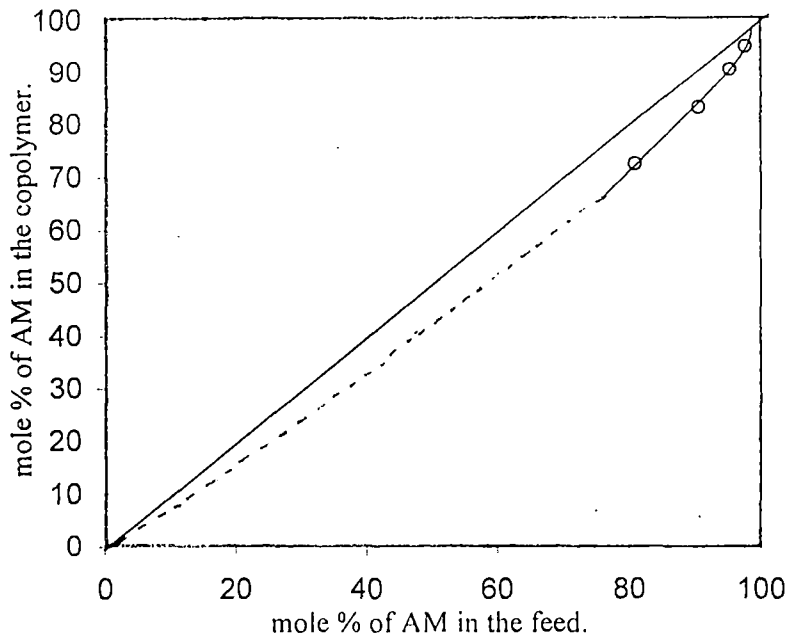


Figure 4.12: Copolymer composition as a function of feed composition for copolymerization of AM with N-t-BAM.

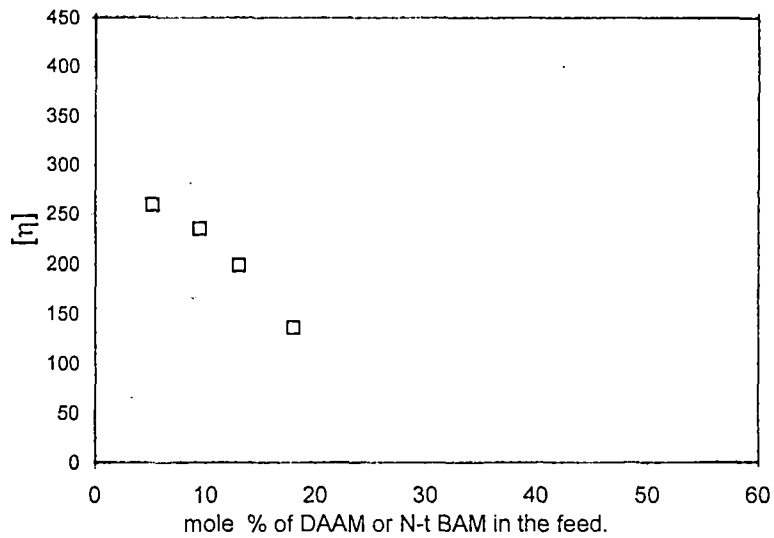


Figure 4.13 :Effect of feed composition on the intrinsic viscosity of AM-N-tBAM copolymer.

explained by the increased cross-termination rates in copolymerization as compared to the very slow rate of termination observed for homopolymerization.

**Table 4.7 Structural data for the copolymers of AM with N-t-BAM. A = AM, B = N-t-BAM.**

Sample number	Composition (mole %)		Blockiness (mole %)		Alternation (mole %) A-B	Mean sequence length		$\mu_A/\mu_B$
	A	B	A-A	B-B		$\mu_A$	$\mu_B$	
10-1	94.79	5.21	89.62	0.04	10.34	18.61	1.010	18.42
20-1	90.53	9.47	81.21	0.15	18.64	9.59	1.016	9.44
30-1	89.00	13.0	74.29	0.31	25.40	5.08	1.034	4.91
40-1	81.99	18.01	64.62	0.65	34.73	2.83	1.075	2.63
10-2	96.23	3.77	92.48	0.02	07.50	18.61	1.010	18.42
20-2	92.37	7.63	84.83	0.10	15.07	9.59	1.016	9.44
30-2	90.13	9.87	80.42	0.16	19.42	5.08	1.034	4.91
40-2	83.46	16.54	67.44	0.53	32.03	2.83	1.075	2.63
10-3	94.29	5.71	88.63	0.05	11.32	18.61	1.010	18.42
20-3	93.71	6.29	87.48	0.06	12.46	9.59	1.016	9.44
30-3	86.14	13.86	72.62	0.35	27.03	5.08	1.034	4.91
40-3	82.56	17.44	65.71	0.60	33.69	2.83	1.075	2.63

**Table 4.8** Reaction parameters for the copolymerization of AM with N-t-BAM at 50°C in aqueous vermiculite microenvironment. (Total monomer concentration 0.42 M).

Monomer conc. in the feed			Time (min)	Conversion (%)	Elemental analysis(Wt %)		Mol% of N-t-BAM	$[\eta]_{\text{ml g}^{-1}}$
[AM]	[N-tBAM]	[AM]/[NtBAM]			C	N		
0.41	0.01	41	90	17.51	43.42	15.79	5.21±0.01	
0.41	0.01	41	150	38.02	42.89	15.88	3.77±0.02	259.4
0.41	0.01	41	210	68.62	43.36	15.67	5.70±0.05	
0.40	0.02	20	90	27.10	43.56	15.04	9.47±0.07	
0.40	0.02	20	150	31.90	43.97	15.52	7.63±0.04	249.04
0.40	0.02	20	210	64.82	43.01	15.43	6.30±0.03	
0.38	0.04	9.5	90	38.45	45.47	15.07	13.0±0.08	
0.38	0.04	9.5	150	61.48	43.97	15.11	9.87±0.0	198.76
0.38	0.04	9.5	210	62.45	45.55	14.96	13.80±0.1	
0.34	0.08	4.25	90	20.00	45.73	14.34	18.01±0.90	
0.34	0.08	4.25	150	29.00	45.07	14.36	16.54±0.10	123.43
0.34	0.08	4.25	210	38.00	45.45	14.34	17.44±0.15	

## SECTION – C

### GENERAL DISCUSSION

The adsorption isotherm for Ce (IV) ion adsorption onto vermiculite exhibit L-type nature, which suggests strong sorbate-sorbent interaction. The maximum saturation corresponds to 0.97 meq/g of the mineral. Figure 4.14 shows that the AM molecules readily adsorbed from the aqueous solution onto the surface of the mineral. Two plateau regions indicating two-stage intercalation of amide molecules characterize the isotherm. The first saturation value is nearly 1.80 mmol/g whereas second one is close to double of the first saturation value. Unlike AM, TU leads to the monolayer formation (adsorption isotherm shown in figure 4.15) only and the maximum capacity is found to be 1.50 mmol/g, which is consistent with that of the monolayer of the AM. Tables 4.9-4.10 give an idea about the strength of intercalation of AM and TU molecules in both HV and CeV interlayer spaces respectively. The distribution coefficient ( $K_D$ ) values are low and of the order of  $10^{-2}$  in the concentration range of AM and TU used for polymerization experiments. The distribution coefficients have been calculated according to the relation:

$$K_D = m_{i(s)} / m_{i(l)} \quad 36$$

Where  $m_{i(s)}$  and  $m_{i(l)}$  are the concentrations of the species in the solid and liquid phase respectively.

As is expected from their nature, the adsorption isotherms do not obey the Langmuir relation:

$$c/(x/m) = 1/K_L (x/m)_{\max} + c/(x/m)_{\max} \quad 37$$

Where,  $c$  = equilibrium concentration of the adsorbate,  $X/m$  = moles adsorbed per gm of adsorbent,  $K_L$  = Langmuir constant. The plots of  $c/(x/m)$  vs.  $c$  are not linear over a range of adsorbate concentrations. However, from the slopes and intercepts of the average line drawn through the points over the concentration of the adsorbate give a rough idea of the  $K_L$  values and which are low. In general, the  $R_p$ 's are somewhat lower in presence of vermiculite than those observed in homogeneous polymerization maintaining the polymer yield ( $X_L$ ) almost same. The interlayer expansion and collapse of vermiculite layers are influenced by the nature of the exchangeable cation as well as by the interlayer liquid.

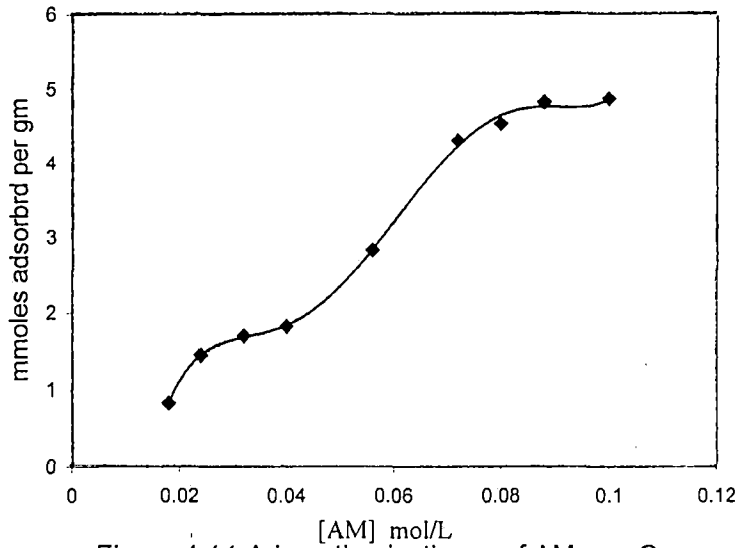


Figure:4.14: Adsorption isotherm of AM on Ce-Vermiculite.

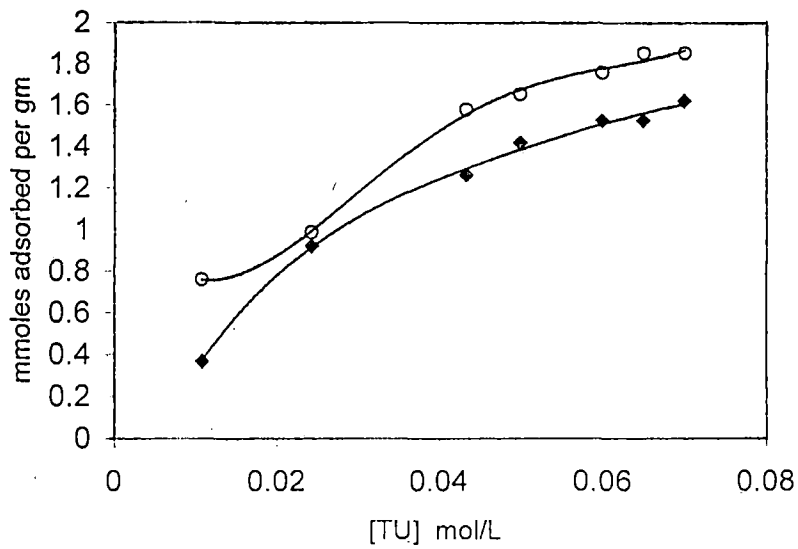


Figure:4.15: Adsorption isotherm of TU on CeV and HV.  
 ♦ CeV ○ HV.

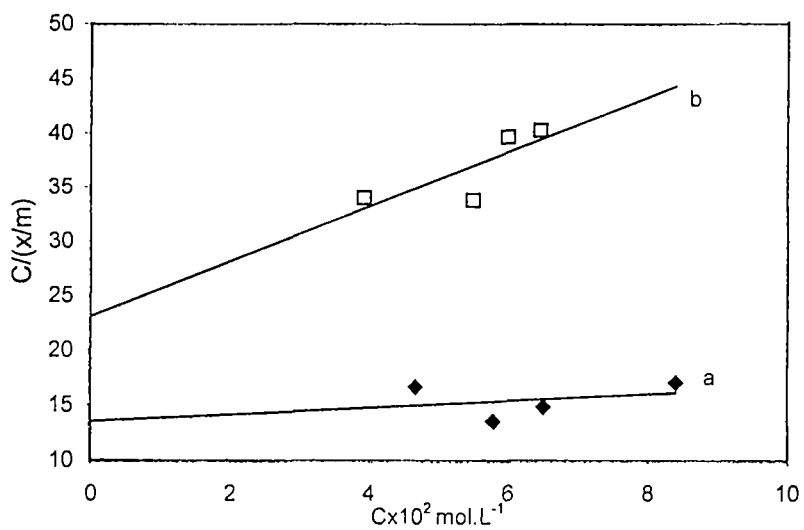


Figure:4.16. Langmuir plots of CeV-AM(a) and CeV-TU (b)systems

**Table 4.9 Intercalation of acrylamide molecules in Cerric-vermiculite (CeV) interlayer spaces.**

Mineral %	Conc. of added AM (mol.L <sup>-1</sup> ) X10 <sup>-2</sup>	Conc. of adsorbed AM (mol.L <sup>-1</sup> ) X10 <sup>-3</sup>	Conc. of free AM (mol.L <sup>-1</sup> ) X10 <sup>-2</sup>	Distribution Coefficient (K <sub>D</sub> )
CeV 0.328	10.00	15.93	8.40	0.19
	8.80	15.80	7.21	0.22
	8.00	14.48	6.51	0.23
	7.20	14.09	5.79	0.24
	5.60	9.27	4.67	0.20
	4.00	5.96	3.40	0.17
	3.20	5.67	2.63	0.21
	2.40	4.75	1.92	0.25
	1.80	2.72	1.53	0.18

Low charge vermiculite may have interlayer expansion characteristic, which bear closer resemblance to those of high charge montmorillonite than to those shown by other vermiculite of high charge. Moreover, its ability to form complexes with organic compounds bears a striking resemblance to that of montmorillonite. Basal spacing measurement from X-ray diffractogram of unoriented powder sample of hydrogen-montmorillonite, TU treated Fe (III)-montmorillonite and Fe (III)-montmorillonite-PAM adduct before and after glycerol treatment show the existence of intercalated PAM in the layered spaces of the mineral. However, intercalation of TU and Fe (III) do not expand the basal spacing of the mineral.<sup>144</sup> Using infrared spectroscopy, Tahaun and Morland have confirmed that amides predominantly protonate on the oxygen atom in the acidic clay system.<sup>151</sup> Comparing the results of adsorption on the surfaces of montmorillonite and vermiculite minerals it may be argued that like montmorillonite phase the bilayer adsorption of acrylamide in the internal surface of the vermiculite also play a pivotal role in affecting the initiation of polymerization and its mechanism as compared to the homogeneous polymerization reaction. In acidic medium, amides may apriori accept a proton on either the oxygen or the nitrogen atom. Spectroscopic as well as solution studies, however, support the possibility of coming about of the former alternative.<sup>152</sup>

**Table 4.10 Intercalation of thiourea molecules in Cerric-vermiculite (CeV) and hydrogen-vermiculite (HV) interlayer spaces.**

Mineral %	Conc. of added TU (mol.L <sup>-1</sup> ) X10 <sup>-2</sup>	Conc. of adsorbed TU(mol.L <sup>-1</sup> ) X10 <sup>-3</sup>	Conc. of free TU (mol.L <sup>-1</sup> ) X10 <sup>-2</sup>	Distribution Coefficient (K <sub>D</sub> )
CeV 0.328%	7.00	5.30	6.47	0.08
	6.50	4.98	6.00	0.08
	6.00	4.98	5.50	0.09
	5.00	4.64	4.53	0.10
	4.34	4.13	3.93	0.10
	2.43	3.02	2.13	0.14
	1.08	1.20	9.60	0.12
HV 0.33%	7.00	6.10	6.39	0.09
	6.50	6.10	5.89	0.10
	6.00	5.80	5.42	0.10
	5.00	5.44	4.45	0.12
	4.34	5.19	3.82	0.13
	2.43	3.26	2.10	0.15
	1.08	2.50	0.83	0.30

Linear termination of aqueous acrylamide polymerization by metal ions was observed long back<sup>150</sup>. While the linear termination by metal ions is a very common phenomenon in solution phase reaction, it is not possible in presence of clay mineral and transfer to Ce (IV) ion is almost controlled in the case of reaction in the layered spaces. Thus it is evident that the modification achieved with respect to kinetics and mechanism of the acrylamide polymerization in the vermiculite phase stems from a number of factors viz.,

1. instead of collision between a monomer molecule and an initiating radical, a monomer pair is involved in the initiating step
2. 'cage effect' is prominent in vermiculite phase reaction where a pair of TU radicals form a potential barrier to hinder diffusion of the radicals and favors their recombination

3. rate of linear termination process decreases significantly because transfer to Ce(IV) ions is highly restricted for the latter's location in the layered spaces of the mineral and diffusion of the living radical through vermiculite gel is rather slow. In general, loading of the oxidant, i.e. metal ions, of the redox couple in the interlayer space of clay minerals offers a potential method of achieving very high degree of polymerization for a redox initiating acrylamide polymerization reaction.

#### 4 D REFERENCES

1. B.K.G. Theng, Clay-polymer Interactions: summary and perspectives, *Clay and Clay minerals*, 30, (1982).
2. J. Bhattacharya, S. K. Chakroborty, S. Talapatra, S.K. Saha and S.C. Guhaniyogi, *J. Polym. Sc., Part A, Polymer Chemistry*, 28, 2249(1990).
3. G.S. Misra, U.D.N. Bajpai and J. Trekoval, *J. Rev. Macromol. Chem. Phys. C* 24(3), 335(1984).
4. M. Fanood, H. Rafi'ee; George and H. Maurice *Polymer*, 29(1), 134(1988).
5. M. Fanood, H. Rafi'ee; George and H. Maurice, *Polymer*, 29(1), 128(1988).
6. T. Ishige and A.E. Hamielec, *J. Appl. Polym. Sci.*, 17(5), 1479 (1973).
7. M. Lazar and J. Rychly *J. Pavlinec., Chem. Zvesti.*, 30(3), 318 (1976).
8. U.C. Singh, S.P. Manickam and K. Venkatarao. *Makromol. Chem.*, 180. 589 (1979).
9. P. Ghanasundaram and H. Kothandaraman, *Polym. J.* 11 (1), 261(1979).
10. T. Miyagawa, T. Nakata and M. Tanaka, *Jpn. Kohai Tokkyo Koho.*79, 133, 583, 17 Oct. 1979, April. 78/41, 568, 08 Apr. 1978, 7 pp.
11. S. Sarasvathy and K. Venkatao, *Curr. Sci.*, 49, 702 (1980).
12. K. Kaliyamurthy, P. Elayaperumal, T. Balakrishnan and M. Santappa, *Polym J. (Tokyo)*, 14, 107 (1982).
13. S. Lenka, P. L. Nayak, S. B. Dash and S. Ray, *Colloid Polym. Sci.*, 261, 40 (1983).
14. A. Kaim, *J. Polym. Sci., Polym. Lett. Ed.*, 22, 203(1984).

15. A. Copalan, S. Paulrajan, S. Vaidyanathan, K. Venkatarao and N.R. Subbaratham, *Eur. Polym. J.*, **20**, 971 (1984).
16. T. Balakrishnan and E. K. Kasilingam, *J.Ind.Chem.Soc.***60**, 1186(1983).
17. J. Barton and V. Juranicova, V. Vaskova, *Macromol.Chem.***186**, 1935(1985).
18. W. Xuanchi and Y. Peng, *Gaofenzi Tongxun*, **6**,499(1984).
19. S. Misra and G. Sahu, *J. Polym. Sci., Polym. Chem. Ed.*, **23**,2647(1985).
20. A.V. Pantar and M.V.R. Rao, *Makromol Chem., Rapid commun.*,**7**,77(1986).
21. M. Cvetkovska and T. Greev, *Hem.Ind.***41**, 188(1987).
22. L.G. Revel'skya and V.I. Kuryankina, *Vyosomol. Soedin. Ser. A.* **29**, 1086 (1987).
23. V. Vaskova, D. Oremusova and J. Barton, *Makromol. Chem.*, **189**, 709 (1988).
24. Y. Liu, X. Song, H. Shi and L. Xu, *Gaodeng Xuexiao Huaxue Xuebao* **11**, 328 (1990).
25. D. Hundeler and A. E. Hamielec. *Polym. Prep.. (Am. Chem. Soc. Div. Polym. Chem.)* **30**(2), 346(1989).
26. Y. Lui, X. Song, H. Shi and Lili Xu, *Huaxue Shijie* **31**,159(1990).
27. R. Vasishtha and A.K. Srivastava, *J. Polym. Sci., Part A: Polym. Chem.* **28**, 1297 (1990).
28. M. Takahashi, *Nippon Kagaku Kaishi*, **12**,2070(1989).
29. L.L. Stupen'kova, T.A. Baiburdiv, V.F. Gromov and E.N. Teleshov, *Vysokomol. Soedin, Ser. A.*, **33**, 1498 (1991).
30. D. Hunkeler, *Macromolecules*, **24**, 2160 (1991).
31. V. A. Bhanu and K. Kishore, *J. Polym. Sci. Part A; Polym. Chem.*, **28**, 3617 (1990).
32. S.K. Ghosh, M. Nazimuddin, S.N. Bhattacharya and B.N. Mandal, *Polym. Sci. Symp. Proc. polym.* **1**,199 (1991).
33. V.F. Kurenkov, E.V. Nurullina and V.A. Mgagchenkov, *Izv. Vyash. Uchebn zaved, Khim.Khim.Tekno.***132**, 96(1989).

34. G.S. Misra and J.J. Rabello, *Makromol. Chem.*, **177**, 21(1976).
35. M.M. Husain A. Gupta and S. Misra, *Makromol. Chem.*, **176**, 2861(1975).
36. G.S. Misra and U.D.N. Bajpai, *J. Macromol. Sci. Chem.*, **13**, 1135(1979).
37. U.D.N. Bajpai and G.S. Misra, *Vysokomol. Soedin, Ser., A*, **21**, 1720(1979).
38. G.S. Misra and S.N. Bhattacharya, *J. Macromol. Sci. Chem. A*, **14**, 907(1980).
39. U.D.N. Bajpai and A.K. Bajpai, *J. Macromol. Sci. Chem. A*, **19**, 487(1983).
40. U.D.N. Bajpai and A.K. Bajpai, *J. Polym. Sci. Polym. Chem. Ed.*, **22**, 1803 (1984).
41. U.D.N. Bajpai and A.K. Bajpai, *Macromolecules*, **18**(11), 2113 (1985).
42. K.C. Gupta, M. Verma and K. Behari, *Macromolecules*, **19**, 548(1986).
43. K. Behari, K.C. Gupta and M. Verma, *Vysokomol. Soedin, Ser., A.*, **28**, 1781 (1986).
44. K. Behari, K.C. Gupta, G.D. Raja and P. Das, *Acta. Polym.*, **42**, 206(1991).
45. U.D.N. Bajpai and A. Ahi, *J. Apl. Polym. Sci.* **40**, 359(1990).
46. U.D.N. Bajpai and G.S. Misra, *Vysokomol. Soedin, Ser. B.*, **21**, 419(1979).
47. S.P. Rout, A. Rout, N. Mallick and B.C. Singh, *Macromol Chem.*, **178**, 1971 (1977).
48. M. Husain and A. Gupta, *J. Macromol. Sci. Chem.*, **All**, 2177(1977).
49. G.S. Misra and G.P. Dubey, *Polym. Bull.* **1**, 671(1979).
50. G.S. Misra and S.N. Bhattacharya, *Colloid Polym. Sci.*, **258**, 954(1980).
51. G.S. Misra and G.P. Dubey, *J. Macromol. Sci. Chem. A* **16**, 610(1981).
52. D. Pramanik and K. Das, *Ind. J. Phys. Nat. Sci.* **1**, 8(1981).
53. G.S. Misra and S.N. Bhattacharya, *J. Polym. Sci. Polym. Chem. Ed.* **20**, 131 (1982).
54. G.S. Misra, P.S. Bassi and S.L. Abrai, *Ind. J. Chem. Soc. A*, **22A**, 286(1983).
55. G.S. Misra and J.I. Khatil, *J. Polym. Sci. Polym. Chem. Ed.*, **21**, 1665(1983).
56. G.S. Misra and A.K. Bajpai, *J. Macromol. Sci. Chem. A* **19**, 487(1983).

57. D. Pramanik and B. Chakraborty, *Bull.Pure.Appl.Sci.Soc.C.2*, 1(1983).
58. K.C. Gupta and K. Behari, *J. Polym. Sci. Part A: Polym Chem.*, **24**,764(1986).
59. A.S. Savac, A. Gocmen and B. Basaran, *J.Soln.Chem.*, **19**,901(1990).
60. K. Qiu, Q.W. Wang and Y. Yang and X. Feng, *Chin.Sci.Bull.*, **34**,1348(1989).
61. W. Wang, Y. Sun, Ye. Song, Kuryan Qiu and Zinde Feng, *Gaofenzi Xuebao.*, **2**, 213 (1990).
62. K. Qui, W. Wang, W. Guo, D. Zhang and X. Feng, *Gaofenzi Xueba.*, **4**,496(1990).
63. K. Qiu and W. Wang, *Gaofenzi Xuebao.*, **3**,355(1989).
64. B. Dincer, S. Bayulken and A.S. Sarac., *J. Appl. Polym. Sci.*, **63**, 12, 1643 (1997).
65. P. Bera and S.K. Saha, *Macromol. Rapid Commun.* **18**, 261(1997).
66. X., Guo, K. Qiu, X. Feng, *Chin.J.Polym.Sci.*, **7**, 165(1989).
67. X., Guo, K.Qiu and X. Feng, *Makromol. Chem.*, **191**, 577(1990).
68. G.P. Patapov M.I. Alieva, Izu, Vyash. Vchebn. Zaved. *Khim. Khim. Tekhnal.*, **34**, 107 (1991).
69. G. Maihot and M. Bolte, *Polyhedron.*, **10**,237(1991).
70. K. Qiu, Y. Yang and X. Feng, *Gaofenzi Xuebao.* **5**, 593(1989).
71. V.F. Kurenkov, T.A. Baiburdiv and L.L. Stupen'kova, *Zh. Prikl. Khim*, **60**, 2311 (1987).
72. V.F. Kurenkov, M.N. Tritonova and V.A. Myagchenkov. *Eur. Polym.J.* **23**, 685(1987).
73. V.F. Kurenkov, T.A. Baiburdiv and L.L. Stupen'kova, *Vyskomol.Soedin, Ser. A.* **29**, 348 (1987).
74. R.M Akopyan, A.M. Kaifadzhyan and N.M. Beileryan, *Arm. Khim. Zh.* **39**, 471 (1986).
75. V.F.kurenkov, T.V. Baiburdiv, L.L. Stupenkova, *Zh. Prikl .Khim.* **60**,2311(1987).

76. X. Guo, K. Qui and X. Feng, *Gaodeng Xuexiao Huaxue Xuelao*, **10**, 1068 (1989).
77. C.Y. Chen and J.F. Kuo, *J. Polym. Sci., Part A: Polym. Chem.*, **26**, 1115 (1988).
78. R.A. Smith, U.S.4, 617,359, 14 Oct. 1986,US Appl. 649, 622,12Sep. 1984. 10pp. Cont in-Part of US Ser No.622 abandoned.
79. X. Wu and J. He, *Gaofenzi Tongxun* **6**,402(1986).
80. T. Balakrishnan and S. Sabbu, *J. Polym. Sci., Part A : Polym. Chem.*, **24**, 2771 (1986).
81. C.Y. Chen and J.F. Kuo, Ch'eng-Kung Ta Hsueh Pao, K'ochi, I. Hsueh Pian, **20**, 193 (1985).
82. T. Grcev and M. Cvetkovska, al-Dabas, Imad. *J. Serb. Chem. Soc.*, **51**, 15 (1986).
83. A.S. Sarac, E. Erbil, A.B. Soydan , *J. Appl. Polym. Sc.*, **47**, 1643 (1993).
84. C. Volga, B. Hazer and O. Torul, *Euro. Polym.J.***33**, 907(1997).
85. A. Gopalan, S. Paulrajan, S. Vaidyanathan, K. Venkatarao and N.R. Subbaratnam, *Eur. Polym.J.*,**20**,971(1984).
86. S. Lenka, P.L. Nayak and S. Roy, *J. Polym. Sci. Polym. Chem. Ed.*, **22**, 959 (1984).
87. M. Cvetkovska, T. Grcev and G. Petrov, *Macromol. Chem.* **185**,429(1984).
88. C. Namasivayam, P. Natarajan, Proc. I.U.P.A.C., Macromol. Symp. 28<sup>th</sup> 1982, 181, Int. Union. Pure Appl. Chem., Oxford, U.K.
89. T.A. Kay, F. Rodriguez, Proc. I.U.P.A.C., Macromol. Symp.28<sup>th</sup> 1982, 77, Int. Union. Pure Appl. Chem., Oxford, U.K.
90. D.V.P.R. Varaprasad and V. Madadevan, *J. Macromol. Sci.,Chem.* **A18**,1429(1982).
91. P. Elayaperumal, T. Balakrishnan, M .Santappa and R. W. Lenz,*J Polym. Sci.,Polym: Chem. Ed.* **20**, 3325(1982).
92. D.V.P.R. Varaprasad and V. Madadevan, *Eur.Polym.J.***17**, 1185(1981).

93. N. Nosa, R.G. Lopez, E.A. Zaragoza, R.D. Peralta, I. Katime, F. Bercea, E. Mendizabal, and J.E.Puig, *Macromolecules*, **33**,2848(2000).
94. G.S. Sur, S.K. Choi, *J. Macromol. Sci.Chem.***A15**,671,(1981).
95. M. Haragopal, A. Jayakrishnan and V. Mahadevan, *Makromol. Chem.*, **183**, 657 (1982).
96. P. Ganasundaram and H. Kothandaraman, *Eur. Polym. J.***15**,399(1979).
97. G.S. Sur, *Yongu Pogoyongnam Taehakkyo Kongop Kishi Yonguso*, **7**, 43 (1979).
98. M.M. Husain, S.N. Misra and R.D. Singh, *Makromol. Chem.*,**179**,295(1978).
99. D.Z. Chshmarityan and N.M. Beileryan, *Arm. Khim. Zh.*,**30**,120(1977).
100. Wrzyszczyński A , *J.Macromol. Sci.*,**38**(3), 281(2001).
101. L. Yinghai, Y. Lanying, L. Junbo, S. Zengqian, D.Kuilin CJI, **5**,96,(2003).
102. W. Bodenheimer, L. rodriguez, *J.Polym. Sci.,Part A1*, 3151(1967)
103. J.J. Fripiat, *Trans. 9<sup>th</sup> Intern. Cong. Soil. Sci. Adelaide*, **1**,691 (1968).
104. B.M. Mandal, U.S. Nandi and S.R. Palit, *J. Polym. Sci.* **A1 8**, 67 (1970).
105. C.W. Hsu, J.F. Kuo and C.Y. Chen, *J. Polym. Sci. Part A : Polym Chem.* **31**, 267 (1993).
106. P. Bera, S.K.Saha, *Ind.J.Chem.Technol.***6**,24(1999).
107. N. Pustelnik and R.Soloniewiez,*Chem.Anal.(Warsaw)*,**21**,503(1976.)
108. D.D. Perrin, *Organic Ligands : IUPAC Chemical Data Series (No.22)*, Pergamon Press, New York (1983).
109. A.E. Martel and R.M. Smith, 'Critical Stability Constant (vol. 3)', New York, (1979).
110. A.L. Barnes, *J. Pet. Tech.* 1147 (October 1962).
111. D.J. Pye, *J. Pet. Tech.* 911(August 1964).
112. H.L. Chang, *J. Pet. Tech.* 1113(August 1978).
113. N.J. Bikales, Ed., 'Water Soluble Polymers Plenum', New York,105-126 (1973).

114. C.L. McCormick, Symposium on Polymeric materials for Basic Energy Needs, Case Western Reserve, 13 (1978).
115. M. T. Szabo, *J.Pet.Tech.* 553 (May 1979).
116. L. Soltesz, K. Rajnai, M. Gerzson, G. Halas, J. Balogh, M. Vraga, Z. Ferninand and J. Ratkovszky et al. Ger. Offer. DE 3,801, 736,27 July 1989, April, Appl. 21 Jan. 1988.
117. W. Baade, D. Hunkeler and A.E. Hamielec, *J.Appl.Polym.Sci.***38** (1), (1989).
118. F. Lafuma and G. Durand, *Polym. Bull.*, **21**(3), 315(1989).
119. N.A. Lavrov, N.F. Nikolaev and A.K. Kuzmina, *Zh. Prikl. Khim*, **62** (20), 429 (1989).
120. X. Yang, H. Yu and Y. Bao, *Shiyan Huagong*, **17**(1), 21(1988).
121. C.L. McCormick and K. Khim, *J. Controlled Release*, **7**(2),101(1988).
122. H. Xu, X. Zhang W. Liu, F. Yanjiu Y. Fushe and G. Xuebao, **3** (3),19(1985).
123. W. Baade, D. Hunkeler and A.E. Hamielec, *Polym. Mater. Sc. Eng.* **57**, 850 (1987).
124. C.L. McCormick and L.C. Salazar, *Polym.Sci.Eng.***57**, 859(1987).
125. C.L. McCormick and G.S. Chen, *J. Polym. Sci. Polym. Chem. Ed.* **20** (3), 817 (1982).
126. Yu. P. Chernenkova, E.N. Zil'berman and G.N. Shvareva, *Vysokomol Soedin, Ser. B.*, **24** (2) 119 (1982).
127. M. Georgieva and E. Georgieva, *Angew Makromol.Chem.*, **66**, 1(1978).
128. V. Vaskova, V. Juranicova and J. Barton, *Makromol. Chem.* **192** (4), 989 (1991).
129. B. Srinivasula, P.R. Rao, E.V. Sundaram, *Angew Makromol. Chem.*, **189**, 97 (1991).
130. B. Srinivasula, P.R. Rao, E.V. Sundaram M. Srinivas and L. Sirdeshmukh, *Eur. Polym. J.* **27** (9), 979 (1991).
131. C.L. McCormick, L.S. Park, G.S. Chen and H.H. Neidlinger, *Polym. Prep.* **22** (1), 138 (1981).

132. C.L. McCormick, T. Nonaka and C.V. Johnson, *Polymer*, **29**(4), 731(1988).
133. C.L. McCormick and K.P. Blackmon, *Angew Makromol. Chem.* **144**, 73(1986).
134. C.L. McCormick and G.S. Chen, *J. Polym. Sci. Polym. Chem. Ed.* **22**(12), 3633 (1984).
135. M. Orbay, R. Laible and L. Dulong, *Makromol. Chem.* **183** (1), 47(1982).
136. H. Sumi, H. Holta, S.H. Iratsuna and A. Yada, *Jpn. Kohai Tokyo Koho Jp* 28. 61, 126, 104, 13 Jan. 1986, April 84/247, 146, 22 Nov. 5 (1984).
137. V.S. Thomas, Pat. 2, 558, 396, June 26, (to American Cyanamid Co.) (1951).
138. J. Bhattacharya, Ph.D. Theses, North Bengal University, India (1988).
139. D.A. Kritskaya and A.N. Ponomarev, *J. Polym. Sc., Ser.* **44**, 551, 2002).
140. A. Rangaraj, V. Vangani, A.K. Rakshit, *J. Appl. Polym. Sc.*, **66**, 45, 1997)
141. Ebril C.; Uyan K N.: *Polym. Int.*, **50**, 792: (2001)
142. Y. Liu, J. Li, L. Yang, Z. Shi, K. Deng., *J. Macromol. Sci., Part A: Pure and Appl. Chem.* **41**, 1025(2004).
143. V.F. Kurenkov, O.A. Zaitseva, D.G. Vazeeva and D.A. Solov'ev, *Russ. J. Appl. Chem.*, **74**. 2001., 813
144. P. Bera, Ph.D. thesis, North Bengal University, India, (1999).
145. C.L. McCormick, K.P. Blackmon and D.L. Elliot, *J. Polym. Sc. Part A: Polymer Chemistry*, **24**, 2619 (1986).
146. M. Fineman and S.D. Ross, *J. Polym. Sci.* **5**, 259 (1950).
147. T. Kelen and F. Tudos, *J. Macromol. Sci., Chem.*, **A9**, 1 (1975).
148. P. Bera. S.K. Saha., *European Polymer Journal*. **36**, 411 (2000).
149. Hardwood HJ. *J Polym Sci*; **25**, 275(1968).
150. E. Collison, F.S. Dainton and G.S. McNaughton, *Trans Faraday Soc.*, **53**, 489 (1997).
151. S. Tahaun and M.M. Morland, *Soil Sci.*, **102**, 248 (1966).
152. B.K.G. Theng, *The chemistry of clay organic reactions*, Adam Hilger, London 111 (1974).

## CHAPTER 5

# STUDIES ON SOLUTION PROPERTIES OF POLYACRYLAMIDE IN WATER – N, N DIMETHYLFORMAMIDE MIXTURES

**SECTION – A**

**STUDIES ON SOLUTION PROPERTIES OF  
UNHYDROLYZED POLYACRYLAMIDE IN WATER- N, N  
DIMETHYL FORMAMIDE MIXTURES**

**5 A 1 INTRODUCTION AND REVIEW OF PREVIOUS WORKS**

The behavior of dilute polymer solutions, expressed by different parameters, viz., the second virial coefficient, the mean dimensions, the intrinsic viscosity  $[\eta]$ , solvent quality and molecular weight domain, can be discussed through different excluded volume theories. The theoretical approaches mutually differ in the mathematical methods of approximations used, but all of them relate the excluded volume effects to measurable quantities by considering different possible interactions. Very high molecular weight polymers have penetrated different application areas, including many advanced technologies.<sup>1</sup> The increase in molecular dimension from monomer to oligomer, from oligomer to usual length polymer and from later one to pleistomer is accompanied by the appearance of new properties. Application of the fundamental laws governing polymer chemistry and physics to new dimensions of these macromolecular chains revealed that many accepted concepts and relations have to be modified or even changed and it is reasonable to presume that an understanding of their behavior will open new research directions and suggest new and unexpected end uses.<sup>2</sup> In the treatment of the properties of very dilute polymer solutions it is convenient to represent the molecule as a statistical distribution of chain elements or segments, about the center of gravity. The average distribution of segments for a polymer molecule is approximately gaussian; its breadth depends on the molecular chain length and thermodynamic interaction between polymer segments and solvent.<sup>3</sup> According to hydrodynamics, the specific viscosity of a Newtonian liquid containing a small amount of dissolved material should depend in the first approximation only upon the volume concentration and the shapes of the suspended particles.

The unperturbed dimension (UD) of a given polymer in a solvent does not depend on the nature of the solvent, as long as the solvent has no influence on the rotation of the chain segments.<sup>4,5</sup> This is true in many cases, especially for nonpolar

polymer-solvent pairs, but in the cases of polar polymer - polar solvent systems, the unperturbed dimension vary considerably with the nature of the solvent. Most of the polymeric materials are soluble only in a limited number of primary solvents, but they could be made soluble in all proportions in mixtures consisting of two or more solvents, which may be individually poor solvent for the polymers.<sup>6</sup> Several mixtures of nonsolvent are also known which produce good solvent systems or at least increase the solvency power of primary solvents.<sup>7</sup> Although some studies on the solution viscosity properties of polyacrylamide in water are available in the literature, similar studies in other solvents or cosolvent systems are surprisingly little.<sup>8-14</sup> The intrinsic viscosity  $[\eta]$  is related to unperturbed dimension ( $K_\theta$ ), molecular weight ( $M$ ), and the hydrodynamic expansion factor, ( $\alpha_n$ ) by the relation.<sup>15-16</sup>

$$[\eta] = \Phi(r_0^2/M)^{3/2} M^{1/2} \alpha_n^3 = K_\theta M^{1/2} \alpha_n^3 \quad 1$$

where  $\Phi$  is universal parameter ( $\Phi = 2.5 \times 10^{23} \text{ mol}^{-1}$ ) and  $r_0^2$  is the unperturbed mean square end-to-end distance. At theta temperature  $\alpha = \alpha_n = 1$  (where  $\alpha$  is molecular expansion factor) and hence evaluation of  $K_\theta$  is possible using this equation. On the other hand, for evaluation of  $K_\theta$  from intrinsic viscosity at temperature other than theta temperature, a number of equations have been proposed. Some of the equations are as follows:

$$[\eta]^{2/3}/M^{1/3} = K_\theta^{2/3} + K_\theta^{5/3} C_T (M/[\eta]) \quad [\text{Fox and Flory (FF)}]^{15} \quad 2$$

$$[\eta]^{2/3}/M^{1/3} = K_\theta^{2/3} + 0.363 \Phi B [g(\alpha_n) M^{2/3}/[\eta]]^{1/3} \quad [\text{Kurata and Stockmayer (KS)}]^{16} \quad 3$$

$$\{([\eta]/M)^{1/2}\}^{1/2} = K_\theta^{1/2} + 0.42 K_\theta^{3/2} B (r_0^2/M)^{3/2} (M/[\eta]) \quad [\text{Berry}]^{17} \quad 4$$

$$([\eta]/M)^{1/2} = K_\theta + 0.51 \Phi B M^{1/2} \quad [\text{Burchard-Stockmayer and Fixman (B.S.F)}]^{18-19} \quad 5$$

Besides these, several other equations have also been reported<sup>20-23</sup>. According to the equations given above, the value of  $K_\theta$  is obtained from the intercepts on the ordinates of the plots of the quantity on the left-hand side versus the function of  $M$  and  $[\eta]$  on the right hand side. Assuming Flory's limiting exponent and utilizing the first order perturbed results for the intrinsic viscosity and the friction coefficient ( $f$ ) of a flexible polymer Tanaka proposed<sup>24</sup>

$$\{([\eta]/M)^{1/2}\}^{5/3} = K_\theta^{5/3} + 0.627 \Phi_0^{5/3} (\langle R^2 \rangle_0/M) B M^{1/2} \quad 6$$

and Bohdanecky<sup>25</sup> derived the following equation

$$([\eta]/M)^{1/2} = 0.80 K_{\theta} + 0.65 K_{\theta} K^{0.7} M^{0.35} \quad 7$$

Qian and Rudin<sup>26,27</sup> described a method for predicting the thermodynamic properties of polymer solutions in which the radius of gyration ( $R_g$ ) is expressed as

$$R_g = \{3[\eta]M/[9.3 \times 10^{24} (1 + ([\eta] - [\eta_0])(1 - \exp(-C/C^*))/[\eta_0])^{1/3}] \quad 8$$

where  $[\eta]$  and  $[\eta_0]$  are intrinsic viscosities in a given solvent and under  $\theta$  conditions, respectively and  $C$  is polymer concentration and  $C^*$  is the critical concentration (or overlap concentration) at which polymer molecules begin to overlap. This model was used for determining the unperturbed dimensions of polymethylmethacrylate with  $12.90 \times 10^6 < M_w < 23.84 \times 10^6$ . It appeared that calculated dimensions decrease with increasing polymer concentration upto a certain concentration; at higher concentrations the dimension remain constant for the same molecular weight and independent of the solvent type.<sup>28</sup> According to the literature it is observed that the relation put forwarded by Lenka and coworkers for the evaluation of the unperturbed dimensions has also been used for ultra high molecular weight polymers

$$6\langle S_0^2 \rangle^{1/2} = 2.204 \times 10^{-8} (M/C^*)^{1/3} \quad 9$$

where  $C^*$  is the overlap point concentration of the polymer in number of solvents, obtained from viscometric data in the semi dilute concentration regime where the macromolecular coils progressively contract and approaches the unperturbed dimensions.<sup>29-31</sup> The unperturbed dimension of polystyrene and poly (2- vinylpyridine) have been measured in solvent - precipitant mixtures of various compositions using the Stockmayer-Fixman representation by Dondos and Benoit.<sup>32</sup> In a resin solvent system, the change in temperature initiates conformational transition in polymer chains and the process of aggregation on precipitation was caused by such transitions.<sup>33-34</sup> Raju and Yaseen reported that the continuous decrease in limiting viscosity number of nylon-6 in m-cresol at temperatures ranging from 20<sup>o</sup> to 75<sup>o</sup>C was due to the contraction of the dimension of the polymer coil.<sup>35</sup> Quoting the view of other workers Haneczek and coworkers explained the partial helix-coil type polymer chain transition occurs in polyamide-6 in solution and results in higher value of limiting viscosity number of Nylon-6 in m-cresol at lower temperatures which in turn favors the dissolution.<sup>36</sup> Chatfield reports that solvent power of an alcohol-ether mixture for nitrocellulose increases with lowering of temperature and at - 50<sup>o</sup>C methyl alcohol alone becomes a solvent for cellulose ethers.<sup>37</sup> Recently Savas and Zuhail

have determined the unperturbed dimension of anionically polymerized poly (p-tert-butyl-styrene) at various temperatures and found the theta temperature of the polymer to be of the order of 31<sup>0</sup> and 32.7<sup>0</sup>C in nitropropane and 2-octanol respectively.<sup>38</sup> Several other workers reported the conformational transition of polymers in solution with the change of temperature.<sup>39,40</sup> Coil dimension of PMMA in the cosolvent medium of CCl<sub>4</sub> and MeOH have been investigated by Maitra and coworker.<sup>41</sup> They observed that the intrinsic viscosity exhibited a maximum for all fractions of polymers at a composition,  $\phi_{\text{CH}_3\text{OH}}=0.33$  while the Huggins constant showed a minimum value at the same composition. The experimental data for the solution properties of poly (N, N-dimethyl acrylamide) and poly (n-isopropylacrylamide) show that the hydrodynamic and configurational characteristics of these two polymers in methanol and water are different, showing a peculiar behavior in water, which cannot be easily interpreted in terms of random coil molecules. Chintore and co-workers found that the behavior of poly (N-methylacrylamide) molecule in aqueous solution was quite abnormal, as indicated by the values of second virial coefficients, lower than those measured in methanol solutions by the large difference of estimated unperturbed dimensions.<sup>42,43</sup> Therefore, the hypothesis was made that the solvation of N-substituted polyacrylamide by water would occur with large dipole interaction and/or hydrogen bonding with the structural units of the polymers in such a way as to give a large chain expansion with low chain flexibility, so that the polymer molecules could no more be treated as random coil in aqueous solutions. It has been pointed out that polyacrylamide, in which the lack of N-substitutions increases the chances of intramolecular interactions, has the highest unperturbed dimensions.<sup>44</sup> The aqueous solutions of polyacrylamide are suspected to contain fibrous aggregates of very high molecular weight. These aggregates were observed by electron microscopy and the disaggregation kinetics studied by viscometry.<sup>45-47</sup> This phenomena is generally attributed to intermolecular hydrogen bonds and is evidenced by an important decrease of viscosity with time. Boyadjian and co-workers have noticed differences of measured molecular weight by light scattering, according to the nature of the solvent and have concluded the presence of aggregates broken up by the effect of salt in pure water but not in formamide<sup>48</sup> However, even for nonhydrolyzed polyacrylamide, there is a lack of reliable data in the literature concerning the chain conformation in salt-water solutions and its relation to intrinsic viscosity, particularly in the range of molecular weight of

interest.<sup>49,50</sup> However, Francois and co-workers were successful in studying molecular weight dependence of radius of gyration, viscosity, sedimentation and diffusion on a set of fractions in the same range of molecular weight.<sup>51</sup> It has been shown recently that the unperturbed dimension of polyacrylamide could be determined by light scattering measurement in methanol-water system.<sup>52</sup> These authors concluded that the high value of the exponent (0.64) of the molecular weight dependence of radius of gyration was not related to a great expansion of macromolecular coil and the determination of unperturbed dimension by extrapolation of viscosity measurements in good solvent at  $M \rightarrow 0$  ( $M = \text{mol. wt.}$ ) should be possible and works of Okada and Yamaguchi provide such determinations.<sup>53,54</sup> Fundamental parameters of poly (2-acrylamido-2-methyl propane sulfonamide), which is soluble in water and formamide are obtained by light scattering, osmometry and viscometry in these good solvents by Gooda and Huglin and has been analyzed by extrapolation procedures to yield the unperturbed dimensions, steric factor and characteristic ratio.<sup>55</sup> There was good accord between the values of these parameters thereby obtained directly and those derived indirectly, the mean values being  $8.73 \times 10^{-9} \text{cm.g}^{1/2}.\text{mol}^{1/2}$ , 4.07 and 32 respectively. Bohdanecky and coworkers investigated the solutions of polyacrylamide fractions (molecular weight 3300-800,000) in water at 25°C and in a mixed theta solvent at 20°C by light scattering, sedimentation and viscometry.<sup>14</sup> Measurement in water gave the configuration characteristic ratio  $C_{\alpha} = 8.5$ .

The fundamental parameters of polyacrylamide obtained previously by viscometry in good solvent and in  $\theta$  solvents have been analyzed by viscosity-molecular weight relationship procedures suggested by several workers (Newman<sup>56</sup> and Misra<sup>13</sup>). High value of excluded volume exponent, as was observed in some cases, once thought to be the result of great expansion of polyacrylamide in aqueous solution as mentioned earlier. This arose doubts on the applicability of the method of extrapolation of the viscosity data in determining unperturbed dimension of the polymer in water. Further study, however, confirmed that high value of exponent of molecular weight dependence of the radius of gyration was not due to great expansion of the macromolecular coil in water and it is now believed that determination of unperturbed dimension by extrapolating viscosity data in good solvents is possible.<sup>52</sup> Bera and coworker have determined the unperturbed dimension of polyacrylamide in water-dimethylsulphoxide mixtures at 30-50°C by

different methods of extrapolation and found a minimum value of unperturbed dimension at  $\phi_{\text{DMSO}} = 0.5$  (ref. 57). From the above literature it appears that in some cases the estimated unperturbed dimensions of chains may depend on whether measurements are made on samples in solutions or in the bulk, in most instances the results from different investigators, in some cases using different methods, are consistent and the extrapolation procedures yield much higher values for unperturbed dimensions as compared to the real one, due to the curvatures appearing in the linear dependences given by the experimental data for high values of the excluded volume. Simionescu, Chee and coworkers performed viscosity measurement on solutions of polyvinylchloride resin in various plasticizers to calculate polymer-solvent interaction parameter,  $\chi_1$  using Flory equation pertaining to the linear expansion factor of the coiling in the solution.<sup>58-61</sup> This very information was then used to estimate lower critical solution temperature. Kathmann and McCormick synthesized and studied the dilute and semi-dilute solution behaviour of the terpolymers of sodium acrylate, acrylamide and the zwitterionic 4-(2-acrylamido-2-methylpropane dimethylammonio) butanoate.<sup>62</sup> The authors observed polyelectrolyte behaviour of the terpolymer at pH 8.5 and the viscosity decreased in the presence of added electrolyte. Hocking and coworkers measured the progressive influence on the hydrodynamic volume and other properties contributed by incorporation of N, N dimethylacrylamide into a series of high molecular weight acrylamide copolymers.<sup>63</sup> Aqueous solution of these polymers showed little or no decrease of radius of gyration when low concentration of sodium chloride were added, in contrast to its effect on solutions of polyacrylamide itself. Shanks and Wu measured the viscosity of polyacrylamide dilute solutions in water with acetone, ethanol, dimethylformamide and ethylene glycol as cosolvent to study the conformation of polymer chains and the degree of polymer solvent interaction.<sup>64</sup> It was found that polymer chain conformation contracted as the acetone, ethanol and the DMF cosolvent composition ratio increased but there was no distinguishing difference of contraction in case of water-ethylene glycol compositions. Alorió and coworkers reported relationship between intrinsic viscosity and molecular weight for narrow molecular weight distribution of polyisoprene and polystyrene samples in  $\text{CCl}_4$  at  $25^\circ\text{C}$ .<sup>65</sup> Conclusions drawn from viscometry that  $\text{CCl}_4$  is a good solvent for both the polymers was supported by second virial coefficient from low-angle light scattering measurements. Azim and Huglin measured the intrinsic viscosities of different

fractions of polystyrene (PS) at 98.5 °C in the mixtures of MC and 1, 2, 3, 4-tetrahydronaphthalene over the whole range of solvent compositions.<sup>66</sup> The theta temperature of PS measured as 98.5 °C in methylcellulose (MC). Solution viscosities of the copolymers and homopolymers of acrylamide were determined at 30, 40, and 50°C by Rakshit and coworkers.<sup>67</sup> The activation parameters of viscous flow, voluminosity, and shape factor were also calculated. The average shape factor was observed to be nearly 2.5 for all the copolymer systems. Viscosity average molecular weights were calculated, and from the intramolecular expansion factor it was observed that copolymers are less flexible than that of homopolymers. The  $dn/dc$  values obtained from differential refractometry are in good agreement with those calculated theoretically. Rakshit and coworkers.<sup>68</sup> also used the viscosity data to calculate the volume related parameter  $V_E$  of the polymer. Recently it has been used to determine the shape of protein and some other acrylate copolymer molecules in solution.  $V_E$  is calculated by plotting  $Y$  against concentration  $C$ , where

$$Y = (\eta_r^{1/2} - 1) / [C (1.35\eta_r^{1/2} - 0.1)], \text{ (here } \eta_r \text{ is relative viscosity)} \quad 10$$

From the plot,  $V_E$  is obtained as an intercept since

$$\text{Lt } C \rightarrow 0 \text{ } Y = V_E \quad 11$$

The shape factor  $v$  is calculated from the relation<sup>69</sup>

$$[\eta] = vV_E \quad 12$$

The value of  $v$  has been shown to be 2.5 for spherical particles.<sup>70</sup>

An Ubbelohde viscometer was used to measure the relative viscosities of polymer solutions (detail in experimental section, chapter 3). The related definitions are as follow:

$$\text{Specific viscosity, } \eta_{sp} = (t - t_0) / t_0 \quad 13$$

$$\text{Reduced viscosity, } \eta_{red} = \eta_{sp} / C \quad 14$$

$$\text{Intrinsic viscosity, } [\eta] = (\eta_{sp} / C)_{C=0} \quad 15$$

$$\text{And the Huggins equation is } \eta_{sp} / C = [\eta] + K_H [\eta]^2 C \quad 16$$

where  $K_H$  is the Huggins constant. The symbol  $\eta$  refers to the viscosity of solution,  $t$  is the efflux time of the solution,  $t_0$  is the efflux time of solvent and  $C$  is the polymer

concentration. For a linear relationship between  $\eta_{red}$  and  $C$ ,  $K_H [\eta]^2$  is the slope and  $[\eta]$  is the intercept.

In the present section, the results of our investigation on unperturbed dimension, interaction parameter and related aspects of unhydrolyzed polyacrylamide in water-DMF mixtures have been described. The intrinsic viscosities of the polymer have been measured for different fractions of the polymer (viz., A type, B type, and C type) in different compositions (water-DMF) of the cosolvent mixture at different temperatures. In the previous chapter, we have reported the technique by which the molecular weight of PAM in aqueous solution may be controlled by trapping the initiator component in the interlayer space of vermiculite. This method has been adopted selectively to prepare polymers of varying molecular weights for the solution property studies as presented in this section of the present chapter. Low molecular weight polymers (viscosity average molecular weight  $2.3 \times 10^5$ , C-type) were prepared via redox polymerization of acrylamide monomer initiated by  $FeCl_3$  and thiourea redox system at  $50^\circ C$ . To obtain medium molecular weight polymers (viscosity average molecular weight  $1.6 \times 10^6$ , B-type) 0.4M monomer and 0.06M TU in aqueous suspension of ferric vermiculite (FeV) were used at  $60^\circ C$  temperature and at pH 1.98. Details are given in chapter 3. High molecular weight polymers (viscosity average molecular weight  $8.9 \times 10^6$ , A-type) were purchased from Across Organics (Belgium). From the relation between  $[\eta]$  and  $M$ , the unperturbed dimension and molecular expansion factor have been measured. The Huggins constant value in each case was also determined in order to study the influence of cosolvent system on the aggregation of the polymer. While DMF is a poor solvent for PAM, water – DMF mixture acts as a cosolvent in certain proportions.

## **5 A 2 RESULTS AND DISCUSSION**

### **INTRINSIC VISCOSITY**

In general for a flexible polymer in poor solvent, the intrinsic viscosity increases with temperature, whereas in good solvent it decreases with temperature. In athermal solvent, however, viscosity is independent of temperature.<sup>71</sup> In absence of any solute the observed physical-chemical characteristics of water-DMF mixtures<sup>72-78</sup> such as dielectric decrement<sup>72</sup> with a maximum around  $\phi_{DMF} = 0.5$ , nonlinear viscosity increment<sup>77-78</sup> at water rich composition and highly nonlinear

concentration dependence of apparent molal volumes with a minimum<sup>75</sup> around  $\phi_{\text{DMF}}=0.20$  have led the investigators to suggest that in presence of water, the self associates of DMF<sup>72-73</sup> undergo disruption due to possible formation of intercomponent H-bonded complexes, resulting in the breakdown of 3-D structures. At the initial water-rich region of DMF-water mixtures, comparatively more monomeric water and DMF molecules and the so-called DMF-water complexes are free to solvate the solute species. However, at higher composition of DMF, free monomeric water and DMF molecules are involved in the possible H-bonded clusters and DMF-DMF aggregate formation. The polymer chains are expanded most at the temperature at which  $[\eta]$  is the maximum. The variation of  $[\eta]$  for all three types of polymer at different temperatures and solution compositions are shown in figure 5.1-5.3. The result shows that an increasing the amount of nonsolvent (DMF) up to a certain limit, intrinsic viscosity also increases for all types of PAM. This variation is, however, distinguishable from the variation observed in case of a pure solvent system. Intrinsic viscosity reaches its maximum value near  $\phi_{\text{DMF}}=0.2$  for the polymer type-A, near  $\phi_{\text{DMF}}=0.3$  for the polymer type-B and near  $\phi_{\text{DMF}}=0.4$  for the polymer type-C. This indicates that energetically the most favorable solvent composition is different for different types of PAM. The higher the molecular weight of the polymer, smaller is the concentration of DMF required for showing the cosolvency effect. The decrease in  $[\eta]$  after the maximum is explained by decrease in unperturbed mean square end-to-end distance. At a higher co-solvency condition, the energetic weighting factor favors the extended configuration of the polymer molecules. The extended long chains are surrounded by the solvated hull and longer the chain lesser is the amount of DMF required for attaining the cosolvency condition. At low value of  $\phi_{\text{DMF}}$  of pure solvent systems, the viscosity should decrease with temperature but in the present ternary system (water+DMF+PAM),  $[\eta]$  is found almost invariant with temperature of the system. Increase in temperature of a polymer solution generates two antagonistic effects.<sup>79-80</sup> Firstly, an increase in temperature generally leads to an increase in the solubility. This results in uncoiling of the polymer chain leading to an increase in intrinsic viscosity with temperature. Secondly, increase in temperature may lower the rotational barrier, thereby enhancing the degree of rotation about a skeletal bond, forcing the molecular chains to assume more compact coiled configuration. This leads to decrease in intrinsic viscosity with the increase in temperature. Plots of Huggins constant as a function of solvent composition are

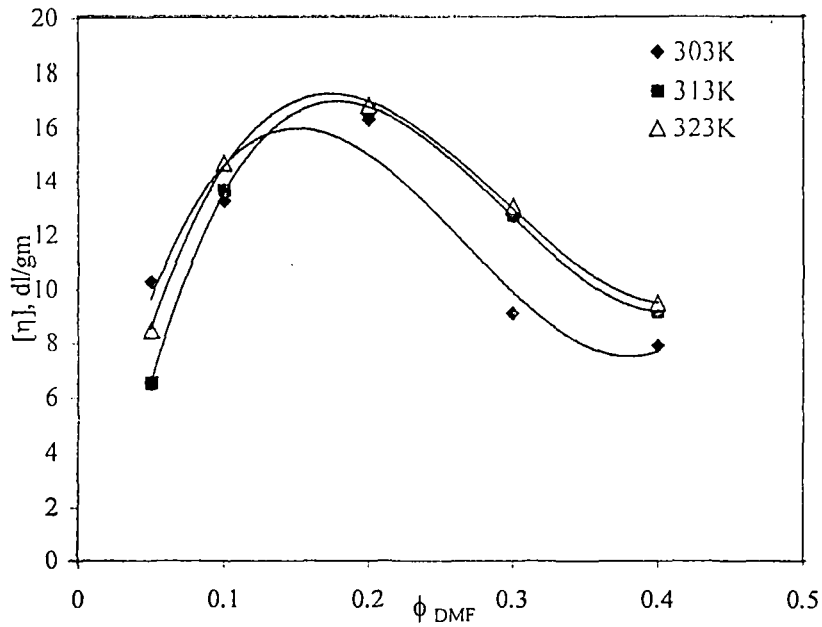


Figure 5.1: Plot of intrinsic viscosity vs. fraction of DMF at various temperatures for PAM type A.

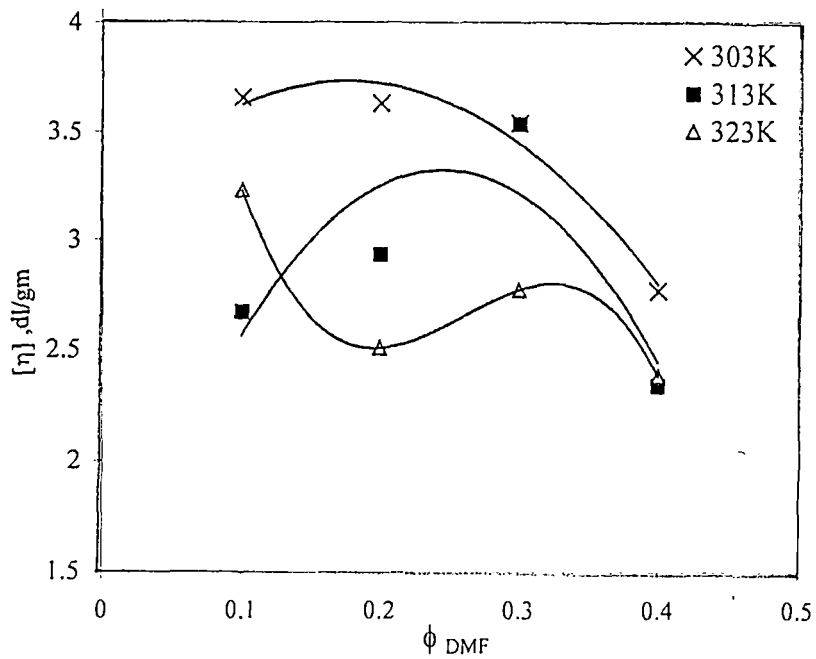


Figure 5.2: Plot of intrinsic viscosity vs. fraction of DMF at various temperatures for PAM type B.

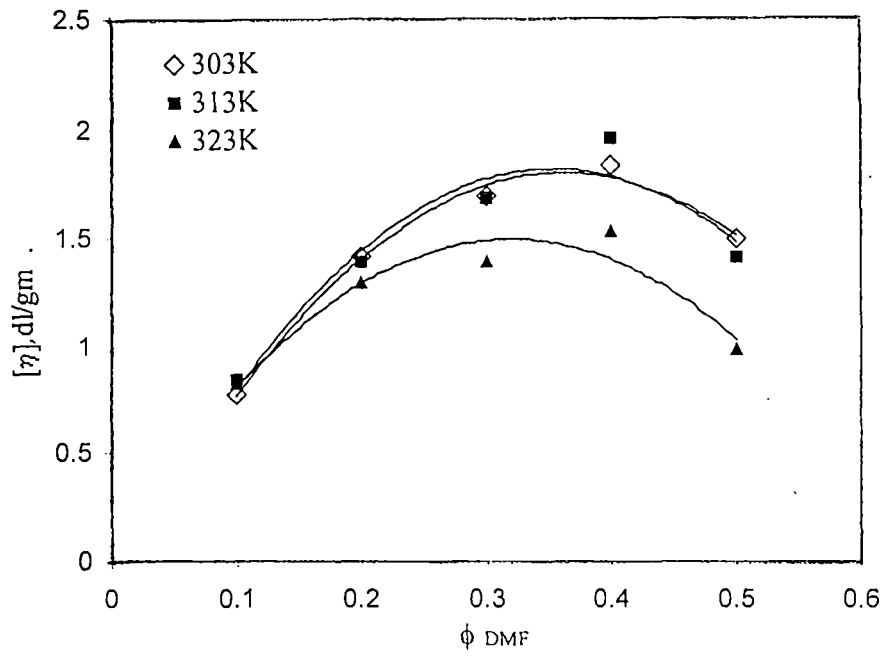


Figure 5.3: Plot of intrinsic viscosity vs. fraction of DMF at various temperatures for PAM type C

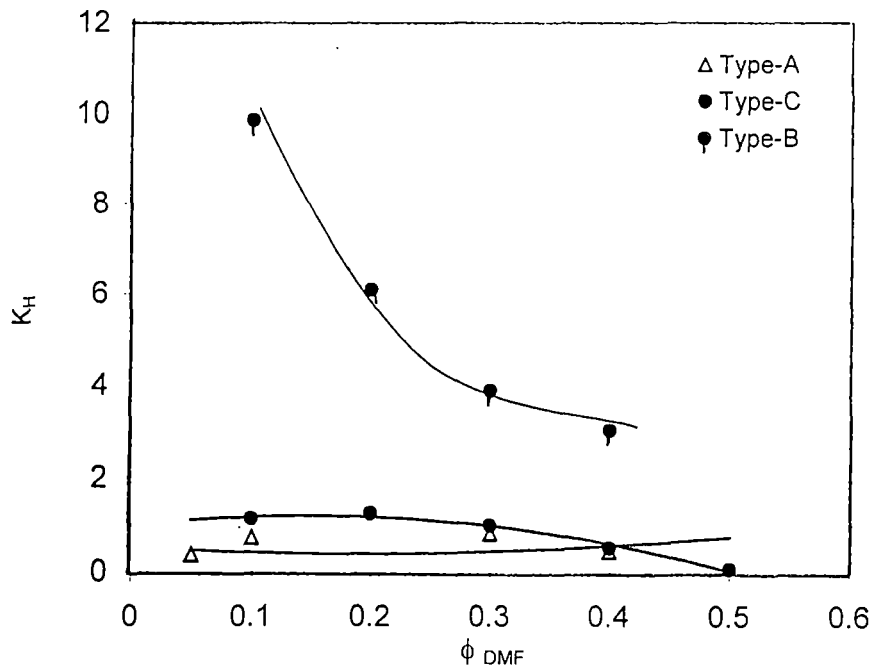


Figure 5.4: Plot of Huggins constant vs. fraction of DMF at 30°C.

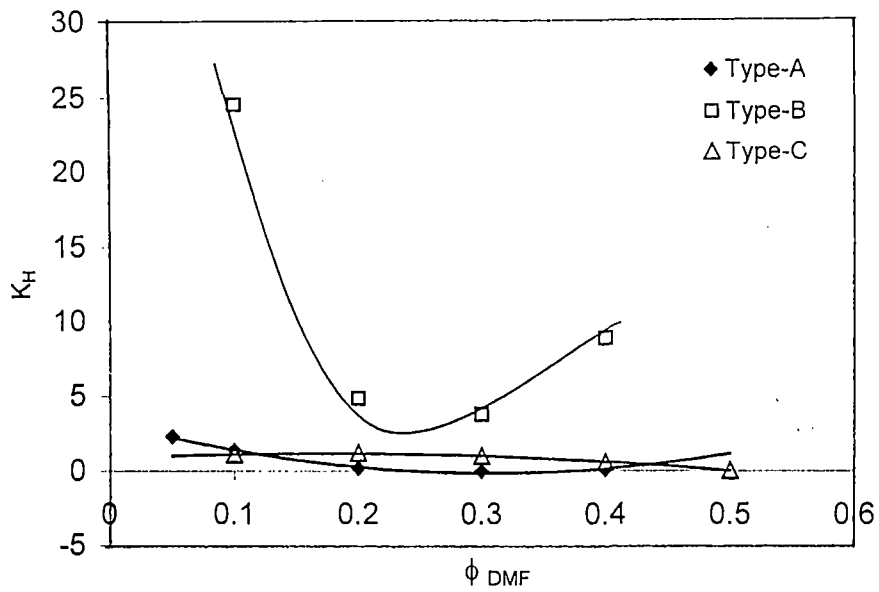


Figure 5.5: Plot of Huggins constant Vs. fraction of DMF at 40°C.

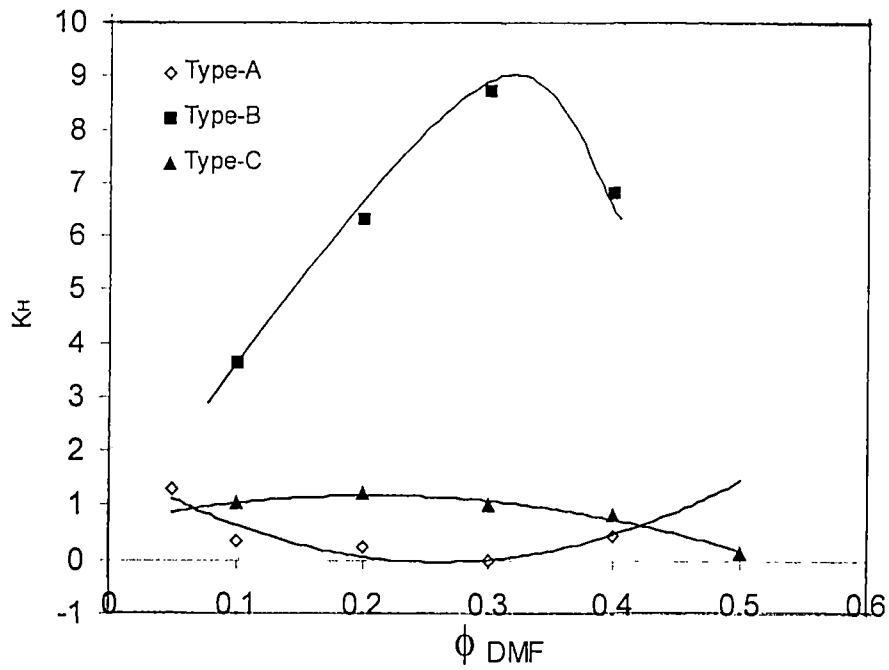


Figure -5.6: Plot of Huggins constant Vs. fraction of DMF at 50°C.

shown in figure 5.4-5.6. It is observed that there is a maximum at the solvent composition  $\phi_{\text{DMF}} = 0.2$  for PAM type C at all the studied temperatures. There are maxima at  $\phi_{\text{DMF}} = 0.3$  for type-B and type-A at  $50^{\circ}\text{C}$  and  $30^{\circ}\text{C}$  respectively and there are minima at  $\phi_{\text{DMF}} = 0.2$  for type-A and type-B at  $50^{\circ}\text{C}$  and at  $40^{\circ}\text{C}$  respectively. Small values of  $K_H$  indicate better cosolvency at this solvent composition and temperature. Very high values of  $K_H$  for PAM type-B are the indication of strong aggregation for polymer molecules at all temperatures studied.

### **UNPERTURBED DIMENSION (UD)**

The UD of the polymer chain is the dimension where volume exclusion due to long-range segmental interaction is nullified by its interaction with a definite solvent (theta solvent).<sup>20</sup> UD is the end-to-end distance of the polymer chain under theta condition and can be determined from intrinsic viscosity measurement at this condition. In the present study, Kurata-Stockmayer equation under non-theta condition<sup>16</sup> has been used to derive  $K_{\theta}$  of PAM in different water-DMF mixtures. The results are summarized in table 5. 1. Some of the K-S plots are shown in figures 5.7-5.12. Plots are essentially linear. The value of  $K_{\theta}$  obtained from various methods of measurements viz. S-F, K-S-F and K-S agree well with each other except for a few composition conditions of the solvents. It is apparent that at  $\phi_{\text{DMF}} = 0.4$  the polymer has the highest unperturbed dimension and this result is in general true for all the adopted methods for  $K_{\theta}$  calculation. Above the  $\phi_{\text{DMF}}$  value of 0.4 the cosolvency of the system is lost and the polymer is precipitated out (for PAM of type-C, precipitation starts at  $\phi_{\text{DMF}} = 0.5$ ) from the solution. At  $\phi_{\text{DMF}} = 0.1$  the polymer shows lowest  $K_{\theta}$  values for all the methods of calculation. The effect of temperature is interesting. With an increase in temperature,  $r_o^2$  and hence  $K_{\theta}$ , decrease due to greater freedom of rotation around the skeletal bonds.<sup>20</sup> However, such a temperature dependence of  $K_{\theta}$  can be attributed not only to the change in flexibility of macromolecular chains but also to the specific polymer solvent interaction. The effect may also be correlated to the cohesive energy density of the polymer and the solvent.<sup>33</sup>

### **TEMPERATURE COEFFICIENT OF UNPERTURBED DIMENSION**

The effect of temperature on UD can be attributed to the change in flexibility of a macromolecular chain as well as to polymer solvent interactions. Some solvents at certain temperatures hinder internal rotations in macromolecules due to favorable

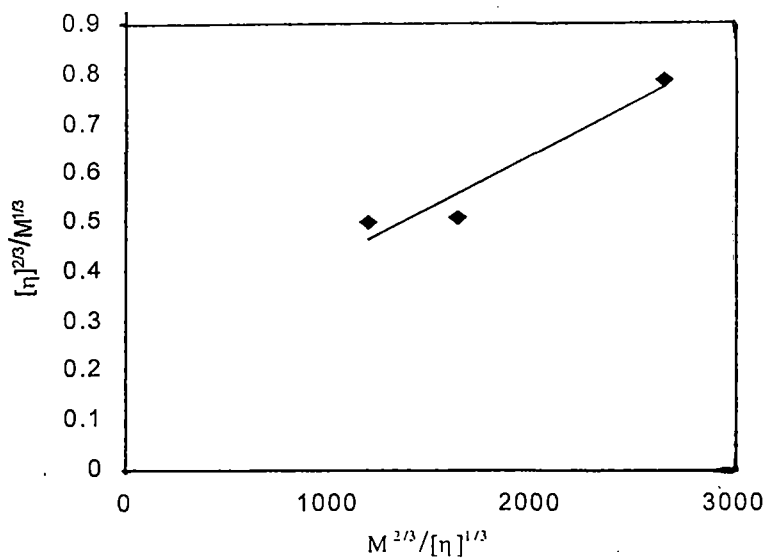


Figure 5.7 :KS Plot at 30°C,  $\phi_{DMF}=0.2$

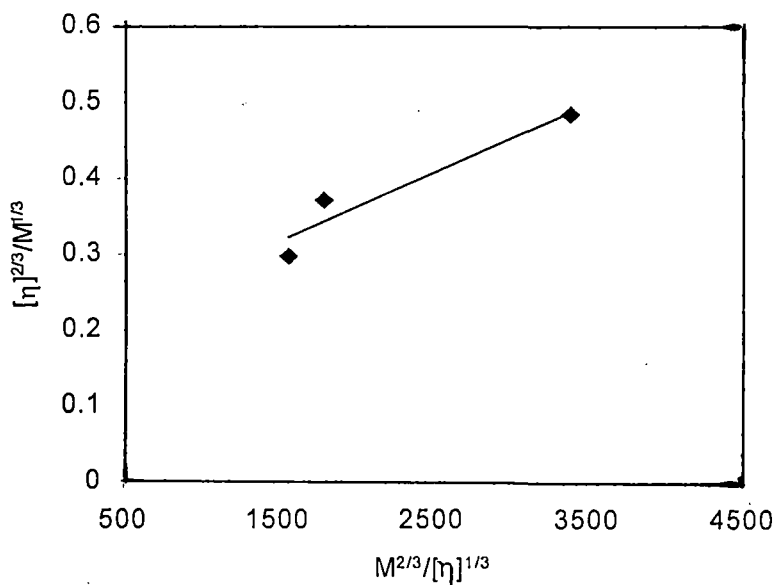


Figure 5.8 :KS Plot at 30°C,  $\phi_{DMF}=0.4$

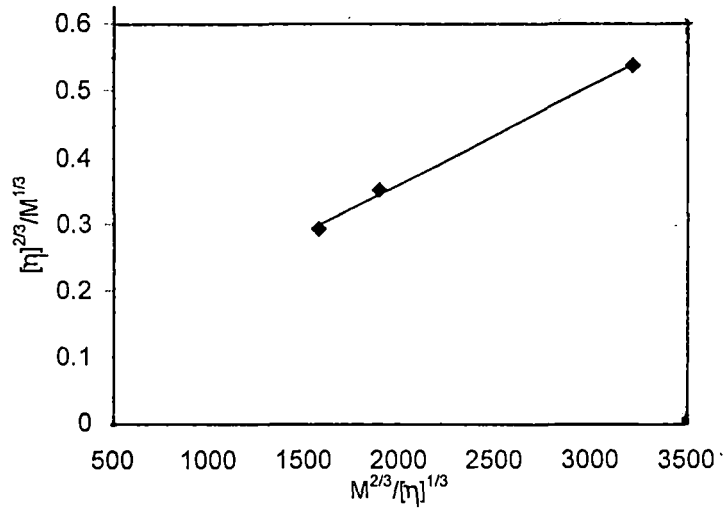


Figure 5.9:KS plot at 40°C,  $\phi_{DMF}=0.4$

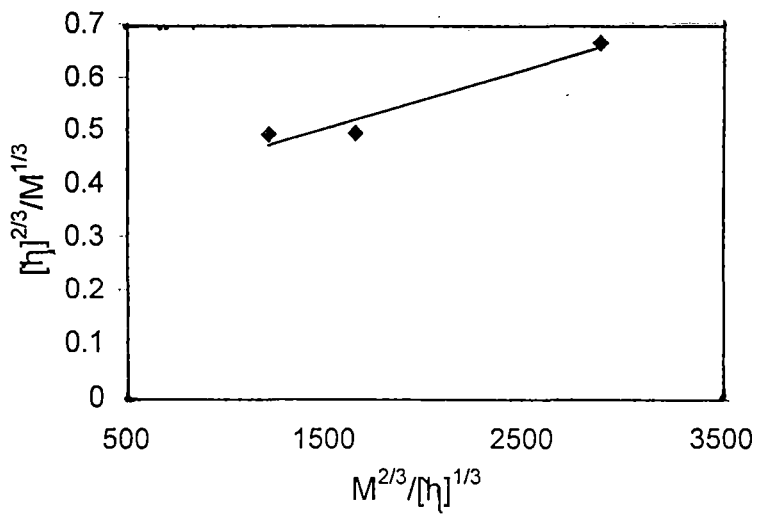


Figure 5.10:KS Plot at 40°C,  $\phi_{DMF}= 0.3$

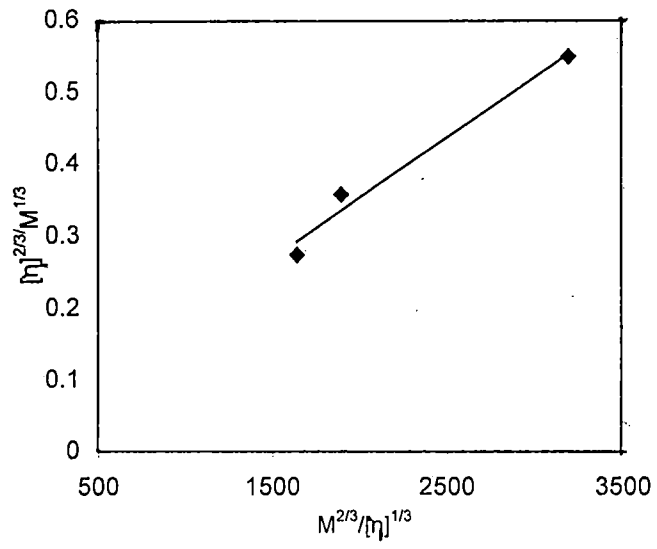


Figure 5.11:KS Plot at 50°C,  $\phi_{DMF}=0.4$

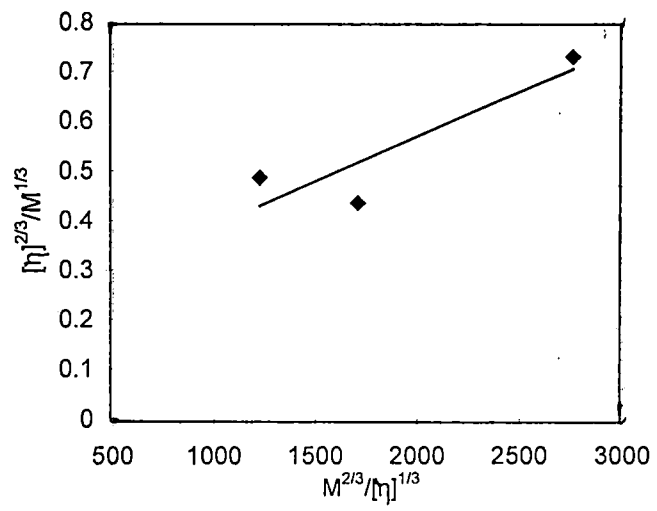


Figure 5.12:KS Plot at 50°C,  $\phi_{DMF}=0.1$

**Table 5.1 Unperturbed Dimension of PAM in water+DMF mixtures at different temperatures determined by different methods.**

Temp. °C	$\phi_{DMF}$	$K_{\theta} \times 10^3 \text{ (cm}^3 \cdot \text{g}^{-3/2} \cdot \text{mol}^{1/2}\text{)}$		
		K-S	S-F	K-S-F
30	0.1	0.484	0.679	1.843
	0.2	1.377	1.399	2.522
	0.3	3.189	3.181	3.261
	0.4	3.391	3.338	3.191
40	0.1	0.328	0.332	1.483
	0.2	1.125	0.958	2.141
	0.3	2.532	2.509	3.041
	0.4	3.367	3.167	3.092
50	0.1	0.260	0.343	1.641
	0.2	0.900	0.578	1.828
	0.3	1.650	1.562	2.301
	0.4	2.423	2.302	2.527

**Table 5.2 Temperature co-efficients of Unperturbed Dimension at different DMF compositions.**

$\phi_{DMF}$	$K' \text{ deg}^{-1}$
0.1	0.0161
0.2	0.0212
0.3	0.0330
0.4	0.0168

interactions, which lead to expanded uncoiled conformation of the polymer. Previous workers attributed this variation in UD to the specific solvent effect resulting from hydrogen bonding or other polar interactions<sup>67</sup>. In the case of mixed solvents, preferential adsorption leads to similar observations and the effects are correlated to cohesive energy density of the polymer and the solvent. Unperturbed dimension ( $K_\theta$ ) is related to statistical parameter ( $r_o^2$ ) and unperturbed mean square end-to-end distance by Flory equation as follows:

$$K_\theta = \Phi_0 [ r_o^2 / M_w ] \quad 17$$

On differentiating the above with respect to T, the temperature coefficient of unperturbed dimension may be obtained

$$d \ln K_\theta / dT = 3/2 [ \{ d \ln (r_o^2) / dT \} ] = K' \quad 18$$

Here  $K'$ , the temperature coefficient of unperturbed dimension provides information about configuration of chain molecules and also predict the configuration-dependent properties of polymer chain and energies of bond conformations in the molecules. From the table 5.2 it is seen that the value of  $K'$  changes with solvent composition. The value of  $K'$  increases up to  $\phi_{DMF} = 0.3$  and then decreases. That is PAM molecules expand more up to  $\phi_{DMF} = 0.3$ . It also reveals the presence of low energy configuration in this solvent composition at high temperature. However, at  $\phi_{DMF} = 0.4$ ,  $K'$  again assumes lower value indicating more compact structure and the existence of high-energy configuration of the polymer.

## MOLECULAR EXPANSION FACTOR

The molecular expansion factor ( $\alpha_n$ ), which represents the effect of long-range interaction, can be described as an osmotic swelling of the chain by the solvent-polymer interaction. It has been calculated from the relation,

$$\alpha_n^3 = [\eta] / K_\theta M_v^{1/2} \quad 19$$

where  $K_\theta$  has been taken from the K-S plot. The actual end-to-end distance,  $\alpha_n K_\theta$ , of the polymer molecule is also computed, which is shown in table 5.3. It is observed that  $\alpha_n K_\theta$  attains its highest value at  $\phi_{DMF} = 0.4$  for all the fractions of the polymer. As the number of segmental interaction of the polymer molecules increases with

molecular weight, the value of  $\alpha_n$  also increases. This trend is observed at all temperatures under the study.

**Table 5.3 Molecular Expansion Factor and Coil Dimensions of PAM at different temperatures in water + DMF mixtures.**

Temperature(°C)	$\Phi_{DMF}$	Type-A		Type-B		Type-C	
		$\alpha_n$	$\alpha_n \times K_{\theta} \times 10$	$\alpha_n$	$\alpha_n \times K_{\theta} \times 10$	$\alpha_n$	$\alpha_n \times K_{\theta} \times 10$
30	0.1	2.260	1.096	1.883	0.912	1.487	0.720
	0.2	1.723	2.373	1.327	1.827	1.287	1.772
	0.3	1.065	3.396	0.995	3.173	1.031	3.288
	0.4	0.996	3.377	0.897	3.042	1.037	3.517
40	0.1	2.602	0.855	1.932	0.635	1.743	0.6727
	0.2	1.845	2.075	1.322	1.516	1.360	1.530
	0.3	1.286	3.257	1.073	2.717	1.111	2.814
	0.4	1.049	3.532	0.851	2.866	1.062	3.576
50	0.1	2.880	0.750	2.224	0.580	1.867	0.486
	0.2	1.994	1.795	1.352	1.217	1.436	1.293
	0.3	1.496	2.468	1.489	2.456	1.203	1.984
	0.4	1.185	3.600	0.955	2.315	1.093	2.648

## CHAIN RIGIDITY

The characteristic ratio ( $C_{\alpha}$ ), which serves as a measure of short-range interactions such as bond angle restrictions and steric hindrances, are also influenced by the torques exerted on the chain by solvent molecules. This effect is, however, small in many cases. The characteristic ratio  $C_{\alpha}$  is a parameter that compares the unperturbed mean square end-to-end distance to the dimension of the chain if each segment was freely jointed. Steric factor ( $\sigma$ ), the characteristic ratio ( $C_{\alpha}$ ), and  $[r_0^2/M]^{1/2}$  are calculated in usual manner from the following equations<sup>81</sup>

$$\sigma = [\langle r^2 \rangle_{of}/M]^{1/2} / [\langle r^2 \rangle_{of}/M]^{1/2} \quad 20$$

$$[\langle r^2 \rangle_{of}/M]^{1/2} = [\langle r^2 \rangle_{of}/N]^{1/2} [1/M_0]^{1/2} \quad 21$$

$$C_{\alpha} = [K_{\theta}/\Phi_0]^{2/3} (M_0/2L^2) \quad 22$$

where  $\langle r^2 \rangle_0$  is the unperturbed mean square end-to-end distance for a freely rotating chain, N is the degree of polymerization,  $M_0$  is the molecular weight of the monomer and L is the backbone bond length ( $L=0.154\text{nm}$ ). For vinyl polymers the value of  $[\langle r^2 \rangle_0/N]^{1/2}=3.08 \times 10^{-8}\text{cm}$  [35]. The computed values of  $\sigma$ ,  $C_\alpha$ , and  $[r_0^2/M]^{1/2}$  for PAM at different solvent compositions and temperatures are given in the table 5.4. Cowie observed that the range of values of  $\sigma$  normally encountered is about 1.5-2.5 (ref. 82). In the present system, however, it ranged between 1.29 and 3.03. Like UD, other parameters viz.,  $\sigma$ ,  $C_\alpha$  and  $\alpha_n K_\theta$  also show their highest values at  $\phi_{\text{DMF}} = 0.4$ .

**Table 5.4 Steric Factor, Characteristic Ratio and Unperturbed Dimension (in  $\text{cm.g}^{1/2}.\text{mol}^{1/2}$ ) of PAM as a function of DMF fraction and temperature.**

Temperature( $^{\circ}\text{C}$ )	$\Phi_{\text{DMF}}$	$r_0^2/M^{1/2} \times 10^9$	$C_\alpha$	$\sigma$
30	0.1	5.787	0.772	1.585
	0.2	8.198	1.549	2.246
	0.3	10.845	2.711	2.971
	0.4	11.070	2.824	3.030
40	0.1	5.084	0.595	1.392
	0.2	7.662	1.353	2.099
	0.3	10.043	2.325	2.751
	0.4	11.043	2.811	3.025
50	0.1	4.706	0.510	1.289
	0.2	7.115	1.167	1.949
	0.3	8.706	1.747	2.385
	0.4	9.897	2.257	2.711

## VOLUME RELATED PARAMETER

The volume related parameter is a function of temperature and a measure of volume of the solvated polymer molecules. The representative plot of Y vs. C (equation no.10) is shown in figure 5.13.  $V_E$  is obtained from the intercept of the straight line on y-axis. Computed data of  $V_E$  and  $\Psi$  are shown in table 5.5. As the temperature increases the solvation decreases and hence,  $V_E$  decreases. This is true

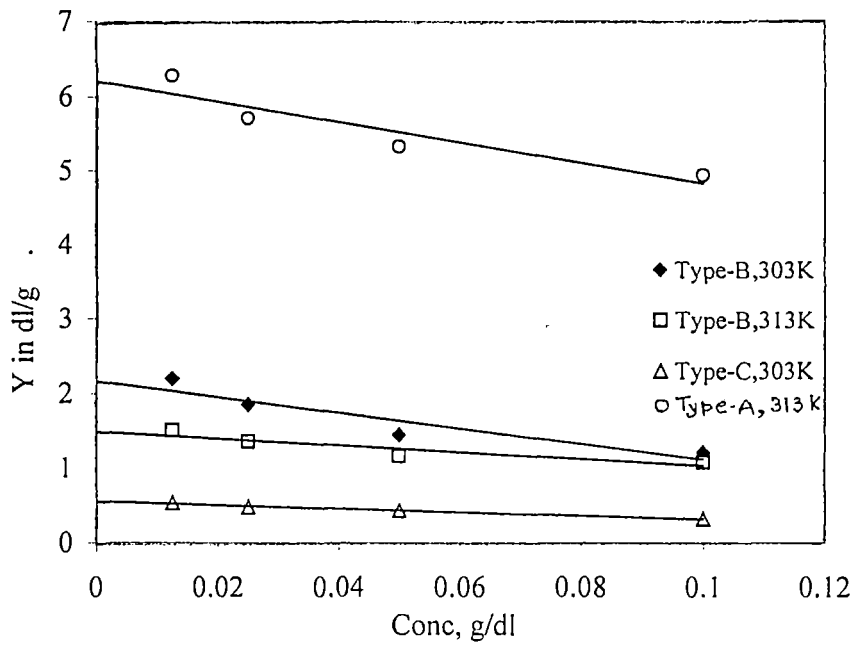


Figure 5.13: Pot of Y vs. Concentration for different fractions of PAM at various temperatures,

in most of the cases except for the polymer of type-A. It is to be noted that as the molecular weight decreases the solvated volume also becomes smaller. A poor solvent system results in the less solvation of the polymer molecules, and hence the nature of variation of  $V_E$  is almost similar to the nature of variation of  $[\eta]$  with  $\phi_{DMF}$ .

**Table 5.5 Volume related Parameter  $V_E$  (in  $dl g^{-1}$ ) and Shape Factor values of PAM at different solvent compositions and temperature**

Temperature( $^{\circ}C$ )	$\Phi_{DMF}$	Type-A		Type-B		Type-C	
		$V_E$	$\nu$	$V_E$	$\nu$	$V_E$	$\nu$
30	0.1	5.27	2.51	1.47	2.50	0.40	---
	0.2	6.31	2.58	2.37	---	0.56	2.54
	0.3	3.42	2.65	1.40	2.52	0.60	2.84
	0.4	3.82	2.07	1.11	2.50	0.60	3.05
40	0.1	5.66	2.41	1.16	2.30	0.40	2.12
	0.2	6.45	2.58	1.56	---	0.53	2.58
	0.3	4.64	2.74	1.40	2.51	0.60	2.88
	0.4	3.77	2.43	1.04	2.34	0.64	3.06
50	0.1	5.75	2.55	1.36	2.37	0.32	2.53
	0.2	6.54	2.57	1.15	2.20	0.45	2.81
	0.3	5.04	2.58	1.17	2.37	0.48	2.88
	0.4	4.04	2.16	1.03	2.32	0.56	2.73

The shape factor  $\nu$  gives an idea about the shape of the polymer molecules in solution. Ideally it is 2.5 for spherical particles. Rakshit and coworker suggested that the conformation of hydrolyzed PAM was other than spherical ( $\nu = 2.5-8.7$ )(ref.83). It is interesting to note that  $\nu$  values (Table-5.5) of unhydrolyzed PAM in the present study are very close to 2.5 and is not affected by solvent, molecular weight and the temperature of the study. This indicates that unhydrolyzed PAM molecules assume globular structure in solution.

## SECTION - B

# STUDIES ON SOLUTION PROPERTIES OF HYDROLYSED POLYACRYLAMIDE IN WATER-N, N DIMETHYLFORMAMIDE MIXTURES

### 5 B 1 INTRODUCTION AND REVIEW OF PREVIOUS WORKS

Water-soluble polymers find a very broad range of industrial applications. Acrylamide based polymers are widely used as flocculants, rheology control agents and additives.<sup>84-86</sup> Paper manufacturing, mining and water treatment processes are among the many fields that benefit from the use of acrylamide-based polymers.<sup>87-91</sup> In solution phase, progressively hydrolyzed polyacrylamide (PAM) develops varied charge densities on the polymer backbone and as such, solution behaviour of the polymer is modified. Hydrolysis of amide groups in the alkaline condition, adsorption of nonionic (unhydrolyzed) [NPAM], anionic and cationic types of PAM on charged surfaces at different pH media are documented in literature.<sup>92-102</sup> If hydrolyzed PAM is dissolved in water<sup>103</sup> it behaves like weak polyelectrolyte with charged  $\text{COO}^-$  on the backbone. In this charged PAM, relative dissociation of the ionic groups is a function of solvent polarity and the distribution and alignment of the charged dipoles along the chain are expected to play decisive role on the final state of conformation of the polymer chain.<sup>101</sup> Partially hydrolyzed PAM is thus expected to develop fascinating solution behavior especially in aqueous-nonaqueous mixed solvents. The effect of hydrodynamic field and the degree of hydrolysis on apparent conformation of hydrolyzed PAM has been discussed.<sup>104</sup> Ludenberg and Phillips studied the viscometric behavior of sulphonated polystyrene in water/tetrahydrofuran mixtures and found the nonpolyelectrolytic behavior without any precipitation when water content reduced below 5-vol%.<sup>105</sup> But the sulphonated polystyrene unit in their polymers was only 1.7 mol%. Tong and coworkers measured the viscosity of copolymers of 2-acrylamido-2-methylpropane sulphonic acids and 2-hydroxypropyl methacrylate in dimethyl sulfoxide and dimethyl sulfoxide / tetrahydrofuran mixed solvents and observed polyelectrolyte behavior even in mixed solvent containing 65% of tetrahydrofuran.<sup>106</sup> The viscosity reduction and precipitation of a copolymer from solution with increasing tetrahydrofuran content was attributed to the dipole-

dipole attraction between ion-pairs formed in less-polar medium. Some workers observed a complicated dependence of  $[\eta]$  on the mole fraction of ethanol in aqueous solution of polymethacrylic acid and interpreted the results in terms of coil to collapsed chain model.<sup>107-110</sup>

In section A of this chapter the results of our investigation on unperturbed dimension, interaction parameter and related aspects of unhydrolyzed polyacrylamide in water-DMF mixtures have been described. In continuation to our studies on physicochemical behavior of water-soluble synthetic polymers, present section of this chapter deals with the variation of  $[\eta]$ , activation entropy and activation enthalpy ( $\Delta S_{vis}^\#$  and  $\Delta H_{vis}^\#$ ), volume related parameter ( $V_E$ ), and the shape factor ( $v$ ) of progressively hydrolyzed PAM with solvent composition in water-DMF system. While DMF is a poor solvent, water-DMF mixtures act as a cosolvent in certain proportions for hydrolyzed PAM also.

## 5 B 2 RESULTS AND DISCUSSION

### INTRINSIC VISCOSITY

It has been pointed out that for polyelectrolyte solutions, Fuoss equation (equation 28) cannot predict explicitly the occurrence of maximum in the reduced viscosity upon dilution under salt free condition.<sup>111</sup> Different models have been proposed to explain such behaviour.<sup>112,113</sup> Witten and Pincus have explained polyelectrolyte viscosity for the semi dilute concentration regime where the polymers overlap.<sup>122</sup> According to the above model

$$\eta = \eta_s Z (C/l)^{3/2} (C/C^*)^{1/2} \quad 23$$

where  $\eta$  and  $\eta_s$  are solution and solvent viscosities, respectively,  $l$  is the solution ionic strength,  $C^*$  is the overlap concentration,  $C$  is the polymer concentration and  $Z$  is the polyion charge. In salt free solution where  $C = l$ . Examination of equation 23, however, reveals that for  $C > C^*$ , the inverse of reduced viscosity  $(\eta_{red})^{-1} \propto C^{1/2}$ , which is in agreement with the equation of Fuoss. In the present system, straight lines are obtained on plotting  $(\eta_{sp}/C)^{-1}$  against  $C^{1/2}$  under semi dilute condition of HPAM (not shown). The variation of  $[\eta]$  of the solutions of, LPAM and HPAM at different temperatures and solvent compositions are shown in figures 5.14-5.15 respectively. The variation of  $[\eta]$  with solvent composition is, however, distinguishable from that

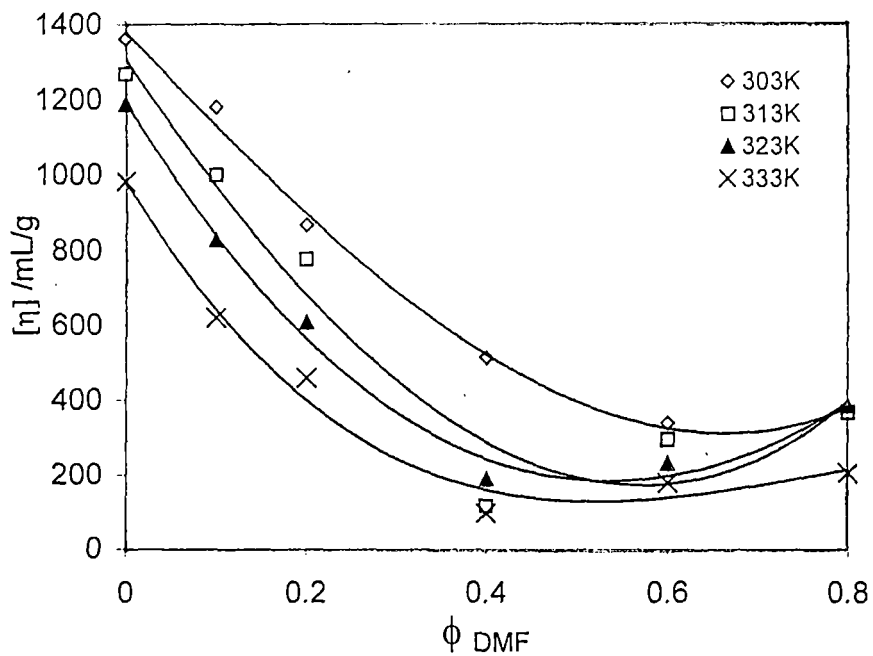


Figure:5.14:Plot of intrinsic viscosity vs. fraction of DMF for HPAM at different temperatures.

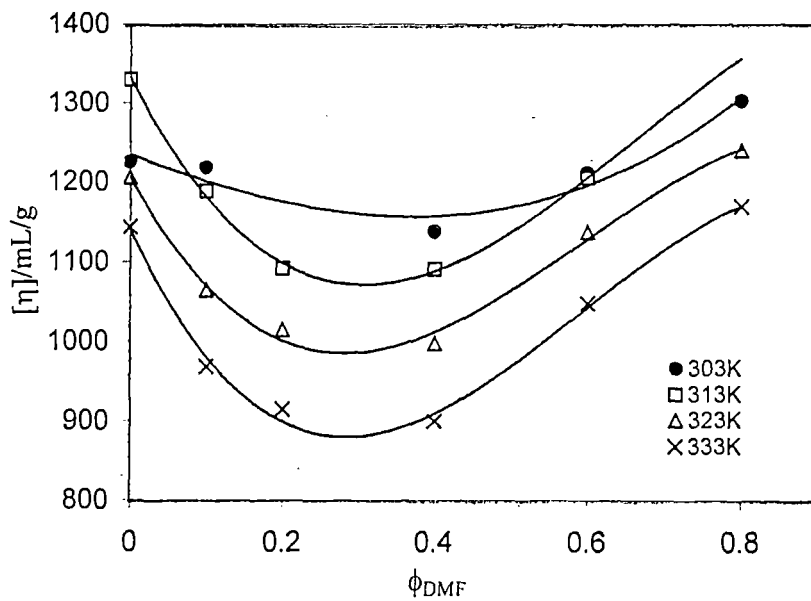


Figure:5.15:Plot of intrinsic viscosity vs. fraction of DMF for LPAM at different temperatures.

observed in case of pure solvent systems. For LPAM and HPAM the nature of variation of  $[\eta]$  with solvent composition is just opposite to that in pure solvent systems. With increasing DMF content (poor solvent),  $[\eta]$  decreases due to the contraction of polymer coils as well as for enhanced degree of intermolecular agglomeration of polymer chain. The negative deviation of  $[\eta]$  as a function of solvent composition of the associated binary solvent can be explained in terms of free volume theory as follows: In the presence of aggregates or complexes, polymer molecules cannot find a free volume and they are contracted. It is found that for LPAM and HPAM,  $[\eta]$  attains a minimum near  $\phi_{\text{DMF}} = 0.4$  indicating energetically most unfavorable solvent composition to be 0.4. H-bonding interactions between neighboring amide and acid groups results in a loss of the number of polymer sites available to interact with solvent molecules and this is prominent upto  $\phi_{\text{DMF}} = 0.4$ . When more DMF is added after  $\phi_{\text{DMF}} = 0.4$ , instead of free monomeric water and DMF molecules H-bonded clusters of water-DMF and DMF-DMF aggregates interact with polymer molecules. The extent of this interaction is more with LPAM where less number of carboxyl sites is present in each polymer chain. On the other hand, for NPAM where no carboxyl groups are present in the polymer chain (figure-5.1 of previous section) the nature of curves are dramatically different. Instead of giving a minimum with the variation of solvent composition, the  $[\eta]$  reaches a maximum near  $\phi_{\text{DMF}} = 0.2$  at all temperatures studied. The maximum intrinsic viscosity at this solvent composition indicates preferential solvation of the polymer due to most powerful cosolvent effect. When the DMF content is increased above  $\phi_{\text{DMF}}=0.2$ , the  $[\eta]$  is decreased due to an enhanced intramolecular interaction causing contraction of the polymer chain. Finally, the polymer is precipitated out from the solvent mixture at high  $\phi_{\text{DMF}}$  value. The cosolvency and intermolecular interaction of polymers are also manifested in the Huggins constant ( $K_H$ ) values when the composition of the solvent was varied.  $K_H$  values can be used to predict the degree of interaction between polymer and the solvent as well. The sign of  $K_H$  is often taken as a measure of the type of interaction in the polymer chain. In general, positive  $K_H$  values, which increase with the ionic strength, indicate enhanced interunit attractive interactions. Plot of  $K_H$  vs.  $\phi_{\text{DMF}}$  for LPAM is shown in the figures 5.16. The  $K_H$  values are calculated from the least square slopes of equation 16. It is observed that there is a maximum in the plot of  $K_H$  vs.  $\phi_{\text{DMF}}$  plot at  $\phi_{\text{DMF}} = 0.4$  for LPAM. However, for NPAM  $K_H$  is the smallest at  $\phi_{\text{DMF}} = 0.2$  where  $[\eta]$  is the greatest. The effect of temperature

upon  $[\eta]$  should strongly depend upon the nature of the solvent. In a poor solvent, the effective molecular shape is more compact and curled than the unbiased statistical mean. Because dissolution of polymer in poor solvent is an endothermic process and the polymer segment will attract each other in solution and squeeze out the solvent between them. In such a solvent, a temperature increase results in an increase in  $[\eta]$ . On the other hand if a solvent is energetically more favorable than the indifferent solvent then in solution the long chain molecule will be surrounded by solvated hull, which tends to prevent polymer-polymer contact. Uncurled configuration will be favored and here a temperature increase should result in the decrease in  $[\eta]$ . The effect of temperature on the intrinsic viscosity of the polymer in present mixed solvent system is interesting. In case of ionic PAM's,  $[\eta]$  decreases with temperature i.e. water-DMF mixtures behave like a good solvent. However, for NPAM, it acts as an athermal solvent as there is either no change or little change in  $[\eta]$  with temperature (figure 5.1). As has already been mentioned, increase in temperature of a polymer solution generates two mutually exclusive antagonistic effects.<sup>79,80</sup> Firstly, an increase in temperature generally leads to an increase in solubility resulting in uncoiling of the polymer chain leading to an increase in  $[\eta]$ . Secondly, an increase in temperature may lower the rotational barrier, thereby enhancing the degree of rotation about a skeletal bond, forcing the molecular chain to assume more compact coiled configuration. This leads to the decrease in  $[\eta]$  value with temperature. In case of NPAM, both of these effects are equally important and the solvent mixture behaves as an athermal system. However, in case of ionic PAM's, some of the H-bonds between amide groups are no longer present and the rotation about the skeletal bonds is enhanced. The former effect is thus superseded by the later and, therefore,  $[\eta]$  decreases with temperature.

## ACTIVATION PARAMETER

Intrinsic viscosity data are used to evaluate activation parameters of viscous flow using Frenkel-Eyring equation as follows:<sup>114</sup>

$$[\eta] = Nh/V \exp (\Delta G^{\#}_{vis}/RT) \quad 24$$

where  $V$ ,  $N$ ,  $h$ ,  $R$ ,  $\Delta G^{\#}_{vis}$  and  $T$  are molar volume of the solution, Avogadro's number, Planck's constant, ideal gas constant, activation free energy for the viscous flow and the temperature in K respectively. The equation 24 can be rewritten as

$$\ln(\eta V/Nh) = \Delta G_{vis}^{\#}/RT = \Delta H_{vis}^{\#}/RT - \Delta S_{vis}^{\#}/R \quad 25$$

where  $\Delta H_{vis}^{\#}$  and  $\Delta S_{vis}^{\#}$  are enthalpy and entropy of activation for the viscous flow respectively. The linearity is observed by plotting  $\ln(\eta V/Nh)$  against  $T^{-1}$  with correlation coefficient of 0.95 or higher for all the systems except NPAM. Some representative plots are given in figure-5.17.  $\Delta H_{vis}^{\#}$  and  $\Delta S_{vis}^{\#}$  values at different polymer concentrations and solvent compositions for hydrolyzed PAMs are shown in table-5.6 and table-5.7. These values were extrapolated to zero polymer concentration to evaluate  $\Delta H_{vis}^{\#0}$  and  $\Delta S_{vis}^{\#0}$ , which are presented in the table-5.8. Positive values of  $\Delta H_{vis}^{\#}$  and  $\Delta S_{vis}^{\#}$  were obtained for LPAM and HPAM.  $\Delta H_{vis}^{\#0}$  and  $\Delta S_{vis}^{\#0}$  values are found to be functions of solvent composition. Interestingly, on plotting  $\Delta H_{vis}^{\#}$  against  $\Delta S_{vis}^{\#}$  a straight line was obtained.

**Table 5.6**  $\Delta H_{vis}^{\#}$  (J.mol<sup>-1</sup>) for HPAM and LPAM in different solvent composition and concentrations of polymers.

$\Phi_{DMF}$	0.97X10 <sup>-3</sup> g/ml		0.58X10 <sup>-3</sup> g/ml		0.35X10 <sup>-3</sup> g/ml		0.21X10 <sup>-3</sup> g/ml	
	HPAM	LPAM	HPAM	LPAM	HPAM	LPAM	HPAM	LPAM
0.0	649	741	145	671	257	263	4705	4441
0.1	187	386	760	453	1276	1483	1176	1771
0.2	867	797	913	165	1284	1090	1675	3348
0.4	453	755	752	96	1565	1876	1526	4552
0.6	380	656	442	1698	962	1006	678	3335
0.8	393	755	312	64	826	1304	1178	3114

**Table 5.7**  $\Delta S_{vis}^{\#}$  (J.mol<sup>-1</sup>.K<sup>-1</sup>) for HPAM and LPAM in different solvent composition and concentrations of polymers.

$\Phi_{DMF}$	0.97X10 <sup>-3</sup> g/ml		0.58X10 <sup>-3</sup> g/ml		0.35X10 <sup>-3</sup> g/ml		0.21X10 <sup>-3</sup> g/ml	
	HPAM	LPAM	HPAM	LPAM	HPAM	LPAM	HPAM	LPAM
0.0	29.35	29.43	31.17	29.84	31.02	24.66	17.25	17.71
0.1	30.74	30.40	29.16	30.24	27.70	26.90	27.90	25.70
0.2	28.70	29.25	28.62	31.20	27.56	28.07	26.10	20.55
0.4	29.96	29.24	29.11	31.12	26.60	25.20	26.34	16.10
0.6	30.35	29.31	30.20	25.50	28.60	27.70	29.30	20.00
0.8	30.27	28.06	30.68	30.06	29.15	26.21	28.02	20.70

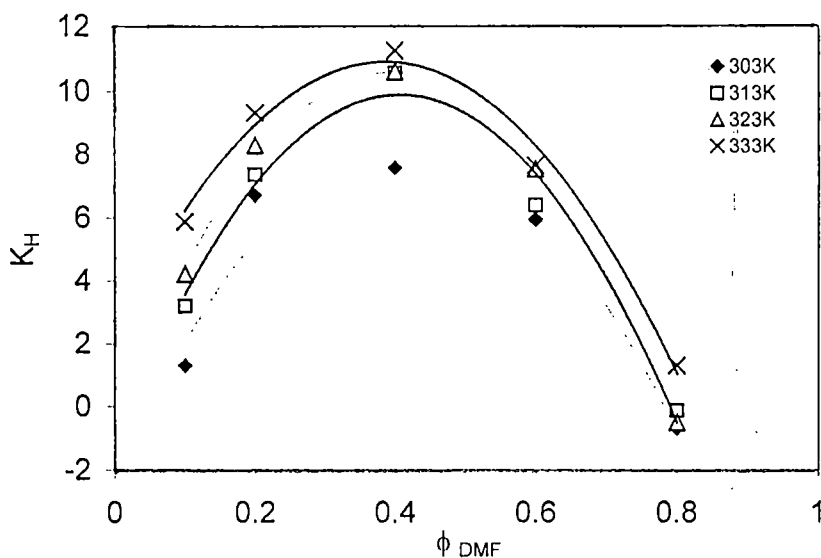


Figure:5.16:Plot of Huggins constant vs. fraction of DMF for LPAM at different temperatures.

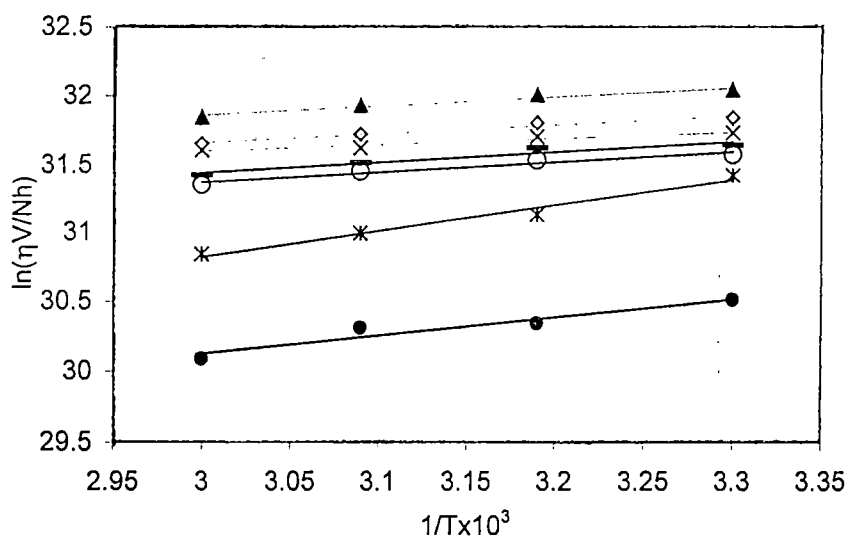


Figure:5.17:Plot of  $\ln(\eta V/Nh)$  vs.  $1/T$  for LPAM and HPAM at different concentrations of polymers and in various solvent compositions.(L is for LPAM and H is for HPAM)

◇ L/0.000972g/mL    ▲ L/0.000582g/mL    × L/0.1/0.000582g/mL  
 \* L/0.4/0.0003499g/mL    ● L/0.8/0.0003499g/mL    — H/0.000972g/mL  
 ○ H/0.4/0.000532g/mL

**Table 5.8 Activation parameters of HPAM and LPAM at infinite dilution.**

$\Phi_{\text{DMF}}$	HPAM		LPAM	
	$\Delta H_{\text{vis}}^{\# 0}$ (J.mol <sup>-1</sup> )	$\Delta S_{\text{vis}}^{\# 0}$ (J.mol <sup>-1</sup> .K <sup>-1</sup> )	$\Delta H_{\text{vis}}^{\# 0}$ (J.mol <sup>-1</sup> )	$\Delta S_{\text{vis}}^{\# 0}$ (J.mol <sup>-1</sup> .K <sup>-1</sup> )
0.0	-----	32.347	3422	17.277
0.1	1610	26.150	2030	24.951
0.2	1708	26.112	3008	21.604
0.4	1907	25.290	5317	16.377
0.6	1138	28.088	3961	20.926
0.8	1273	27.410	2962	21.095

Such a free energy relationships has been reported previously for many systems<sup>83</sup>. The slopes of the plots that yield the values of structural temperatures are found to be different for different solvent systems. Structural temperature is the temperature at which free energy of activation for the viscous flow is assumed to be independent of the entropic forces and solely depends on enthalpic forces<sup>68</sup>. Observed structural temperatures are found to increase with DMF content of the solvent mixture.

### **VOLUME RELATED PARAMETER**

Reduced viscosity values of different types of PAM were used to calculate the volume related parameter ( $V_E$ ) of the polymer solutions. The volume related parameter is a function of temperature and is a measure of volume of the solvated polymer molecules. Values of  $V_E$  (table-5.9) for HPAM show that initially the polymer molecules become less solvated and at higher fraction of DMF the polymer molecules become highly solvated. For NPAM (table-5.5), however, just opposite trend is observed; initially the polymer molecules are highly solvated and at higher DMF content the polymer are assuming compact coiled configuration. This variation of  $V_E$  with fraction of DMF is similar to that of intrinsic viscosity. Poorer is the solvent lesser is the degree solvation and this is well reflected in the corresponding  $V_E$  values. This result is expected from  $[\eta]$  vs.  $\phi_{\text{DMF}}$  plot also. In case of LPAM the said trend is observed only at 323K. The effect of temperature on  $V_E$  is rather interesting.

**Table 5.9** Volume related parameter ( $V_E \text{ dl g}^{-1}$ ) of HPAM and LPAM in different solvent compositions at different temperatures.

$\phi_{\text{DMF}}$	303K		313K		323K		333K	
	HPAM	LPAM	HPAM	LPAM	HPAM	LPAM	HPAM	LPAM
0.0	6.02	6.93	6.21	4.91	6.10	4.48	5.90	4.61
0.1	4.57	4.78	4.65	4.09	4.49	3.75	3.83	3.23
0.2	2.08	3.73	4.35	3.82	4.05	3.55	3.52	3.27
0.4	3.06	3.28	4.23	2.49	3.57	2.16	3.11	1.99
0.6	3.48	2.16	4.32	1.62	4.02	0.80	3.63	1.68
0.8	4.71	1.45	5.00	1.45	4.68	1.41	4.21	0.96

In the case of HPAM, initially  $V_E$  increases with temperature and then decreases. For NPAM also the volume related parameter,  $V_E$ , increases with increasing temperature. On the other hand, in the case of LPAM a decrease in  $V_E$  is observed with an increase in temperature. An increase in temperature may lower the rotational barrier, thereby enhancing the degree of rotation about a skeletal bond, forcing the molecular chain to assume more compact coiled configuration. The difference in behaviour between HPAM and LPAM may be due to the difference in their ion content. From table 5.5 it is found that the value of  $v$  for NPAM is  $\sim 2.5$ . Obviously, the nonionic polyacrylamide molecules assume near-spherical shapes in solution. The shape factors,  $v$ , for HPAM and LPAM are presented in table 5.10. The values of  $v$  suggest that shapes of LPAM and HPAM molecules are not always spherical, particularly when the cosolvent effect is poor. However, at high cosolvent condition the polymer molecules, particularly those of LPAM, assume spherical shape in solution.

## EXPANSION FACTOR

The molecular expansion factor ( $\alpha$ ), which represents the effect of long-range interaction, can be described as an osmotic swelling of the chain by the solvent-polymer interaction. From the theory of polymer it is known that.<sup>16</sup>

$$[\eta] = \Phi (r_o^2/M)^{3/2} M^{1/2} \alpha^3 = KM^{1/2} \alpha^3 \quad 26$$

where  $\Phi$  = Flory constant =  $2.84 \times 10^{23}$  for intrinsic viscosity expressed in mL/g (independent of polymer, solvent and the temperature),  $r_o^2$  = mean square end-to-end

unperturbed distance of the polymer coil (independent of solvent and temperature),  
 $M$  = molecular weight of the polymer and  $\alpha$  = expansion factor of the polymer.

**Table 5.10 Shape factor ( $\nu$ ) of HPAM and LPAM in different solvent compositions at different temperatures.**

$\phi_{\text{DMF}}$	303K		313K		323K		333K	
	HPAM	LPAM	HPAM	LPAM	HPAM	LPAM	HPAM	LPAM
0.0	2.09	1.73	2.30	2.73	2.35	2.43	2.55	1.54
0.1	2.50	2.50	2.17	2.44	2.25	2.21	2.50	1.93
0.2	2.63	2.33	2.51	2.03	2.32	1.71	1.83	1.40
0.4	2.30	1.56	2.45	2.44	2.45	2.45	1.58	1.99
0.6	2.48	1.57	2.62	1.83	2.42	2.90	2.55	1.06
0.8	2.59	2.60	2.50	2.53	2.42	2.73	2.45	2.14

**Table 5.11 Expansion factors of HPAM and LPAM in different solvent compositions at different temperatures.**

$\phi_{\text{DMF}}$	303K		313K		323K		333K	
	HPAM	LPAM	HPAM	LPAM	HPAM	LPAM	HPAM	LPAM
0.1	1.002	0.953	0.960	0.923	0.960	0.887	0.950	0.858
0.2	0.910	0.860	0.940	0.850	0.940	0.800	0.930	0.776
0.4	0.980	0.723	0.940	0.450	0.940	0.542	0.930	0.463
0.6	0.990	0.630	0.970	0.615	0.980	0.580	0.970	0.570
0.8	1.020	0.651	0.940	0.661	1.010	0.687	1.000	0.586

For a given polymer, the unperturbed dimension of the polymer chain ( $k_0$ ) is constant.  
Therefore,

$$\ln[\eta]/[\eta]_0 = (\alpha/\alpha_0)^3$$

27

where  $[\eta]$  and  $[\eta]_0$  are intrinsic viscosities of the polymer in the solvent mixture and in pure water respectively.  $\alpha$  and  $\alpha_0$  have the same significance as the expansion factors. From table-5.11 it is seen that the expansion factor  $\alpha$  of HPAM and LPAM decreases as  $\phi_{DMF}$  increases and at  $\phi_{DMF} = 0.4$  there is a minimum (indeed according to the table the value of  $\phi_{DMF}$  for that minimum depends slightly on temperature) that means the unperturbed end-to-end distance of both LPAM and HPAM increases with  $\phi_{DMF}$  initially and then decreases passing through a maximum. Interestingly, like ionic polymers, the unperturbed end-to-end distance for NPAM (table-5.3) also increases with  $\phi_{DMF}$  at the water rich region.

### 5 B 3 APPLICATION OF HUGGINS EQUATION BELOW THE OVERLAP CONCENTRATION

Classically, the apparent divergence of the reduced viscosity at small polymer concentrations is linearized with a so-called Fuoss-Strauss plot based upon the empirical equation<sup>115-117</sup>

$$\eta_{sp}/C = (A + B C^{0.5})^{-1} \quad 28$$

In the recent polyelectrolyte literature, some theoretical explanations for the meaning of the terms (A & B of equation 28) involved in the equation are given. More recent study has shown that the above equation is basically an empirical equation and physical meaning of the constants A & B is not as clear as originally suggested by Fuoss.<sup>118</sup> Similar results were reported by Kim and others for sulphonated PS ionomers and discussed in terms of a recent theory of polyelectrolyte viscosity.<sup>122-124</sup> Reduced viscosity increases with the decrease in concentration of the polymer and reaches its maximum at the overlap concentration. It can be assumed that polymer molecules have reached a final state of expansion in this range of concentration and that the reduced viscosity then decreases at lower concentrations according to Huggins' equation.<sup>122,123</sup> In the present investigation, viscosities are measured at different concentrations below the overlap concentration, which vary linearly and the intrinsic viscosity is determined by extrapolating the straight line to zero concentration (straight lines are drawn by least square method). Following discussion is based on calculations avoiding Fuoss linearization. Figure 5.18 – 5.21 show that if the reduced viscosity of HPAM solutions is plotted against the concentrations of polymer solutions, it passes through a maximum. The sharp increase in reduced viscosity with

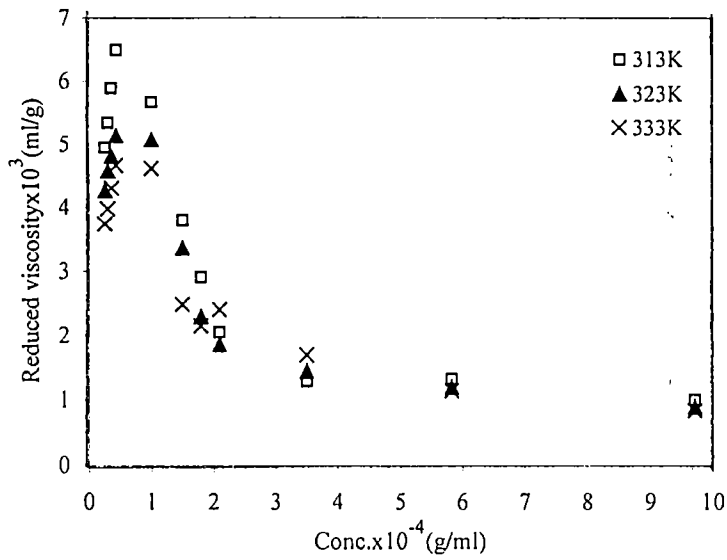


Figure 5.18: Reduced Viscosity vs. concentration (above and below overlap concentration) plot for HPAM in pure water at different temperatures.

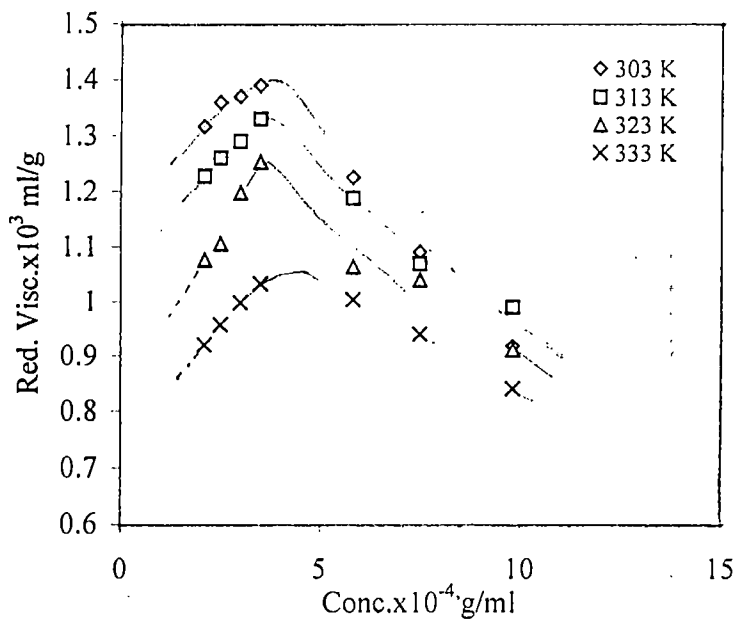


Figure 5.19: Reduced viscosity vs. concentration plot for HPAM in water-DMF mixture ( $\phi_{\text{DMF}}=0.1$ ).

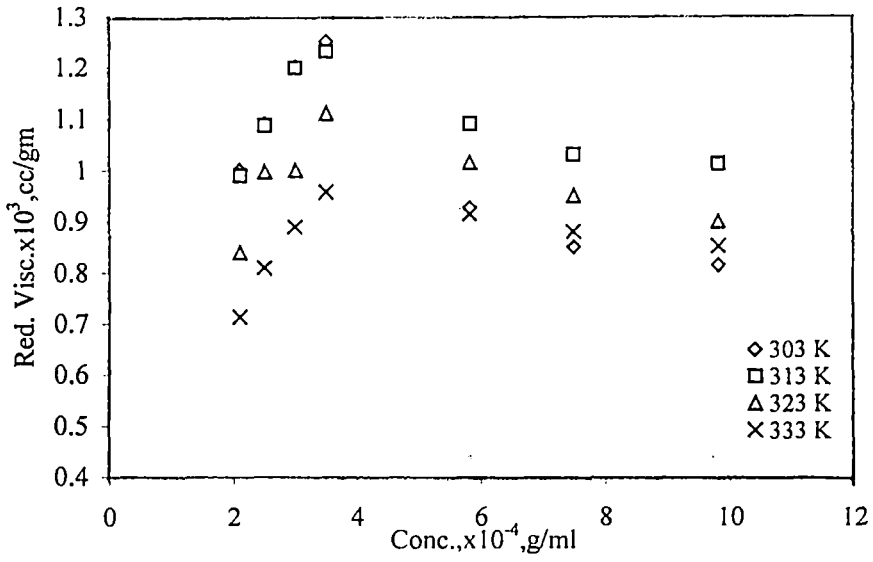


Figure:5.20 :Reduced viscosity vs. concentration plot for HPAM in water-DMF mixture( $\phi_{DMF}=0.2$ )

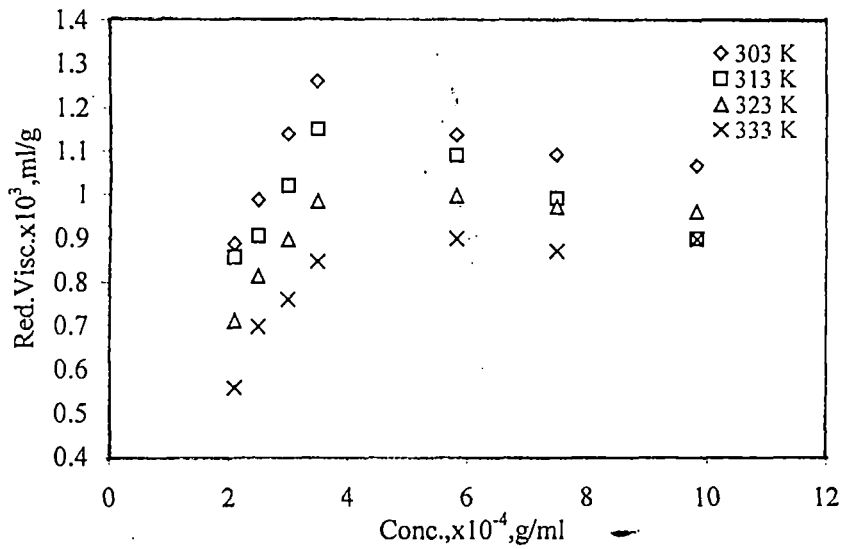


Figure:5.21 :Reduced viscosity vs. concentration plot for HPAM in water-DMF mixture( $\phi_{DMF}=0.4$ ).

decreasing concentration of polymer can be accounted for in terms of progressively enhanced dissociation of the ionisable groups on dilution. The maximum, which corresponds to the overlap concentration, is found to be different for different compositions of solvent. At this point it is assumed that molecules have reached a final state of expansion and below this concentration the reduced viscosity decreases according to the Huggins equation. In section 5.B it was not possible to discuss on the values of  $K_H$  for HPAM because it could not be measured due to the manifestation of polyelectrolyte behavior in HPAM with respect to its solution viscosity and the analysis of data was made by using Fuoss equation in the semi dilute regime. Plot of Huggins' constant vs. solvent composition is shown in the figure 5.23. Intrinsic viscosity measured using above method is plotted against the solvent composition and is shown in the figure 5.22. Interestingly, when these plots are compared with those obtained using Huggins equation although a small difference in intrinsic viscosity values is observed there was practically identical trend of intrinsic viscosity variation with solvent composition. Small difference in intrinsic viscosity values may be attributed to the limitations of the applicability of Fuoss's empirical equation through the whole concentration range of the polyelectrolyte solution. It is observed from the figure 22 & 23 that there is a maximum in the plot of  $K_H$  vs.  $\phi_{DMF}$  at  $\phi_{DMF}=0.4$  for HPAM.

**Table 5.12** Volume related parameter ( $V_E$  dl $g^{-1}$ ) of HPAM in different solvent compositions at different temperatures

$\phi_{DMF}$	303K	313K	323K	333K
0.1	4.87	4.93	3.50	3.01
0.2	2.39	2.56	2.21	2.01
0.4	1.38	1.59	1.31	1.09
0.6	1.75	2.81	2.71	2.65
0.8	4.98	5.17	4.59	4.21

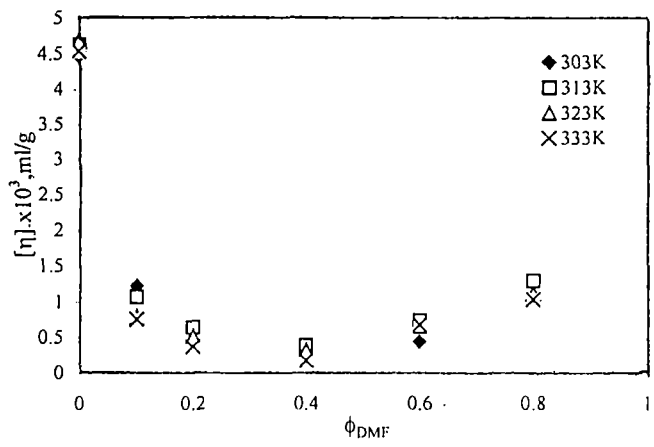


Figure: 5.22 :Variation of intrinsic viscosity of HPAM with the fraction of DMF in water-DMF mixtures at different temperatures.

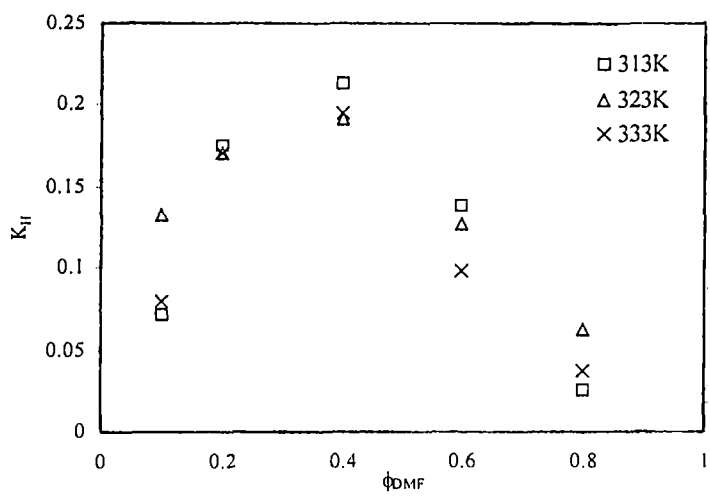


Figure: 5.23 :Variation of Huggins constant with the fraction of N,N dimethyl formamide in water-DMF mixture at different temperatures

**Table 5.13** Shape factor ( $\nu$ ) of HPAM in different solvent compositions at different temperatures.

$\Phi_{\text{DMF}}$	303K	313K	323K	333K
0.1	2.68	2.55	2.40	2.53
0.2	4.45	2.51	2.50	2.60
0.4	3.72	2.60	2.80	2.90
0.6	3.50	2.80	2.83	2.86
0.8	2.80	2.20	2.65	2.77

**Table 5.14** Expansion factors of HPAM in different solvent compositions at different temperatures.

$\Phi_{\text{DMF}}$	303K	313K	323K	333K
0.1	0.83	0.79	0.77	0.78
0.2	0.67	0.68	0.67	0.61
0.4	0.54	0.57	0.58	0.49
0.6	0.58	0.71	0.73	0.76
0.8	0.85	0.84	0.87	0.87

As expected intrinsic viscosity is minimum at this solvent composition. Like LPAM the cosolvency and intermolecular interaction of HPAM are also manifested in the values of  $K_H$  when the solvent composition is varied. The viscosity measured by the above method is used to determine the volume related parameter ( $V_E$ ), molecular expansion factor ( $\alpha$ ) and the shape factor ( $\nu$ ). These values are tabulated in tables 5.12-5.14. In this case also same trend of variation of the above parameters with solvent composition is observed. Values of  $V_E$  (table-5.12) for HPAM show that initially the polymer molecules become less solvated and at higher fraction of DMF the polymer molecules become highly solvated. Values of  $\nu$  (table-5.13) suggest that shapes of LPAM and HPAM molecules are not always spherical, particularly when the cosolvent effect is poor. From table-5.14 it is seen that the expansion factor  $\alpha$  of

HPAM decreases as  $\phi_{\text{DMF}}$  increases and at  $\phi_{\text{DMF}}=0.4$  there is a minimum. Explanation pertaining to the variation of the values of these parameters with the solvent composition is already given in the previous section.

## 5 C REFERENCES

1. C.I. Simionescu, B.C. Simionescu and S. Ioan. *J. Macromol. Sci. Chem.*, **A22**, 765 (1985).
2. S. Ioan, M. Bercea, C.I. Simionescu and B.C. Simionescu. In: Salamon JC, editor. *The polymeric encyclopaedia: synthesis, properties and applications*, 11. Boca Raton FL: CRC Press, 8417 (1996)
3. P. Debye and I.M. Krieger (unpublished) have shown that the average distribution of each segment about the centre of gravity is exactly Gaussian for random chain unperturbed by intramolecular interactions.
4. A. Dondos and H. Benoit, *Macromolecules*, **4**(3), 279 (1971).
5. R. Tajero, C. Gómez, B. Celda, R. Gavara, and A. Campos, *Makromol. Chem*, **189** (7), 1643 (1988).
6. I.A. Katime and J.R. Quintana, *J. Macromol. Chem.*, **189**(6), 1373 (1988).
7. L. Katime and J.R. Schio, *Eur. Polym. J.*, **20**(1), 99 (1984).
8. T. Schwartz, J. Sabbadin, and J. Francois, *J. Polymer*, **22**, 609 (1979).
9. J. Francois, D. Sarazin, T.S. Schwartz and G. Weill, *Polymer*, **20**, 969 (1979).
10. T. Schwartz, J. Francois, and G. Weill. *Polymer*, **21**, 247 (1980)
11. W. Scholtan, *Macromol Chem*, **14**(1), 169, (1954)
12. S. Newman, S. Krigbaum, W.R. Laugier, and P.J. Flory, *J. Polym Sci*, **14**, 451 (1954).
13. G.S. Misra and S.H. Bhattacharya, *Eur Polym J.*, **15**, 125 (1979).
14. M. Bohdonecky, V. Petrus and B. Sedlacek, *Makromol Chem*, **184**, 2061 (1983).
15. P.J. Flory and T.G. Fox, *J Am Chem Soc*, **73**:1904 and 1915. (1951).

16. H. Kurata, W.H. Stockmayer and A. Roig, *J Chem Phys*, **33**(1), 151 (1960).
17. G.C. Berry and E.F. Casassa, *J Polym Sci-Macromolecular reviews*, **4** (1), 1-66. (1970)
18. W. Buchard, *Makromol. Chem.* **50**, 20(1960).
19. W.H. Stockmayer and M. Fixman, *J. Polym. Sci.*, **C 1**,137 (1963).
20. J.M.G. Cowie, *Polymer*; **7**(10), 487(1966).
21. A. Dondos and H. Benoit, *Polymer*, **19**(5), 523.(1978).
22. M. Ueda and K. Kajitani, *Macromol Chem*, **108**(1), 138(1967)
23. M.A Bohdanecky, *J Polym Sci (B)*, **3**(3), 201(1965)
24. G. Tanaka, *Macromolecules*. **15**, 1028(1982).
25. M. Bohdanecky, *J. Polym. Sci.*, (B), **3**,201(1965).
26. J. W. Qian and A. Rudin, *Eur Polym J.*, **28**, 725 (1992)
27. J.W. Qian and A. Rudin, *Eur Polym J.*, **28**, 733. (1992)
28. S. Ioan, M. Bercea, S. Ioan and B.C. Simionescu, *Eur. Polym. J.* **23**, 69 (1987).
29. B.C. Simionescu, S. Ioan, M. Bercea and C.I. Simionescu, *Eur. Polym. J.*, **27**, 589 (1991)
30. C.I. Simionescu, S. Ioan, A. Flondor and B.C. Simionescu, *Makromol Chem.*; **189**, 2331. (1988)
31. S.L enka, P. Nayak and M. Dash, *J. Macromo. Sci. Chem.* **A19** (3), 321 (1983).
32. A. Dondos and H. Benoit, *Macromolecules*. **6**(2), 242(1973).
33. P.J. Flory, *Principles of Polymer Chemistry*, Cornell University Press, Ithaca, N.W., chap. XIV,(1953).
34. I.W. Vanden Berg, G. V. Ridder and C.A. Smoldevs, *Eur. Polym. J.* **17**, 935 (1981).
35. G. Tanaka, K.V.S.N. Raju and M. Yaseen, *J. Appl. Polym. Sci.* **43**, 1533 (1991).
36. H. Haneczek and E. Turska, *Polymer*. **24**, 1590 (1983).

37. H.W. Chatfield, "Varnish Constients", Leonard Hill Ltd., London, 412, 419 (1953).
38. K. Savas and K. Zuhai, *Polymer Communications*, **31(1)**, 35 (1990).
39. P. Vasudevan and M. Santappa, *Makromol. Chem.*, **137**, 261 (1970).
40. I. Nishio, S. T. Sun, G. Swislow and T. Tanaka, *Nature*, **281**, 208 (1979).
41. B. Maitra and A.K. Nandi, *Polymer*, **34(6)**, 1260 (1993).
42. O. Chintore, M. Guaita and L. Trossarelli, *Makromol. Chem.* **180**, 2019 (1979).
43. O. Chintore, M. Guaita and L. Trossarelli, *Makromol. Chem.* **180**, 969 (1979).
44. M. Kurata, Y. Tsunashima, M. Iwama and K. Kamada, in: "Polymer Handbook", edited by J. Brandrup and E.H. Immergut, 2<sup>nd</sup> edition, Wiley-Interscience, New York, IV-36, (1975).
45. S. Newman, W.R. Krigbaum, C. Laugier and P.J. Flory, *J. Polym. Sci.*, **14**, 451 (1954).
46. W.P. Shyluk and F.S. Stow, *Jr. J. Appl. Polym. Sci.* **13**, 1023 (1969).
47. N. Narkis and M. Rebhun, *Polymer*, **6**, 507 (1996).
48. R. Boyadjian, G. Seytre, P. Berticat and G. Vallet, *Eur. Polym. J.* **12**, 401 (1975)
49. W. Scholtan, *Makromol. Chem.*, **14**, 169 (1954).
50. E. Collison, F.S. Dainton and G.S. Mcnaughton, *Trans Faraday Soc.*, **53**, 489 (1997).
51. J. Francois, D. Sarazin, T. Schwartz and G. Weill, *Polymer*, **20**, 969 (1979).
52. T. Schwartz, J. Sabbadin and J. Francois, *Polymer*. **22**, 609 (1981).
53. C. Okada, K. kamada, T. Yoshihara, J. Hosoda and A. Fumuro, 'Reports on Progress in Polymer Physics in Japan' XX5, (1977).
54. N. Yamaguchi; N. Onda and Y. Hirai, 'Reports on progress in Polymer physics in Japan' XXI, 63 (1978).
55. S.R. Gooda and M.B. Huglin, *Polymer*. **34(9)**, 1913 (1993).
56. S. Newman, W.R. Krigbaum, C. Laugier and P.J. Flory, *J. Polym. Sci.*, **14**, 451 (1954).

57. P. Bera and S.K. Saha, *Eur. Polym. J.*, **37**, 2327 (2001)
58. C.I. Simionescu, S. Ioan, and B.C. Simionescu, *Rev Roum Chim.*, **31**, 995 (1986).
58. M. Bercea, S. Morariu, S. Ioan and B.C. Simionescu, *Synth Polym J.*, **1**, 81 (1994)
60. M. Bercea, C. Ioan, S. Morariu, S. Ioan, and B.C. Simionescu, *Polym Plast. Technol. Eng.*, **37**, 295,(1998).
61. K.K. Chee, *Eur. Polym. J.***31 (2)**, 1559 (1995).
62. E.E. Kathmann and C.L. McCormick *J.Polym.Sci.Part A:Polymer Chemistry.*, **35**, 23(1997).
63. M.B. Hocking, K.A. Klimchuk and S. Lowen, *J. Polym. Sci. Part A : Polymer Chemistry*, **38**, 3128(2000).
64. Shahui Wu and R. A. Shanks, *J.Appl.Polym.Sci.*,**89**,3122(2003).
65. S. Alorio, S. Pispas, E. siakali-Kioulafa and N. Hadjichristidis, *J.Polym. Sci.Part B : Polymer physics.* **33**, 2229(1995).
66. A. Abdel-Azim and M.B. Huglin *Eur.Polym.J.*, **18**,735(1982).
67. A.K.M. Asaduzzaman, A.K. Rakshit, S. Devi, *Colloid Polym. Sci.*, 281 (2003).
68. A.K.M. Asaduzzaman, A.K. Rakshit and S. Devi, *J. Appl. Polym Sci*, **47(10)**, 1813 (1993).
69. R. Simha, *J Phys Chem*, **44(1)**, 25 (1940).
70. A.B. Mandal, S. Ray, A.M. Biswas and S.P. Moulik, *J Phys Chem*, **84(8)**: 856-859. (1980).
71. T. Alfrey, A. Bartovics and H. Mark *J Am Chem Soc.*, **64**, 1557 (1942).
72. P. Rohdewald and M. Moldner, *J Phys Chem.*, **77**, 373 (1973).
73. K. Rehm and H.J. Bittrich, *Z Phys Chem (Leipzig)*. , **251**, 109 (1972).
74. C.D. Visser and G. Somsen,*J Soln Chem.* **8**,593 (1974).
75. C.D. Visser and G. Somsen,*Z Phys Chem NF.*,**92**,S159 (1974).

76. F. Kawaizumi, M. Ohno and Y. Miyahara, *Bull Chem Soc Japan*, **50**, 2229 (1977).
77. P. Asarsson and F. R. Eirich, *J Phys Chem.*, **72**, 2710 (1968).
78. T.T. Herskovis and T.M. Kelley, *J Phys Chem.*, **77**, 381 (1993).
79. I. Noda, T.T. Suge and M. Nagasawa, *J Phys Chem*, **74**, 710 (1970).
80. V. Vangani and A. K. Rakshit, *J Appl Polym Sc*, **60**(7), 1005 (1996).
81. J.F. Rabek, (Ch-2) Study of Interaction between Polymers and Solvents. *Experimental Methods in Polymer Chemistry*; Wiley-Interscience: New York, (1983).
82. J. Brandrup, and E.H. Immergut, Ch-VIII, in *polymer Handbook*, 3<sup>rd</sup> ed.; Wiley Interscience, New York, (1989).
83. A. Rangaraj and A. K. Rakshit *J. Surface Sci. Technol.* **16**,246 (2000).
84. W.M. Thomas and D.W. Wang *Acrylamide Polymers: Encyclopedia of Polymer Science and Engineering*, 2<sup>nd</sup> Ed. Mark HW, Bikales NM, Overberger CG, Menges G. Eds. Wiley & Sons: New York. **1** : 169- 211(1986).
85. J. Bock, D.N. Schulz and C.L. McCormick, 'Water Soluble Polymers: *Encyclopedia of Polymer Science and Engineering*, 2ndEd. Mark HW, Bikales NM, Overberger CG, Menges G. Eds. Wiley & Sons: New York. **17**:730 (1986);
86. E.L. Carpenters and H.S. Devis, *J Appl Chem.*, **7**,671 (1957).
87. G.J. Hoear F.L. Hudson and J. West, *J Appl Polym Sci* **21**, 1-16 and 29-43 (1977).
88. L.H. Allen and R.H. Pelton, *Colloid Polym Sci*; **261**,485 (1983).
89. M.F. McCarty and R.S. Olson, *Mining Engineering*; **11**,61 (1959).
90. G. Moody, *Minerals Engineering.*, **5**,479 (1992).
91. M. Smollen, *Water S.A.*; **12** (3),127 (1986).
92. N. Schamp and J. Huylerbroeck, *J Polym Sci Symp*, **42**,533 (1973).
93. T.H. Stutzmann and B. Siffert, *Clay Min*; **25**,392 (1977)

94. P. Somasundaran, Y.H. Chia, R. Gorelik, E.D. Goddard and B. Vincent, editors. *ACS Symp. Ser.*, **240**, 393 (1984)
95. E.N. Pefferkorn and A. Carroy, *J Colloid Inter Sci.*, **106**, 94 (1985).
96. G. Atesok, P. Somasundaran and L. Morgan. *J. Powd. Technol.*, **54**, 77 (1988).
97. L.T. Lee, R. Rahbari, J. Lecourtier and G. Chauveteau, *J Colloid Inter Sci.*, **147**, 351 (1991).
98. A.G. Clark and T.M. Herrington, *Colloids Surf.*, **44**,247 (1990).
99. R.I.S. Gill and T.M. Herrington, *Colloids Surf*, **22**, 51 (1986).
100. R.I.S. Gill and T.M. Herrington, *Colloids Surf.*, **28**, 41(1987).
101. M. Mandel and T. Odijk, *Ann Rev Phys Chem.*, **35**, 75 (1984).
102. S.H. Pinner, *J Polym Sci*; **10**,379 (1953).
103. A. Sirivat, *J Polym Sci Part B Pol. Phys.*, **36**,743 (1998).
104. N.V. Sastry, P.N. Dave and M.K. Valand, *Eur Polym J.*, **35**,517 (1999).
105. R.D. Ludenberg and R.K. Phillips, *J. Polym. Sci, Polym. Phys. Ed.* **20**, 1143 (1982).
106. X. liu, O. Hu, Z. Tong, *J. Polym. Sci B, Polym.Phys*, **35**, 1433 (1997).
107. J. Yamanaka, H. Matsuoka, H. Katino and M. Hasegawa and N. Ise, *J. Am. Soc.*, **112**, 92 (1990).
108. R.M. Davis and W.B. Russel, *Macromolecules*, **20**, 518 (1987).
109. A. Katchalsky and H. Eisenburg, *J.Polym.Sci.6*, 145, 9(1951).
110. Z. Priel and A.Silberberg.*J.Polym.Sci.A* **28**, 689(1970).
111. H. Eisenberg and J. Pouyet, *J Polym Sci*, **13**, 85 (1954).
112. Y. Rabin, J. Cohen and Z. Priel, *J Polym Sci Polym Lett.*, **26**,397(1988).
113. T.A. Witten and P. Pincus, *Europhys. Lett.*, **3**,345 (1987).
114. G.V. Vinogradov and A.Y. Malkin, *Rheology of Polymers*, 106.Mir, Moskow (1980).
115. R.M.Fuoss and J. Strauss, *J. Polym. Sci.* **3**, 246(1948).

116. R.M. Fuoss and J. Strauss. *J. Polym. Sci.*, **3**, 603 (1948).
117. R.M. Fuoss and J. Strauss. *J. Polym. Sci.* **4**, 96 (1948).
118. C. Wolf, *J.Phys.***39**, C2-169 (1978).
119. M.W. Kim and D. G. Piefer, *Europhys. Lett.* **5**, 321(1988).
120. T.A. Witten and P.Pincus, *Europhys. Lett.* **3**:315, (1987).
121. J. Cohen, Z. Priel and Y. Rabin, *J. Chem. Phys.*, **88**, 7111(1988).
122. G.S. Misra and S. L. Dubey *J. Pol. Sc.*, **17**, 1393(1979).
123. J. Yamanaka, H. Matsuoka, H. Kitano, M. Hasegawa and N. Ise, *J. Am. Chem. Soc.*, **112**, 587 (1990).

## CHAPTER 6

# STUDIES ON DILUTE SOLUTION BEHAVIOUR OF PROGRESSIVELY HYDROLYZED POLYACRYLAMIDE IN AQUEOUS SOLUTION

# **DILUTE SOLUTION BEHAVIOUR OF PROGRESSIVELY HYDROLYZED POLYACRYLAMIDE IN AQUEOUS SOLUTION**

## **6.1 INTRODUCTION AND REVIEW OF PREVIOUS WORKS**

In recent years the study of polyelectrolytes has been stimulated by the use of newly available experimental techniques and the introduction of new theoretical concepts. Solutions of polyelectrolyte exhibit a behavior that may differ considerably from that of either uncharged macromolecules or low-molar-mass electrolytes. The origin of this specificity lies in the combination of properties derived from those of long-chain molecules with properties that results from charge-charge interactions. Physical properties of polyelectrolyte solutions have been studied for more than 50 years, but several of them have not yet found a satisfactory theoretical explanation. In many cases a qualitative understanding is available but a quantitative interpretation is still lacking. The study of polyelectrolyte solution has been much more extensively done in aqueous solution than in nonaqueous solution.<sup>1,2</sup> A series of research studies conducted by Fuoss's group in the late 1940s and 1950s demonstrated the general nature of polyelectrolyte behaviour and made an important contribution in establishing major concepts of polyelectrolyte solution.<sup>3-4</sup> Subsequent studies, however, have concentrated on aqueous solution behaviour of polyelectrolyte.<sup>5,6</sup> With respect to the concept of chain expansion due to intramolecular repulsion, scattering techniques were used in addition to classical studies of viscosity.<sup>1,2</sup> The concept of counterion condensation was tested by conductometric measurements of a polyelectrolyte solution, in which the dielectric constant of the solvent was altered and the polyelectrolyte was a copolymer of 4-vinylpyridine and styrene quaternized by n-butyl bromide and the solvent was nitromethane-dioxane mixture covering the dielectric constant from 16.0 to 39.4 (ref. 7). Polyelectrolyte behaviour with respect to solution viscosity was observed for sulphonated polystyrene (PS) ionomers (Na salt) in DMSO, alpha methoxy methanol as well as in DMF (ref.8) This polymer shows similar behavior in acid form also due to dissociation of protons. It was demonstrated by Fuoss and Strauss in one of the first explorations of synthetic polyelectrolyte solution viscosity, that the effect of

charging a polymer chain complicates interpretation of viscosity experiments considerably.<sup>9,10</sup> Unbound rise of reduced viscosity with decreasing concentration for polymethacrylic acid, 2-vinylpyridine-methacrylic acid copolymer, sodium salts of pectin, carboxy methyl cellulose and polyacrylic acid was reported by a number of investigators.<sup>11-14</sup> Yamanaka, Pal and co-workers for dilute solution of sulfonated polystyrene demonstrated very strong shear rate dependence of the reduced viscosity.<sup>15,16</sup> Isoionic dilution method was used by Davis and Russel in their studies on sulfonated polystyrene and the authors found a variation of Huggins constant,  $K_H$  from 20 at low ionic strength to 0.8 at maximum ionic strength near 0.1M.<sup>17</sup> Measuring the reduced viscosity as a function of pH Katchalsky and coworkers observed an abrupt increase in reduced viscosity as pH varied above pH 6 for fractions of polymethacrylic acid.<sup>18</sup> Priel and Silberberg observed a complicated dependence of  $[\eta]$  on the mole fraction of ethanol in aqueous solution of polymethacrylic acid and interpreted the results in terms of coil to collapsed chain model.<sup>19</sup> Noda and co-workers observed an increase in the excluded volume parameter as the concentration of added salt decreased for polyacrylic acid and an increase in the apparent excluded volume parameter with the degree of ionization of the polyelectrolyte.<sup>20</sup> McCormick and Johnson<sup>21</sup> have focused their efforts on tailoring macromolecules so that their (three series of N-alkylacrylamide/ acrylamide copolymers containing up to 0.75 mol% of C8, C10, and C12 N-alkylacrylamide monomers) solution viscosity is determined by interplay between intermolecular hydrophobic or ionic interactions of certain chain segments and strong hydration of other segments. Bock and coworkers<sup>22</sup> studied the relationship between the structure and property of hydrophobically associating polymers using a series of copolymers of acrylamide and N-substituted acrylamides and also terpolymers that contain anionically charged carboxyl group. Their results show that hydrophobic association could dominate polymer conformation in solution. Intrinsic viscosities of sodium polystyrene sulfonate (PS) of narrow molecular weight distribution in the absence of coexisting salt were also measured by Ise and coworkers<sup>23</sup>. The possibility of adsorption of the macroions on the glass wall of the viscometer capillary was confirmed to be negligible.

In the polyelectrolyte expansion theory the concentration of low molar mass electrolyte is assumed to be such that electrostatic interactions produce only a perturbation on the inherent dimension of the flexible polyion chain. In a salt free

solution where the electrostatic screening length is controlled by the counter ions of the polyion, by the auto dissociation of water or by dissolved impurities ( $\text{CO}_2$ ), the assumption is not expected to apply. Under these conditions monotonic rise in reduced viscosity is observed and it was suggested that the same results may be found from the chain expansion of the polymer to a rod like conformation. The evidence for this assumption came from an extrapolation of reduced viscosity ( $\eta_{\text{red}}$ ) using Fuoss equation to obtain apparent intrinsic viscosity. Several groups of authors subsequently demonstrated that the initial rise of reduced viscosity to a maximum during dilution of salt free polyelectrolyte solution is followed by a decrease. It appears that decreasing reduced viscosity at low concentrations following the viscosity maximum can be extrapolated to apparent intrinsic viscosity. It was argued that chains were entangled and decreased in size with concentration in the range where the Fuoss equation was applicable.<sup>24</sup> Similar arguments, based on the homogeneously entangled semi dilute polyelectrolyte solutions, are given by using a scaling approach.<sup>25,26</sup> Some researchers studied the characteristics of polyelectrolyte behaviour using polystyrene based ionomers that had ionic groups randomly distributed along the chain.<sup>27</sup> In their work, the role of intra- and intermolecular interaction on polyelectrolyte behaviour of random ionomer was studied by changing the number of ionic groups per chain, since it was expected that the importance of intramolecular interaction decreased with decreasing number of ionic groups per chain. It was observed that even ionomers with small number of ions per chain showed characteristic polyelectrolyte behaviour. It was suggested that the essential factor causing polyelectrolyte behaviour was intermolecular interactions not intramolecular interactions as is usually assumed in conventional explanations.<sup>28</sup> The use of aqueous polymer solutions in secondary oil recovery has been subject of great interest. It has been reported that<sup>29</sup> more oil may be recoverable by addition of only small quantity of polymers to injection water. The choice of polymer to be added to injection water must take into consideration a number of parameters - the pH of the reservoir, the nature and concentration of salts. The effectiveness of the polymers is related to their molecular weight, the absence of branched chains and solubility in water. The enhanced recovery seems to be a consequence of molecular expansion that results from electrostatic repulsion between the charges carried by the polymer chains. As has already been mentioned that water-soluble synthetic polymers of high molecular weight have given rise to much interest due to their practical application

including the recent application in the preparation of highly viscous solutions in the secondary oil recovery process. One of the widely applied polymers for the above application is carboxyl-modified polyacrylamide (PAM). To understand the role of charged groups on factors that govern the efficiency of PAM in the above use especially in the salt rich waters, a complete molecular characterization is required. In the case of charged PAM the relative dissociation of the ionic groups and the distribution and alignment of the charged dipoles along the chain are expected to play a decisive role on the final state of conformation of the polymer chain.<sup>30</sup> The effect of hydrodynamic field on the viscosity of partially hydrolyzed PAM has been discussed in the literature.<sup>31</sup> The effect of various salt ions on the characteristic of polyelectrolyte in the aqueous solution and the site-binding interaction of salt ions and polymer using Huggins equation has been investigated.<sup>32-36</sup>

Keeping in mind the above, we have investigated the behaviour and properties of unhydrolyzed and hydrolyzed PAM according to the function of factors known to effect the expansion of polyelectrolyte molecules that is, the degree of ionization, polymer concentration and the concentration of added salt. PAM is of interest because it is possible to obtain high molecular weight samples that are easily soluble in water. Moreover, the controlled hydrolysis of PAM samples yield polymers of various charge densities. The effectiveness of the polymer with respect to the above application is related to the extension of the polymer chain. Since the extension of the dissolved chain is related to the charge densities the hydrolysis is thought to be a powerful chemical variable. Moreover, degree of hydrolysis increases salt tolerance of the polyelectrolytes with respect to its solution viscosity. The object of the work is two fold (1) to examine polyelectrolyte behavior of progressively hydrolyzed polyacrylamide with a view to ascertain the degree of polyelectrolytic property shown by an ionomer (LPAM) (2) to examine how the polyelectrolyte behavior is affected on screening of charges of the polyelectrolyte. In view of the above the results of physicochemical studies on dilute solution properties of high carboxyl content (HPAM) and low carboxyl content polyacrylamide (LPAM) in aqueous solution as a function of concentration, pH, added salt and the temperature are reported in this chapter.

---

In chapter 6 onwards, sometimes unhydrolyzed PAM is also designated as non ionic PAM or NPAM.

## 6. 2 RESULTS AND DISCUSSION

### INTRINSIC VISCOSITY

Factors, which affect the intrinsic viscosity of a polymer, include molecular weight, temperature; shear rate, chain stiffness and topology etc. Values of Huggins coefficient depend on the shear rate, temperature and molecular weight. For expanded neutral polymers in good solvents or for polyelectrolytes, the dependence of  $[\eta]$  on the shear rate can be considerable; shear rate extrapolation of the reduced viscosity is needed for quantitative comparison of experiment to theory. The effect of shear rate on the reduced viscosities of dilute polymer solutions in the presence and in the absence of added salts is shown in figures 6.1-6.4. Shear thinning behaviour is observed from the figures. Similar shear thinning behaviour was reported earlier for polystyrenesulphonic acid and its sodium and potassium salts.<sup>37</sup> HPAM and LPAM both are showing shear thinning behavior. The carboxyl content of HPAM is 72 mol% and that of LPAM is 8.2 mol%. Quite obviously the effect of electrical charges should be more for HPAM than that of LPAM. As the concentration of the polymer decreases the effect of shear on solution viscosity increases. On the other hand, as the concentration of added salt increases the polymer solutions become less sensitive to the shear flow. The substantial shear thinning effect of salt-free dilute solutions of hydrolyzed PAM may be attributed to the second order electroviscous effects, which is caused by an electrostatic interaction between macro ions to form an ordered arrangement. For linear macro ions, the flexible nature and orientation of the polymer chains in streaming solvent would also be related to the shear thinning behavior. Concentration dependence of reduced viscosity of HPAM and LPAM in salt free aqueous solutions and in the presence of 0.0125(M) NaCl for HPAM is shown in Figures 6.5-6.10. The reduced viscosity passes through a maximum in reduced viscosity vs. concentration plots. After the maximum point, reduced viscosity decreases continuously on dilution. The sharp increase in reduced viscosity with decreasing concentration can be explained in terms of the expansion of the polymer chain due to progressively enhanced dissociation of the ionisable groups. The more marked dependence of reduced viscosity at lower concentrations seems to be consistent with this explanation. At the maximum point, which is known as overlap concentration, it can be assumed that molecules have reached a final state of expansion and below this concentration the reduced viscosity decreases according to

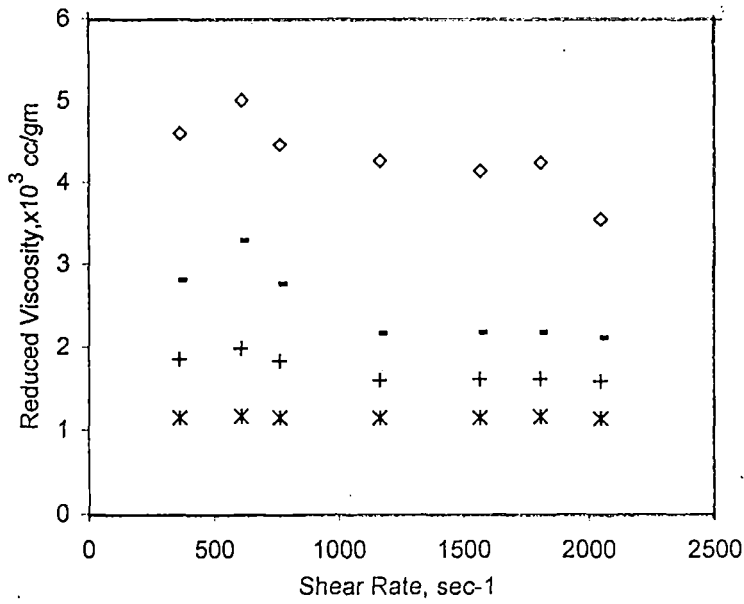


Figure:6.1:Reduced viscosity vs. shear rate for LPAM at different concentrations.

\*0.00244gm/cc +0.00122gm/cc ■0.0006gm/cc ◇0.0003gm/cc

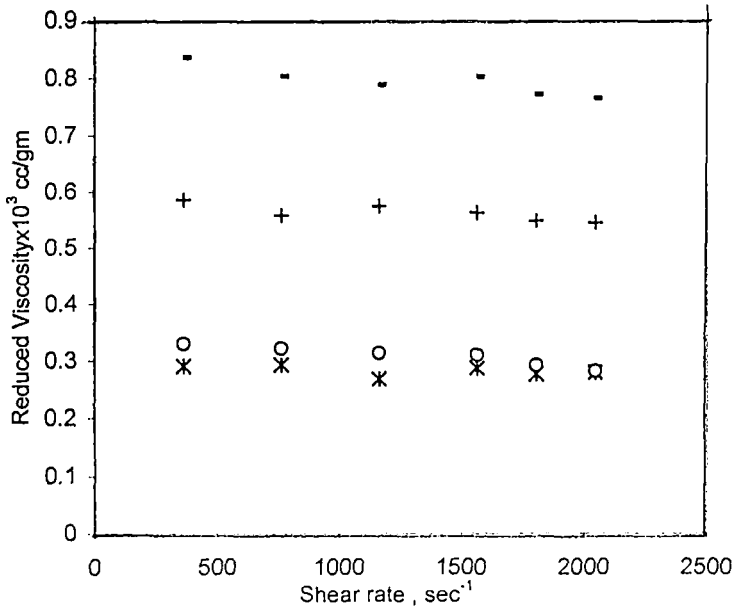


Figure:6.2:Reduced viscosity vs.shear rate of HPAM (conc.=0.00061gm/cc) in presence of various concentration(N) of NaCl.

\*0.25(N)NaCl ○0.12(N) NaCl +0.05(N)NaCl ■0.025(N)NaCl

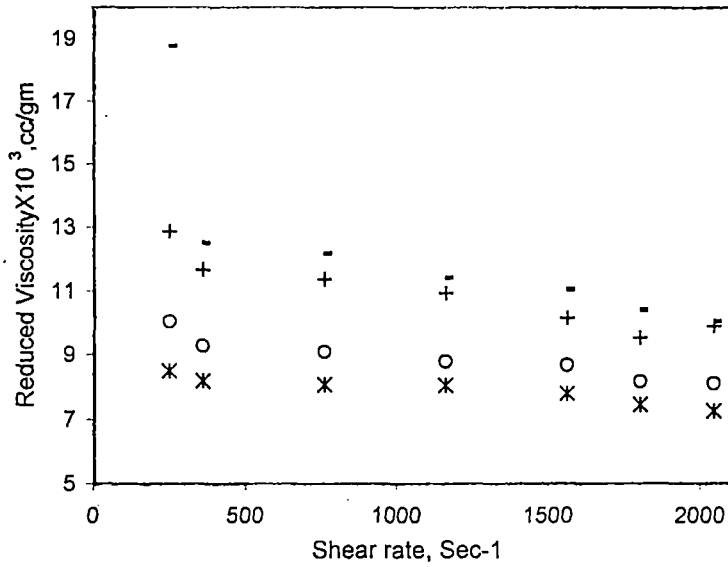


Figure 6.3: Reduced viscosity vs. shear rate of HPAM at different concentration (gm/cc): Legends are same as that LPAM.

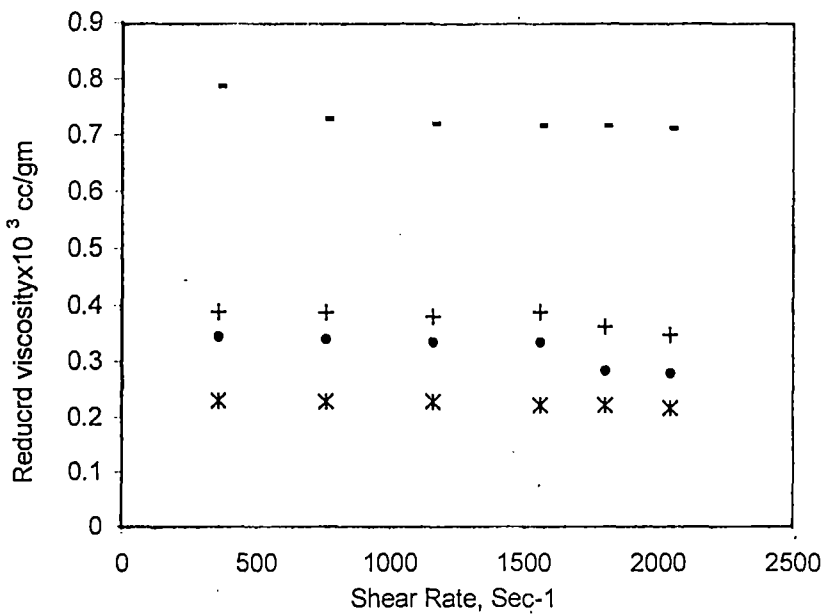


Figure 6.4: Reduced viscosity vs. shear rate of LPAM (conc. = 0.00061 gm/cc) in presence of various concentration (N) of NaCl.

$\times$  0.1(N) NaCl  $\bullet$  0.05(N) NaCl  $+$  0.025(N) NaCl  $-$  0.0125(N) NaCl

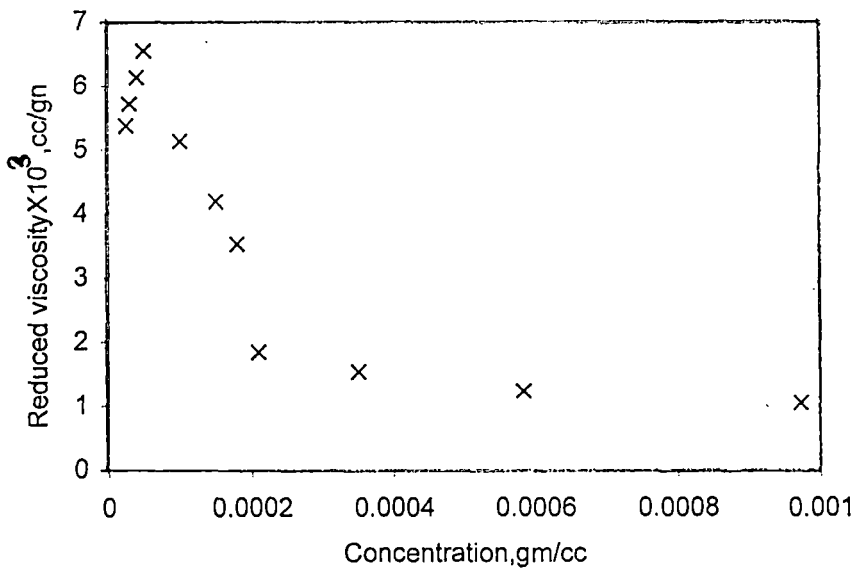


Figure:6.5:Reduced viscosity vs. concentration (below and above overlap concentration) plot for HPAM at 303K.

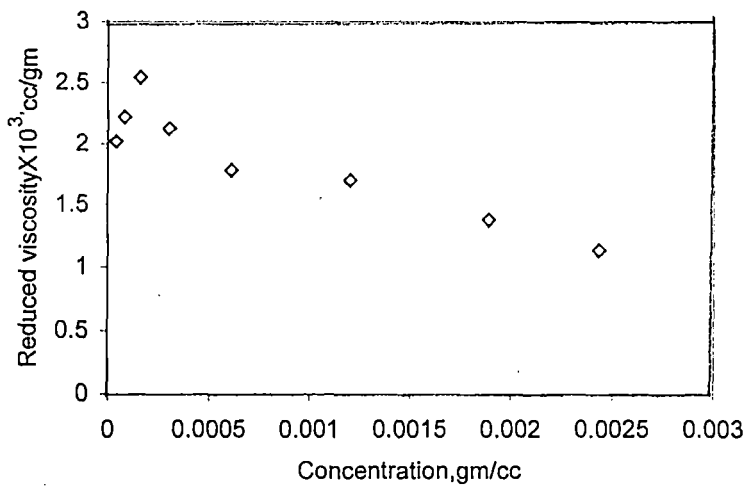


Figure:6.6:Reduced viscosity vs.concentration(below and above overlap concentration) plot for HPAM in presence of 0.0125(N) NaCl at 303K .

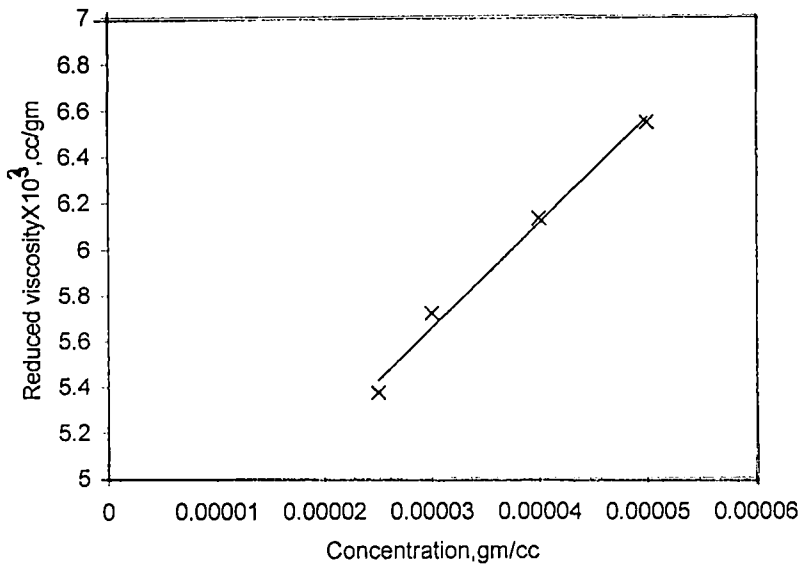


Figure:6.7:Reduced viscosity vs concentration (below overlap concentration) plot for HPAM .

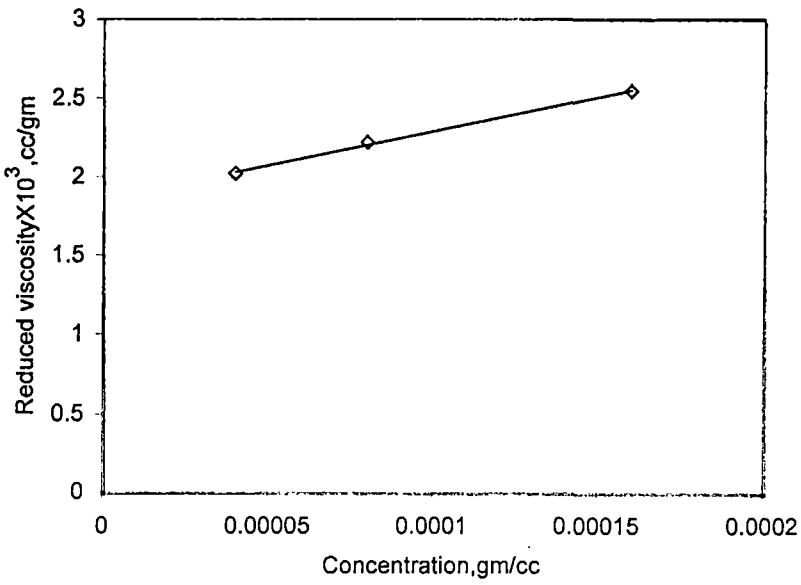


Figure:6.8:Reduced viscosity vs. concentration (below overlap concentration) plot for HPAM in presence of 0.0125(N) NaCl .

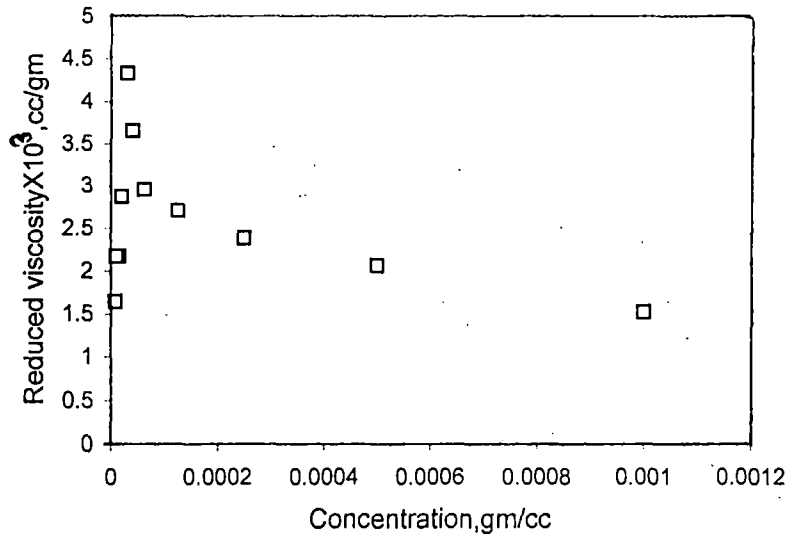


Figure:6.9: Reduced viscosity vs. concentration(below and above overlap concentration) plot for LPAM.

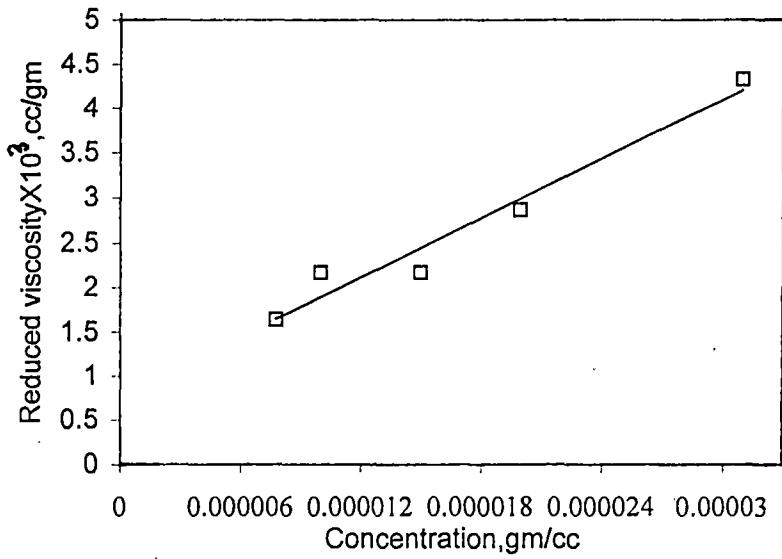


Figure:6.10: Reduced viscosity vs. concentration(below overlap concentration) for LPAM at 303K.

Huggins equation as has already been mentioned in chapter 5. The overlap concentration ( $C^*$ ) depends on the added salt concentration and on the ion content of the polymer. The magnitude of the reduced viscosity at the maximum decreases when salt concentration increases and the ion content of the polymer decreases. This behavior may be attributed to the electrostatic long-range interactions above the overlap concentration of the polymer. The  $C^*$  values of HPAM and LPAM are found to be  $5.0 \times 10^{-5}$  and  $3.0 \times 10^{-5}$  g/ml respectively. The overlap concentration of LPAM in the presence of 0.0125M NaCl and above is not detectable but for HPAM it is  $1.6 \times 10^{-4}$  in presence of 0.0125M NaCl. This value of overlap concentration is substantially higher than that in the absence of salt. At lower concentration regions ( $C < C^*$ ), the reduced viscosity decreases linearly with dilution and the extrapolation to zero concentration yields the intrinsic viscosity  $[\eta]$ .<sup>38</sup> Hydrolyzed PAMs exhibit higher reduced viscosity than their neutral counterpart.

The effect of NaCl concentration on the shear corrected reduced viscosity of LPAM and HPAM is also examined. The effect of various NaCl concentrations ranging from 0.20 to 0.0125M on the reduced viscosity of HPAM and LPAM is illustrated in figure 6.11. A significant decrease in reduced viscosity apparently occurred with an increase of NaCl concentrations. Linear extrapolation of reduced viscosity to zero polymer concentration, which is normally done to determine intrinsic viscosity for non-ionic polymers, could not be applied in the present system because of the deviation from linearity. However, at high concentration of NaCl, 0.1M for HPAM and 0.05M for LPAM, a simple linear extrapolation is possible for reduced viscosity – concentration linearity due to nonpoelectrolytic nature of the polymers under this condition. Addition of NaCl to the polymer solution increases the ionic strength of the solution outside the polymer coil relative to that of inside and also reduces the thickness of the bound layer. As a result, contraction of the polymer chain takes place. When the polymer solution is diluted in presence of a low but fixed NaCl concentration the overall ionic strength decreases. This decrease in overall ionic strength results in an increase in the distance over which electrostatic interaction can be manifested. This causes an increase in intermolecular interactions and the expansion of the polymer chain occurs. On the other hand, the decrease in zero shear reduced viscosity with polymer concentration at higher concentration of NaCl may be ascribed to the complete screening of the electrostatic potential around the bound charges resulting in the manifestation of nonpoelectrolytic behaviour.

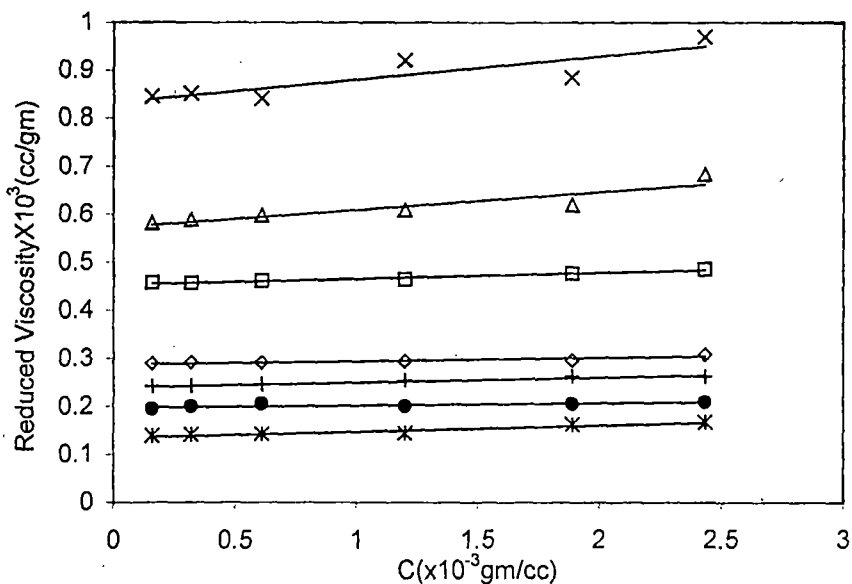


Figure:6.11 :Reduced Viscosity vs. Concentration plot for HPAM and LPAM in presence various concentration of NaCl.

$\diamond$  0.2(N),HPAM  $\square$  0.1(N),HPAM  $\Delta$  0.05(N),HPAM  
 $\times$  0.025(N),HPAM  $*$  0.1(N),LPAM  $\bullet$  0.05(N),LPAM

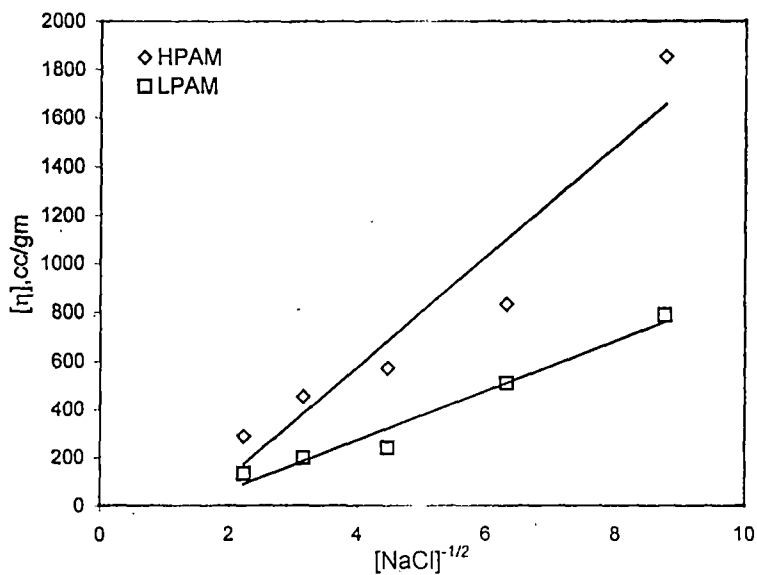


Figure:6.12:Intrinsic viscosity of carboxyl modified polyacrylamide as a function of NaCl concentration.

HPAM requires more NaCl than LPAM for the screening of bound charges due to presence of higher numbers of carboxyl sites per polymer chain. It may be recalled that the number of carboxyl sites are 8.2 and 72 mole% for LPAM and HPAM respectively. Intrinsic viscosities of HPAM and LPAM in salt free solution and in the presence of various amount of NaCl are shown in the Table-6.1. The above concept of chain contraction of the anionic polymers in presence of NaCl is clear from the presented data. A plot of intrinsic viscosity vs.  $C_{\text{NaCl}}^{-1/2}$  for both the polymers is presented in figure-6.12. This linear behavior is typical of polyelectrolytes. In the presence of added electrolytes, charge-charge repulsions between the anionic sites are shielded, leading to a decrease in the hydrodynamic volume because the polymer coils assume less extended conformation. These results have demonstrated that the viscosity behavior of a random ionomer (LPAM) is basically similar to that of a polyelectrolyte in aqueous solution. The above observation that even ionomer (LPAM) with small ion content show characteristic polyelectrolyte behavior is important. The chain expansion due to intramolecular electrostatic repulsion, which is used to explain the observed increase in reduced viscosity with concentration, may not necessarily be sufficient to cause a marked increase in viscosity at low polymer concentration for LPAM. In this context it may be argued that there is still a possibility that some polymer chains may have larger number of ionic groups in random ionomers and may lead to some chain expansion due to mutual repulsion of like charges resulting in an increase in viscosity.

**Table 6.1 Intrinsic Viscosity of hydrolyzed PAM in presence of various concentrations of NaCl.**

Conc. of NaCl (M)	HPAM, $[\eta]$ , cc.g <sup>-1</sup>	LPAM, $[\eta]$ , cc.g <sup>-1</sup>
0.2000	287	123
0.1000	452	134
0.0500	571	197
0.0250	830	239
0.0125	1853	511

## EFFECT OF pH

Since hydrolyzed PAMs behave as polyelectrolytes, the effect of pH on the reduced viscosity should be important. The results of our investigation on the reduced viscosity of carboxyl modified PAMs at different pH are shown in figure 6.13-6.14 (Only a few representative concentrations of each PAM are shown in figures). For LPAM, the reduced viscosity increases with pH and it reaches its maximum value at pH 6 and decreases at higher pH. However, for HPAM, although similar trend in reduced viscosity vs pH plot is observed, reduced viscosity is found to be maximum at pH 9. At low pH when degree of ionization is small and the repulsive interaction between undissociated carboxyl and amide groups is absent an impermeable hypercoiled conformation of the polymer chain results. On the other hand when the pH is increased overall negative charge increases due to higher degree of ionization. As a consequence polymer chain experiences more inter-unit repulsion resulting in an extended rod like structure. In the case of LPAM, ionization is almost complete (detail in next section) at pH 6.0 and it shows highest reduced viscosity at this pH. Similarly, HPAM also exhibits maxima in its reduced viscosity vs. pH plot at pH 9.0, where the ionization of the carboxyl sites are almost complete. After complete dissociation of ionizable groups, reduced viscosity decreases with pH due to shielding of the charge repulsion between charged groups of the LPAM chains. In the case of HPAM, however, this shielding is not apparent in the presence of larger number of charged groups in the chain. Similar observation has also been reported previously in the studies performed on fractions of poly methacrylic acid over a concentration range of 2 to 17 mg/ml<sup>18</sup>.

## VOLUME RELATED PARAMETER

The volume related parameter ( $V_E$ ) is a function of temperature and is a measure of volume of the solvated polymer molecules. Viscosity values of LPAM and HPAM are used to calculate the volume related parameter ( $V_E$ ) of the polymer. As has been mentioned recently,  $V_E$  can be used to determine the shape of protein molecules and some acrylate copolymers<sup>39</sup> in solutions.  $V_E$  is obtained by plotting  $Y$  against  $C$  (concentration of polymer), where

$$Y = (\eta_r^{0.5} - 1) / C \quad (1.35 \eta_r^{0.5} - 0.1) \quad 1$$

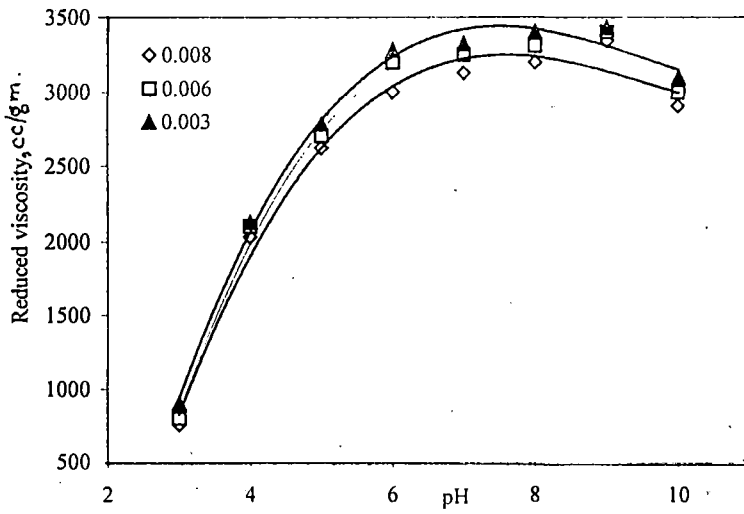


Figure:6.13 :pH vs. reduced viscosity for HPAM at different of polymer concentration (gm/ml).

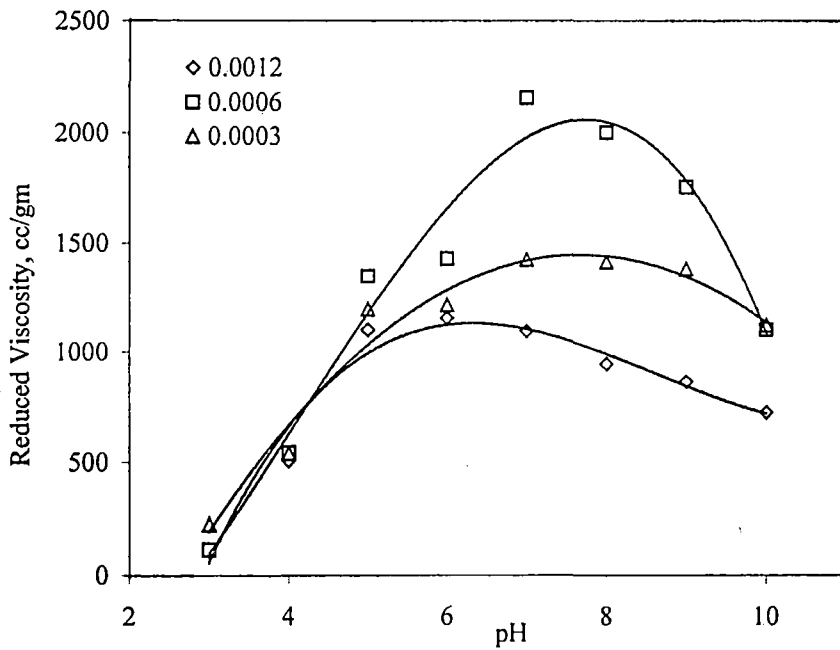


Figure:6.14:pH vs. reduced viscosity for LPAM at different concentrations (gm/ml) of polymer.

(here  $\eta_r$  is relative viscosity). The plot is linear and when it is extrapolated to  $C=0$  the intercept yielded  $V_E$  as

$$\lim_{C \rightarrow 0} Y = V_E \quad 2$$

Plots are shown in the figure 6.15-6.16. From table 6.2 it is seen that with an increase in salt concentration the volume related parameter of LPAM as well as HPAM molecules decreases. This result is expected from their intrinsic viscosity data. Shape factor values of LPAM suggest that polymer molecules are of rigid sphere configuration in presence of low concentration of added salt. On the other hand, HPAM molecules have the tendency of attaining a shape other than spherical in such a solution. Both the polymer molecules, however, assume spherical shape in presence of higher concentration of salt.

**Table 6.2 Shape factor and volume related parameter for hydrolyzed PAM in presence of various concentrations of NaCl.**

NaCl (N)	HPAM		LPAM	
	$V_E(\text{dl.g}^{-1})$	$\nu$	$V_E(\text{dl.g}^{-1})$	$\nu$
0.2000	111	2.58	48	2.56
0.1000	153	2.95	53	2.53
0.0500	159	3.59	78	2.52
0.0250	294	2.82	93	2.57
0.0125	-	-	181	2.82

## POTENTIOMETRIC MEASUREMENTS

Values of dissociation constant ( $pK_a$ ) were calculated using Henderson-Hasselbalch equation <sup>40</sup> (eq. 3). The mole % ionic character of the polymers was found to be 72 and 8.2 for HPAM and LPAM respectively.

$$pK_a = \text{pH} - \log \frac{\alpha}{1-\alpha} \quad 3$$

where  $\alpha$  is degree of ionization of the polymer sites. Plots of pH vs.  $\log \frac{\alpha}{1-\alpha}$  (figure 6.17) are made to determine  $n$  value (equation 4), which measures the

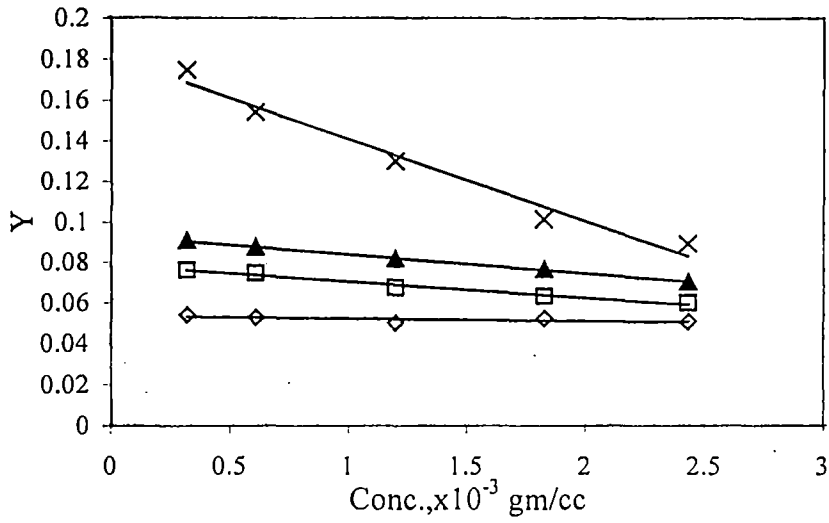


Figure:6.15:Y vs. Conc. for LPAM in presence of various concentration of NaCl.

◇ 0.1000(N) □ 0.0500(N) ▲ 0.0250(N) × 0.0125(N)

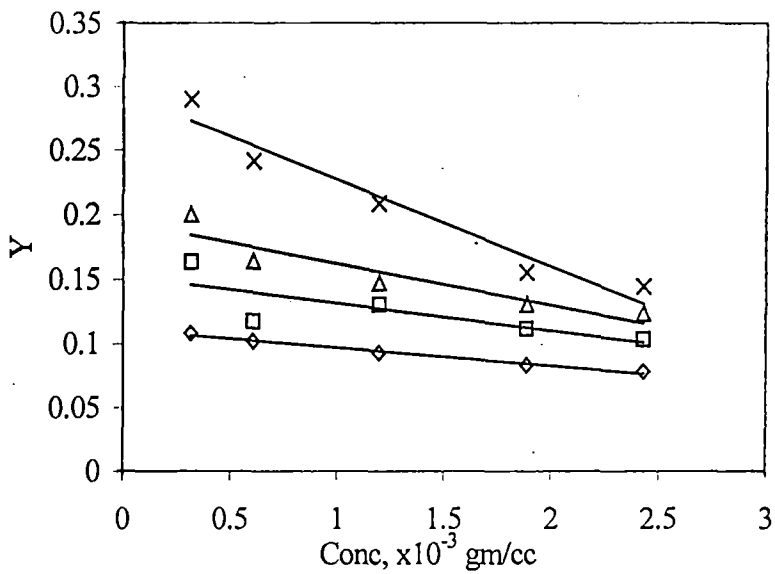


Figure:6.16:Y vs. conc. for HPAM in presence of various conc. of NaCl.

◇ 0.2000(N) □ 0.1000(N) △ 0.0500(N) × 0.0250(N)

average electrostatic repulsion between charges on the chain according to the modified Henderson-Hasselbalch equation

$$\text{pH} = \text{pK}' + n \log \alpha/1-\alpha. \quad 4$$

Calculated values of  $\alpha$ ,  $\text{pK}_a$ ,  $\text{pK}'$  and  $n$  are given in the table 6.3. In water, both  $\text{pK}'$  and  $n$  are higher for HPAM (5.78 and 2.08 respectively) than that of LPAM (4.96 and 1.33 respectively). This is a result of greater charge-charge repulsion due to higher charge density along the chain of HPAM. The increased electrostatic repulsion with increasing carboxyl content causes decreased stability of ionic groups, thereby raising the  $\text{pK}_a$  value<sup>40</sup>.

**Table 6.3 Acid strength (pKa) and degree of dissociation of hydrolyzed PAM.**

HPAM					LPAM				
pH	$\alpha$	$n$	pKa	$\text{pK}'$	pH	$\alpha$	$n$	pKa	$\text{pK}'$
4.18	0.143		4.96		3.7	9.33		4.68	
4.86	0.286		5.26		3.9	16.0		4.62	
5.53	0.428		5.65		4.3	3.30		4.60	
6.11	0.571	2.08	5.98	5.78	4.6	46.6	1.33	4.65	4.96
6.69	0.714		6.29		5.0	62.66		4.77	
7.32	0.857		6.54		5.6	77.33		5.06	
					6.6	92.0		5.54	

The  $\text{pK}'$  values in salt free solution show a greater conformational changes. At low degree of dissociation where there is little charge-charge repulsion, the polymers appear to be in a compact, random coil conformation. As the degree of dissociation increases, the repulsion between charges increases and the conformation of the chain changes to an extended almost rod like molecule with maximum size coming at  $\alpha = 1$ .

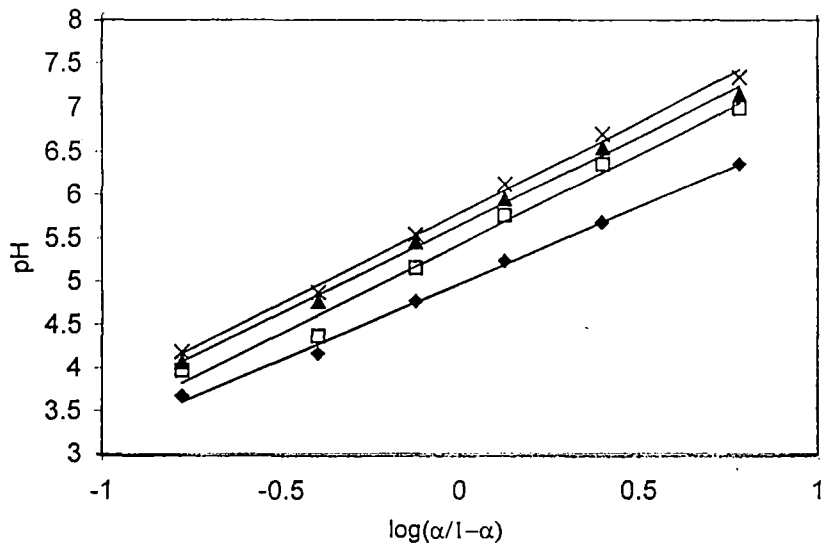


Figure 6.17: Plot of pH vs.  $\log(\alpha/1-\alpha)$  for HPAM in presence of various concentration of KCL.

◆ 0.1(N)KCl □ 0.01(N)KCl ▲ 0.001(N)KCl × Pure water

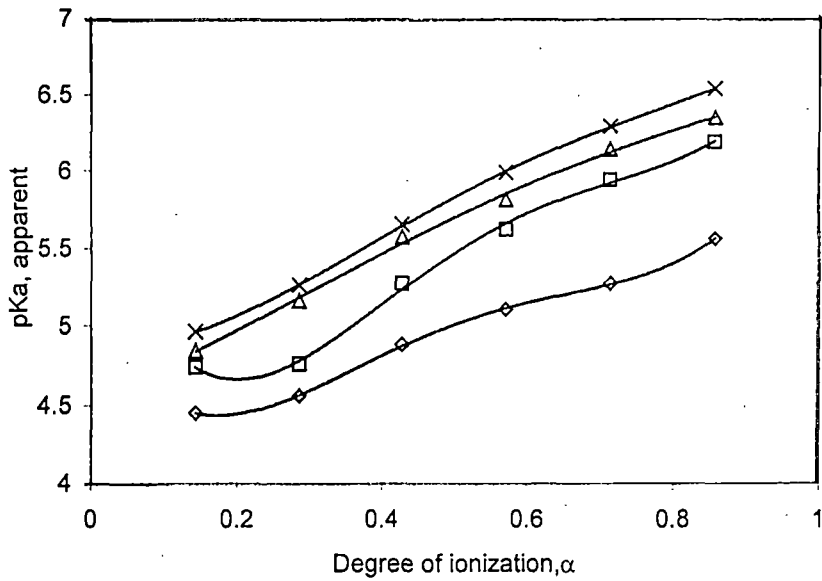


Figure:6.18: Potentiometric titration of HPAM in presence of various concentration of KCl; pKa vs.  $\alpha$   
 ◇ 0.1(N)KCl □ 0.01(N)KCl Δ 0.001(N)KCl × Pure water.

**Table 6.4 Acid strength (pKa) of hydrolyzed PAM in presence of various concentrations of added salt.**

System	pK'	n
Pure Water	5.78	2.08
0.001(N) KCL	5.64	2.06
0.010(N) KCl	5.42	2.02
0.100(N) KCl	4.97	1.76

To investigate the effect of added electrolyte on the chain conformation of the polymers, potentiometric titration were also performed in presence of various concentration of KCl in aqueous solution. From the table 6.4 it is seen that as the electrolyte concentration increases pK' values as well as the n decrease. This may be explained by the slight acidity of the KCl solution and the greater stability of the anionic groups of the polymer chain caused by association with potassium cation. Furthermore, the polymer chains are much more tightly coiled in an electrolyte solution and thus enhancing the possibility of H-bond formation between the carboxylate groups and acrylamide units in the chain due to their closer proximity. The pK' vs.  $\alpha$  curves in figure 6.18 for various concentration of KCl demonstrate a flatter profile for higher concentration of KCl than in water or at lower concentration of KCl due to removal of charge-charge effects in the salt solutions.

## **CONDUCTOMETRIC MEASUREMENTS**

To gain insight on the concepts of counterion condensation, which have been used to attribute the results of viscometric and potentiometric measurements, conductometric measurements were also performed. Manning theory has played a leading role in developing experimental researches on solution properties of polyelectrolytes. According to this theory the equivalent conductivity ( $\Lambda$ ) of a polyelectrolyte solution in the absence of added salt is given by<sup>41-47</sup>.

$$\Lambda = f (\lambda_c^0 + \lambda_p) \quad 5$$

where f is the free fraction of counter ion,  $\lambda_c^0$  is the equivalent conductance of the counter ion in pure solvent and  $\lambda_p$  is the equivalent conductance of the polyion

species in the solution. In the above equation free fraction of counterion,  $f$  is defined as

$$f = 0.866/\xi \quad 6$$

where  $\xi$  is the charge density parameter of the polyion and is defined by

$$\xi = e^2/bDk_B T \quad 7$$

(where  $e$  is the protonic charge,  $D$  is the relative permittivity of the medium,  $b$  is the spacing between charged groups along the axis of the polyion chain,  $k_B$  is the Boltzman constant and  $T$  is the temperature).

$\lambda_p$  has been derived theoretically for the cylinder model of polyelectrolytes and it follows for counterions with a charge of  $z_c$  that :

$$\lambda_p = 279|z_c|^{-1}|\ln ka|/[1+43.2A(|z_c| \lambda_c^0)^{-1}|\ln ka|] \quad 8$$

where the parameter  $a$  is the radius of the polymer chain, while

$$A = Dk_B T/3\pi \eta_0 e \quad 9$$

with  $\eta_0$  being the coefficient of the viscosity of the solvent. In the above equation  $k$  is the Debye screening constant, which is defined by

$$k^2 = 4 \pi \eta^2 \xi^{-1} n_e |z_c|/Dk_B T \quad 10$$

To calculate the charge density parameter  $\xi$ , segment length of 3.8 angstrom<sup>46</sup> and a cylindrical radius of 3 angstrom are used for the present analysis<sup>47</sup>. Experimental data and theoretical predictions of equivalent conductivity of HPAM are shown in figure 6.19. The charge density parameter of LPAM is found to be 0.312 in the present case which is much lower than 1 and equation 7 is valid only for  $\xi > 1$ . Therefore, it is not possible to determine the equivalent conductivities of LPAM with the help of the above equations. For HPAM, experimentally obtained equivalent conductivities are found to be considerably lower than the theoretically predicted values. Concentration dependence of equivalent conductivity is also found to deviate from the theoretically predicted trends. In the case of flexible polyelectrolytes like HPAM, effective charge density parameter should be higher than the value obtained from structural data because of locally curved or coiled conformation of the polyion.<sup>48</sup> The counter ions then see an effective charge being more highly charged than in fully stretched chain. Hence their mobility is lowered concomitantly. Another important

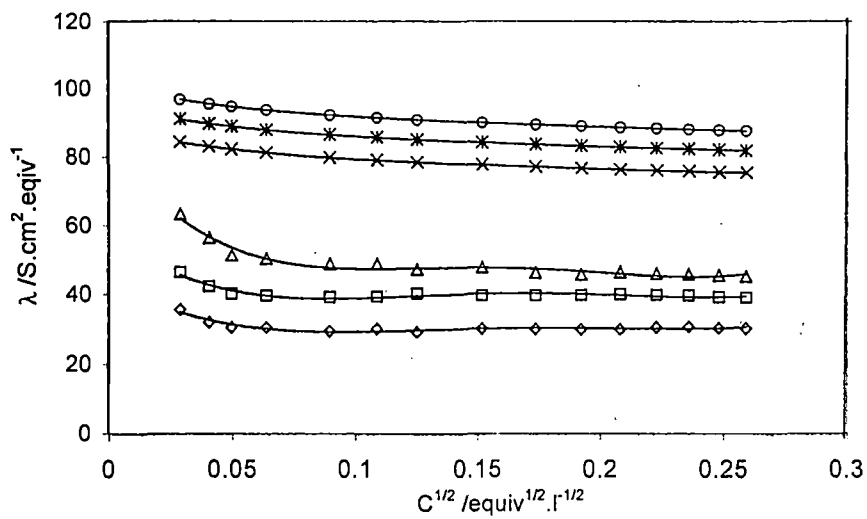


Figure 6.19: Comparison of the experimental values of the equivalent conductivity of solutions of HPAM with those predicted the Manning theory at different temperatures.

◇ 303K,EXP.      □ 313K,EXP.      △ 323K,EXP.      × 303K,THE.  
 \* 313K,THE.      ○ 323K,THE.

EXP and THE stand for experimental and theoretical respectively.

reason for the observed differences between the theoretical and experimental values includes deviation from the rod like model because of kinking in the structure of the polyelectrolyte. In this context it may be noted that viscosity measurement of present polymer system also predicted more or less spherical shape of the polymer molecules (shape factor 2.5) in aqueous solution as well as in aqueous-nonaqueous mixtures (discussed in chapter 6 and chapter 5 respectively), which also support deviation from rod like structure.

### 6.3 REFERENCES

1. S.A. Rice and N. Nagasawa, Polyelectrolyte solutions, Academic Press, New York, (1961).
2. F. Oosawa, Polyelectrolyte, Marcel Dekker, New York, (1971).
3. D. Edelson and R.M. Fuoss, Chain Electrolytes, *J. Am. Chem. Soc.*, **70**, 2802 (1948).
4. R.M. Fuoss and U.P. Strauss, *J. Polym. Sci.*, **3**, 246 (1948).
5. R.M. Fuoss and W. N. Maclay, *J. Polym. Sci.*, **6**, 305 (1950).
6. R.M. Fuoss, *J. Polym. Sci.* **12**, 185 (1954).
7. J.P. Cottonand, M. Moan, *J. Phys. Lett.*, **37**, 75 (1976).
8. B.J. Berne and R. Pecora, Dynamic Light Scattering, Wiley, New York., (1976).
9. G.I. Cathers and R.M. Fuoss, *J. Polym. Sci.*, **4**, 121 (1949).
10. R.D. Ludenburg and R. R. Phillips, *J. Polym. Sci. Polym. Phys. Ed.* **20**: 1143 (1982).
11. R.M. Fuoss and U. P. Strauss, *J. Polym. Sci.*, **3**, 602 (1948).
12. R.S. Fuoss, *Discuss. Faraday Soc.*, **11**, 125 (1952).
13. A. Oth and P. Doty, *J. Chem. Phys.* **56**, 43 (1952).
14. T. Alfrey and H. Morawetz, *J. Am. Chem. Soc.* **74**, 436 (1952).
15. J. Yamanaka, H. Matsuoka, H. Katino and M. Hasegawa, N. Ise, *J. Am. Soc.* **112**, 92, (1990).

16. D.T.F. Pal and J.J. Hermans, *Recl.Trav.Chim.***71**, 433(1952).
17. R.M. Davis and W.B. Russel, *Macromolecules*, **20**, 518(1987).
18. A. Katchalsky and H. Eisenburg, *J.Polym.Sci.*,**6**,145(1951).
19. Priel and A.Silberberg.*J.Polym.Sci.A-28*: 689(1970).
20. Noda, I. Suge, T.T., and Nagasawa, M. *J. Phys. Chem.*, **74** (Feb.19): 710(1970).
21. C.L. McCormick and C.B. Johnson Polymers in aqueous Media (J.E. Glass, ed), *Advances in Chemistry Series 223*, Am. Chem. Soc. Washington D.C, 317 (1989).
22. J. Bock, D.B. Siano, P.L. Valint, Jr., and S.J. Pace., Polymers in aqueous Media (J.E. Glass, ed), *Advances in Chemistry Series 223*, Am. Chem. Soc. Washington D.C., 1989, pp 411-424.
23. Junpei Yamanaka,Hideki Matsuoka, Hiromi Kitano, Masanori Hasegawa and Norio Ise, *J. Am. Chem. Soc.*,**112**,587(1990).
24. M. Mandel ,T. Odijk *Ann Rev. Phys Chem*:**35**:75(1984).
25. S.I. Klein, S.Y. Lubina, I.A. Baranovskaja, E.N. Bykova, B.P. Makagon and, V. Amolotkov, *Soed; Ser. A*, **32**, 439 (1990)
26. U.P. Strauss, D. Woodside, and P.Wineman, *J. Phys. Chem.*,**61**, 1353 (1957).
27. U.P. Strauss and Y.P. Leung, *J.Am.Chem.Soc.*,**82**,1311 ( 1960).
28. L. Kotin and M. Nagasawa, *J.Chem.Phys.*,**36**,873(1962).
29. J.S .Tan and P.R. Marcus, *J. Polym. Sci, Polym.Phys.Ed.*,**14**,239(8)(1976).
30. W.F. Lee and C.C. Tsai, *Polymer*, **36**,357(1995).
31. C. Wolff, *J. Phys (Les Ulis,Fr.) C2-39*,169 (1978).
32. T. Odijk, *Macromolecules*,**12**, 688 ( 1979).
33. deGennes, P.G. Pincus, P. Velasco, R.M. Brochard, F. JJ. *Phys (Les Ulis, Fr).*, **37**, 1461 (1976).
34. M. Hara and J. A. H.Lee ,*Macromolecules*, **21**,2214 ( 1988).

35. M. Mandel, *Encycl. Polym. Sci. Eng.* **11**,739(1987).
36. G. Muller, J. P. Laine and J.C. Fenyo, *J. Pol.Sc., Polymer Chem. Ed.*, **17**, 1979, 659 (1969).
37. H.J. Vink,. *Chem. Soc.Faraday Trans.*, **83**,801(1987).
38. M. Rinaudo and R. Borsali, *Polymer*,**34**,379(1993)
39. A.K. M.Asaduzzaman, A.K. Rakshit and S. Devi, *J Appl Polym Sci*, **47** (10) : 1813 (1993)
40. C.L. McCormick, K.P. Blackmon and D.L. Elliot., *J. Polymer Sci. Part-A : Polymer Chemistry*, **24**,2619(1986).
41. G.S. Manning, *J.Phys.Chem.*,**51**,934(1969).
42. G.S. Manning *Ann.Rev.Phys.Chem.*,**23**,117 (1972).
43. G.S. Manning, *Biopolymers*,**9**,1543 (1970).
44. G.S. Manning *J.Phys.Chem.*,**51**,924(1969).
45. G.S. Manning, *Ann.Rev.Phys.Chem.*,**23**,117(1972).
44. F. Oosawa, *Polyelectrolytes, Scienceand Technology* : Hara, M.Ed.; Marcel Dekker : New York; 202(1993).
45. G.S. Manning, *Ann.Rev.Phys.Chem.*,**79**,262(1975).
46. M. Kowblansky and P. Zema, *Macromolecules*, ,**14**,1451(1981).
47. Vandana K Datye and Philip L Taylor, *Macromolecules*, **17**,1 704(1984).
48. P. Nandi and B. Das, *J. Phys. Chem. B*, **109**, 3238(2005).

## CHAPTER 7

# STUDIES ON SOLUTION PROPERTIES OF POLYMER- NONIONIC SURFACTANT MIXED SYSTEM

# **SOLUTION PROPERTIES OF POLYMER-NONIONIC SURFACTANT MIXED SYSTEM**

## **7.1 INTRODUCTION AND REVIEW OF PREVIOUS WORKS**

Complex water-based fluids containing polymers and surfactants find important practical applications in various domains such as detergency, paints, cosmetics, oil recovery etc. They also play a key role in many biological systems. When surfactants are employed in practice they are almost without exception mixed with various substances either accidentally or intentionally for improving their performances. This is also true for polymers in solution. When a surfactant and a polymer happen to be mixed in aqueous solutions, often significant changes in properties of the individual species appear. These may arise because polymer and the surfactant both belong to the group of substances whose solution property shows marked deviation from regularities. Thus polymer surfactant interactions are not only of a diverse industrial interests but also stimulate academic investigations. The practical importance of polymer-surfactant systems has led to a significant experimental effort to study their behaviour. The interactions between synthetic or natural polymers and surfactants were intensively studied during last few decades. In most cases a strong cooperative association is observed between polyelectrolytes and oppositely charged surfactants and a rather weak interactions are observed between nonionic polymers and ionic surfactants. Interactions between ionic polymers and nonionic surfactants have only been reported in cases where hydrogen bond between polymer and the surfactant is effective<sup>1</sup>. Indeed, a variety of experimental techniques have been utilized to probe the nature of polymer-surfactant interactions including viscosity and conductivity measurements, dialysis, fluorescence spectroscopy, NMR and neutron scattering techniques.<sup>2, 3</sup> Typically hydrophilic nonionic polymers showed no sign of interactions with polyoxyethylated nonionic surfactant.<sup>4</sup> No binding between polyvinyl pyrrolidone (PVP) and TritonX-100 was found, however, mildly hydrophobic nonionic polymers such as propylene oxide and partially hydrolyzed polyvinyl acetate interact with nonionic surfactants.<sup>5</sup> In spite of the above general observations, it was found that nonionic surfactants do interact with polyacrylic acid and other polymers.<sup>6,7</sup> Some of the systems are having solutions

of nonionic polymers and ionic surfactants. These include aqueous solutions of polyethylene oxide (POE) and sodium dodecyl sulphate.<sup>8, 9</sup> Contrary to anionic surfactant, cationic surfactants interact very weakly with POE or PVP and this has been explained by the fact that these surfactants have a very large head group which prevents polymer penetration in their micelles. It has been suggested that the overlap between hydration shells of the polymer and the surfactant head group in the micelles largely determines the effect of the surfactant charge type.<sup>10-12</sup> It was observed that above a critical surfactant concentration, known as critical aggregation concentration (CAC), some ionic surfactants could bind cooperatively to nonionic polymers.<sup>13</sup> The CAC is usually much smaller than critical micelle concentration (cmc), which signals the onset of micelle formation in the corresponding polymer free surfactant solution. In dilute solutions, the polymer-surfactant complex is viewed as composed of a series of spherical micelles with their surfaces covered by polymer segments and connected by strands of the same polymer molecule. Results of NMR studies also provided ample evidence that in these complexes water-soluble polymers do not penetrate into the hydrophobic micellar core, but instead adsorb at the micelle surface and remain in close contact with the surfactant hydrophilic moieties. In addition to the above, neutron scattering studies at the air/water interface show that the water of hydration around the ionic head group extends a short distance down the alkyl chain.<sup>14</sup> Thus aggregate formation of ionic surfactants on hydrophobic polymers is promoted both by hydrophobic interaction of the polymer chain near the head group of ionic surfactant and by increasing the distance between ionic groups compared to a simple micelle. In contrast, nonionic surfactants having weaker repulsion between the head groups show much weaker association.<sup>15</sup> However, association between ethoxylated nonionic surfactants and polyacids has been reported.<sup>17</sup> In these systems, hydrogen bonding between the COOH and the oxygen of the ethylene oxide chain as well as hydrophobic interactions promotes surfactant aggregation on the polymer chain. Association between polyethylene oxide and polyacrylic acid at low pH has been observed and attributed to hydrogen bonding between the polymer and the surfactant.<sup>18,19</sup> Cartalas and coworkers studied the interaction between hydrophobically modified poly (sodium acrylate) and a series of oligoethylene glycol mono dodecyl ether surfactants.<sup>20</sup> The alkyl groups of the modified polymers were found to associate with the surfactant aggregates, which induced dramatic changes in rheology of these systems. It was argued that at least

two different types of gel structures could be recognized in solutions containing hydrophobically modified polymers and surfactant aggregates. Similar viscosity behavior was found when anionic or cationic surfactants were added to hydrophobically modified poly (sodium acrylate) or some other hydrophobically modified polymer aqueous solutions.<sup>21-24</sup> The interaction between ethyl (hydroxyethyl) cellulose and the anionic surfactant sodium dodecyl sulfate has been studied by Lindman and co-workers in dilute aqueous solutions at different temperatures with the aid of viscometry.<sup>25</sup> The delicate interplay between hydrophobic interactions of surfactant and polyelectrolyte is demonstrated through the reduced viscosity data. At surfactant concentration slightly above the CAC the intrinsic viscosity data suggest a sharp collapse of the polymer surfactant aggregates. In presence of moderate amount of surfactant the molecular complexes expand due to amended thermodynamic conditions and enhanced electrostatic repulsion between chains decorated with SDS.

It is very interesting to check if this behavior could occur also with other polymer/surfactant systems. For this reason present work on the interaction of flexible polymers (anionic and nonionic PAM) and nonionic surfactant (Triton-X-100) has been undertaken. The polymers are of high molecular weight nonionic polyacrylamide and anionic (bearing 8.2 and 72 mole% acid) polyacrylamide. The objective of the present work is thus to gain insight into the factors that control the viscosity behavior in dilute solution of nonionic and anionic polyacrylamide under various conditions of temperature and surfactant addition. On the other hand, the variation of CAC and polymer saturation point (PSP) as a function of polymer concentration are of interest because it allows monitoring the complex formation between the polymer and the surfactant as well as provide at least qualitative idea regarding the stoichiometry of such complexes. In view of this a study has also been undertaken on the variation of CAC and PSP of Triton-X-100 as a function of concentration and the nature of the added polymer (NPAM, HPAM, LPAM) with the help of surface tension measurement. In addition to this, thermodynamics of the interaction has also been studied by monitoring the above changes as a function of temperature.

## 7. 2 RESULTS AND DISCUSSION

### VISCOSITY

The intrinsic viscosity  $[\eta]$  is a measure of the hydrodynamic volume in solution since

$$[\eta] \propto S^3/M \quad 1$$

where  $S$  is the radius of gyration and  $M$  is the molecular weight of the polymer. Intrinsic viscosity  $[\eta]$  data of NPAM, LPAM and HPAM in presence of various concentrations of surfactant (0.001-0.1%) at different temperatures are presented in table-7.1 - 7.3. Dramatic drop of  $[\eta]$  at the initial addition of surfactant for all the polymers is observed. A drop in  $[\eta]$  during the formation of polymer-surfactant complex has been reported earlier for nonionic ethyl (hydroxyethyl) cellulose in presence of SDS.<sup>25-26</sup> The marked drop of intrinsic viscosity may be attributed to a strong contraction of polymer-surfactant entities at the onset of surfactant binding to polymer. Above critical aggregation concentration (CAC) micelles begin to form inside the macromolecule, accompanied by collapse of the polymer chain as a result of cooperative binding of surfactant molecule. In a recent theoretical study it was suggested that in a flexible polymer-surfactant system the critical aggregation concentration (CAC) is associated with a considerable change in polymer statistics and polymer-surfactant interactions lead to an effective reduction in the second virial coefficient of the polymer.<sup>27</sup> As a result of this, the polymer is assumed to undergo partial collapse at the CAC. Furthermore, in another theoretical study of binding of small molecules to semiflexible polymers, it was argued that bound molecules might modify the local characteristics of polymer conformations e.g. change its local stiffness.<sup>28</sup> In a recent viscosity study on the dilute aqueous solution of hydrophobically modified (hydroxypropyl) guar polymer in the presence of TX-100 an abrupt drop in  $[\eta]$  was observed at surfactant concentration close to its critical micellization concentration (cmc).<sup>29</sup> This effect was explained in terms of intense intramolecular hydrophobic association junctions. It is interesting to note that drop in the  $[\eta]$  is true for all the polymers under the present study and the intrinsic viscosity minima lies in the CAC range of the surfactant (CAC is measured tensiometrically, shown in table 7.12. It was argued previously that nonionic surfactant could bind cooperatively with ionic polymers only. But present investigation indicates that nonionic polymers also can bind cooperatively with nonionic surfactant. At higher

**Table 7.1 Intrinsic viscosities (dl.g<sup>-1</sup>) of NPAM in presence of various concentrations of surfactant at different temperatures.**

Temperature (°C)	0.00	0.001	0.01	0.100
30	16.31	14	15.93	16.12
35	16.51	14	16.11	16.43
40	16.49	14.6	16.90	16.47
45	16.43	14.6	16.76	16.44
50	16.39	14.6	21.38	16.40
55	16.38	14.7	16.87	16.38
60	16.35	14.2	18.12	16.12

**Table 7.2 Intrinsic viscosities (dl.g<sup>-1</sup>) of HPAM in presence of various concentrations of surfactant at different temperatures.**

Temperature (°C)	0.00	0.001	0.01	0.100
30	43.92	35.18	41.43	44.43
35	40.45	35.96	37.48	44.81
40	44.01	36.93	41.20	45.70
45	45.34	37.07	42.25	46.44
50	46.04	40.43	43.59	47.01
55	47.24	39.15	42.79	48.24
60	47.63	39.30	43.63	49.22

surfactant concentration, (0.01 and 0.1 %, w/v), it is seen that  $[\eta]$  rises at all the experimental temperatures and the conformational expansion as observed is most probably a result of enhanced excluded volume effect due to improved thermodynamic condition (table 7.1-7.3).

**Table 7.3 Intrinsic viscosities (dl.g<sup>-1</sup>) of LPAM in presence of various concentrations of surfactant at different temperatures.**

Temperature (°C)	Surfactant concentration (%)			
	0.00	0.001	0.01	0.100
30	26.7	15.5	20.0	23.14
35	25.9	19.1	20.3	23.15
40	27.3	19.0	21.5	23.54
45	27.1	18.5	20.8	23.64
50	29.7	19.7	21.7	24.00
55	31.6	20.6	22.0	24.12
60	33.5	20.7	22.9	23.19

**Table 7.4 Voluminosity (dl.g<sup>-1</sup>) of NPAM in presence of various concentrations of surfactant at different temperatures.**

Temperature (°C)	Surfactant concentration (%)			
	0.00	0.001	0.01	0.100
30	8.51	5.12	5.25	5.33
35	8.61	5.19	5.33	5.37
40	8.69	5.25	5.39	5.42
45	8.72	5.25	5.41	5.45
50	8.78	5.31	5.49	5.54
55	8.81	5.32	5.50	5.56
60	8.93	5.31	5.99	8.56

Therefore, at concentrations higher than CAC the system can be considered to consist of necklace type of configuration.<sup>31</sup> According to necklace model suggested by K. Shirahama polymer chains are wrapped around the surfactant aggregates with their hydrophobic segment penetrating into the Stern layer of the aggregates by displacing water molecules.<sup>32</sup>

Viscosity values of aqueous solution of different types of PAM (NPAM, LPAM and HPAM) were used to determine the volume related parameter ( $V_E$ ), shape factor

( $V$ ) and molecular expansion factors ( $\alpha$ ) (ref. 33) of the polymer in presence of different concentrations of the surfactant adopting the methods discussed in chapter 5. Values of  $V_E$  (table 7.4 - 7.6) for the polymers are found to decrease at the initial addition of surfactant; subsequent addition of surfactant results in an increase in the value of the volume related parameter. This is, however, expected considering the observed variation of  $[\eta]$  with the concentration of surfactant because both are basically a measure of the hydrodynamic volume of the polymer chain. The value of  $v$  has been shown to be 2.5 for spherical particles. From table 7.7- 7.9 it is observed that for HPAM, LPAM and NPAM the values of  $v$  in most cases deviate from 2.5 at all temperatures and surfactant concentrations under investigation. This result suggests that the shape of the polymer molecules is other than spherical in presence of nonionic surfactant. In this context it may be noted that the shape of the above polymers molecules are found to be spherical in aqueous and aqueous-organic mixtures in the presence or in absence of salts. The change in the shape of the polymer molecules in presence of nonionic surfactant is, however, not surprising. It has already been suggested that the bound ions or molecules may significantly modify the local stiffness of the polymer chain resulting in the restructuring of the overall shape. Moreover, according to the necklace model polymer chain are wrapped around the surfactant aggregates with their hydrophobic segments penetrating with the Stern layer.<sup>32</sup>

**Table 7.5 Voluminosity ( $\text{dl.g}^{-1}$ ) of LPAM in presence of various concentrations of surfactant at different temperatures.**

Temperature ( $^{\circ}\text{C}$ )	Surfactant concentration (%)			
	0.00	0.001	0.01	0.10
30	7.81	7.24	7.19	7.15
35	7.83	7.26	7.15	7.13
40	7.87	7.33	7.14	7.12
45	7.81	7.26	7.08	7.07
50	7.88	7.35	7.20	7.11
55	7.90	7.40	7.21	7.14
60	7.93	8.15	7.20	7.18

**Table 7.6 Voluminosity (dl.g<sup>-1</sup>) of HPAM in presence of various concentrations of surfactant at different temperatures.**

Temperature (°C)	Surfactant concentration (%)			
	0.00	0.001	0.01	0.100
30	8.8	8.65	8.66	8.66
35	8.84	8.68	8.69	8.69
40	8.89	8.72	8.74	8.74
45	8.81	8.71	8.72	8.72
50	8.93	8.82	8.83	8.83
55	8.89	8.84	8.86	8.87
60	8.91	8.85	8.89	13.36

**Table 7.7 Shape factor of NPAM in presence of various concentrations of surfactant at different temperatures.**

Temperature (°C)	Surfactant concentration (%)			
	0.00	0.001	0.01	0.100
30	1.92	2.72	3.03	3.00
35	1.92	2.75	3.02	3.06
40	1.89	2.78	3.13	3.03
45	1.89	2.78	2.98	3.01
50	1.86	2.75	3.89	2.96
55	1.86	2.76	3.06	2.94
60	1.83	2.67	3.02	1.91

The expansion factors ( $\alpha$ ), determined following the methods already described in chapter 5, are presented in the table 7.10. For all the above polymers, it is found that on the initial addition of surfactants the end-to-end distance decreases but on further addition of surfactant the end-to-end distance increases. This is expected from their intrinsic viscosity data also. The initial addition of surfactant causes wrapping of the surfactant molecules by the polymer segments to take place

and further addition of surfactant molecules (micelles) force the chains to expand. Such results were also observed in case of SDS-poly (vinyl pyrrolidone) system previously.<sup>34</sup>

**Table 7.8 Shape factor of LPAM in presence of various concentrations of surfactant at different temperatures.**

Temperature (°C)	Surfactant concentration (%)			
	0.00	0.001	0.01	0.100
30	3.42	2.14	2.78	3.23
35	3.30	2.63	2.83	3.24
40	3.47	2.59	3.01	3.30
45	3.46	2.54	2.93	3.34
50	3.77	2.68	3.01	3.37
55	4.00	2.78	3.05	3.37
60	4.22	2.53	3.18	3.22

**Table 7.9 Shape factor of HPAM in presence of various concentrations of surfactant and at different temperatures.**

Temperature (°C)	Surfactant concentration (%)			
	0.00	0.001	0.01	0.100
30	4.99	4.06	4.78	5.01
35	4.57	4.14	4.31	5.15
40	4.95	4.23	4.71	5.22
45	5.14	4.25	4.84	5.32
50	5.15	4.58	4.93	5.32
55	5.31	4.43	4.83	5.43
60	5.34	4.44	4.90	3.68

Viscosity data are used to evaluate activation parameters of viscous flow using Frenkel-Eyring equation as follows (detail in chapter 5). Linear variation is observed in the plot of  $\ln(\eta V/Nh)$  against  $T^{-1}$  with correlation coefficient of 0.96 or higher for all the systems studied. Some representative plots (Frenkel-Eyring) are shown in figure 7.1 - 7.3.

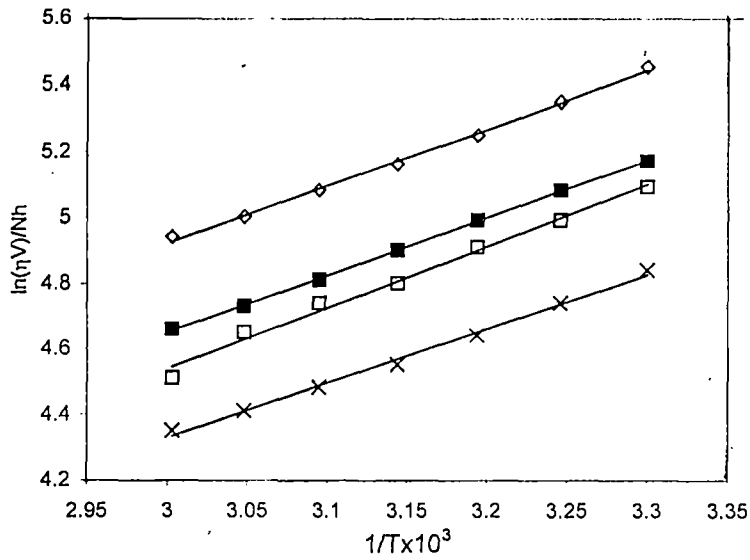


Figure:7.1:F.E.Plot for LPAM.

- ◇ 0.007gm/cc, Tx=0.1%
- 0.0035gm/ccTx=0.1%
- 0.0035gm/cc, Tx=0.01%
- × 0.00178gm/cc, Tx=0.01%

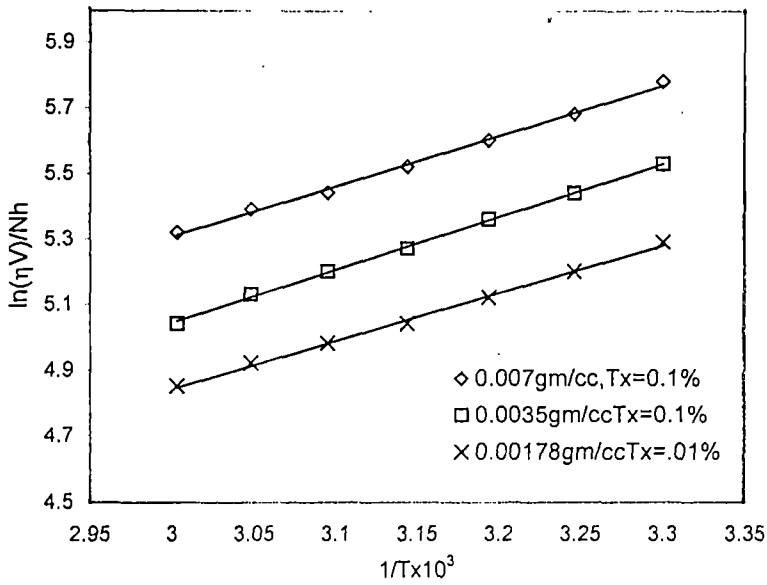


Figure:7.2:Plot of  $\ln(\eta V/Nh)$  vs  $T^{-1}$  for HPAM in presence of different concentrations of Tx-100.

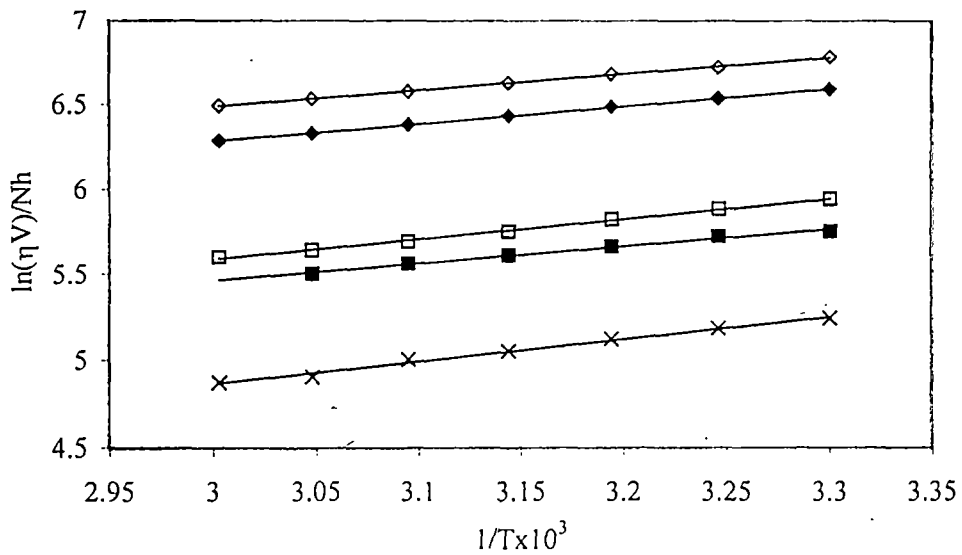


Figure:7.3 :F.E.Plot for NPAM in presence of different concentration of surfactant at various concentration of polymer.

- $\diamond$  0.0036gm/cc,  $T_x=0.1\%$
- $\times$  0.0009gm/cc,  $T_x=0.01\%$
- $\blacksquare$  0.00178gm/cc,  $t_x=0$
- $\square$  0.00178gm/cc,  $T_x=0.1\%$
- $\blacklozenge$  0.0036gm/cc,  $T_x=0$

**Table 7.10 Expansion factors for polymers in presence of different concentrations of surfactant.**

Temp. <sup>o</sup> C	NPAM			LPAM			HPAM		
	$\alpha_1$	$\alpha_2$	$\alpha_3$	$\alpha_1$	$\alpha_2$	$\alpha_3$	$\alpha_1$	$\alpha_2$	$\alpha_3$
30	0.95	0.99	0.98	0.98	0.99	0.99	0.99	0.99	0.99
35	0.95	0.99	0.98	0.98	0.99	0.99	0.99	0.99	0.99
40	0.96	1.00	0.98	0.98	1.00	0.99	0.99	1.00	0.99
45	0.96	1.00	0.98	0.98	1.00	0.99	0.99	1.00	0.99
50	0.96	1.09	0.98	0.98	1.0	0.99	0.99	1.00	0.99
55	0.96	1.01	0.98	0.98	1.00	0.99	0.99	1.00	0.99
60	0.95	1.03	0.98	0.98	1.01	0.99	0.99	1.00	0.99

$\Delta H_{vis}^{\#}$  and  $\Delta S_{vis}^{\#}$  values at different polymer concentrations and solvent compositions for hydrolyzed and nonhydrolyzed PAM's are determined. These values were extrapolated to zero polymer concentrations to estimate  $\Delta H_{vis}^0$  and  $\Delta S_{vis}^0$  values, which are shown in the table 7.11. Positive values of  $\Delta H_{vis}^0$  and  $\Delta S_{vis}^0$  were obtained for all the systems. The slope of the plot of  $\Delta H_{vis}^0$  vs.  $\Delta S_{vis}^0$  for all the systems together yields the value of structural temperature of the system. This parameter is found to be 28.2<sup>o</sup>C. It may be noted that at this temperature free energy of activation for the viscous flow becomes independent of the entropic forces and solely depends on enthalpic forces.<sup>35, 36</sup> It is interesting to note that the structural temperature value obtained in the present case is very close to that observed previously (e.g. 305K) for similar polymer but with different degree of hydrolysis.<sup>37</sup>

**Table 7.11 Viscosity activation parameters of the polymers in presence of various concentrations of Tx-100.  $\Delta H_{vis}^0$ ,  $\Delta S_{vis}^0$  in kJ.mol<sup>-1</sup> and J.mol<sup>-1</sup>.K<sup>-1</sup> respectively.**

Tx-100 (%)	NPAM		LPAM		HPAM	
	$\Delta H_{vis}^0$	$\Delta S_{vis}^0$	$\Delta H_{vis}^0$	$\Delta S_{vis}^0$	$\Delta H_{vis}^0$	$\Delta S_{vis}^0$
0.001	11.93	30.51	13.30	23.74	15.19	28.99
0.010	12.40	29.90	14.24	25.54	12.50	27.89
0.100	11.38	25.54	14.30	23.71	13.11	25.65

## SURFACE TENSION

To understand the nature of interaction between polymers and the surfactants in bulk aqueous solution, as well as at interfaces is of great importance. Indeed, a variety of experimental techniques have been utilized to probe the nature of polymer-surfactant interaction. Surface tension measurement study is one such important technique, which is especially useful in this area. Figures 7.4 – 7.6 are representative plots of surface tension vs. logarithm of concentration of TX-100 ( $\log [Tx100]$ ) for NPAM, LPAM and HPAM respectively. Each of these plots exhibit two transition points. Three regions of surfactant concentration representing the distinct stages of surfactant-polymer interactions in aqueous solution are observed. In the first region, which is located at lower concentration region of the surfactant, the surface tension decreases gradually till the first break point comes. Before the first break point, surfactant molecules bind cooperatively to polymers. This break point is known as critical aggregation concentration (CAC)<sup>38</sup>. The CAC values are found to be much smaller than cmc, which indicates the onset of micelle formation in the corresponding polymer free surfactant solution due to locally accumulated high concentration of the bound surfactants. This cooperative binding result in the formation of polymer surfactant complexes in solution. The binding of the surfactant to polymer begins at CAC and it continues till the second transition, called the critical micellization concentration of the polymer surfactant complex or the polymer saturation point (PSP) reaches. In general, the binding of surfactant to the polymers is similar to micellization and the CAC values are lower and PSP is higher than the cmc of surfactant in water. The cmc values, thermodynamic parameters and interfacial adsorption parameters for pure TritonX100 are taken from literature.<sup>37</sup> The CAC values are more independent of temperature than PSP. Further, CAC is independent of polymer concentration. The cmc decreases with temperature initially (0.234 mM at 30°C and 0.195 mM at 45°C) and then increases passing through a minimum. It was suggested that when the surfactant is present in excess and as the concentration of micelles are relatively high, the micelle/water and the air/water interfaces compete progressively for the polymer. Thus surface tension values eventually attain same values as that of pure surfactant. But for the present system the surface tension values are somewhat different from the pure surfactant solutions at polymer saturation point and at higher concentrations. Therefore, it may be suggested that complete transfer of polymer does not occur from air/water interface. The air/water

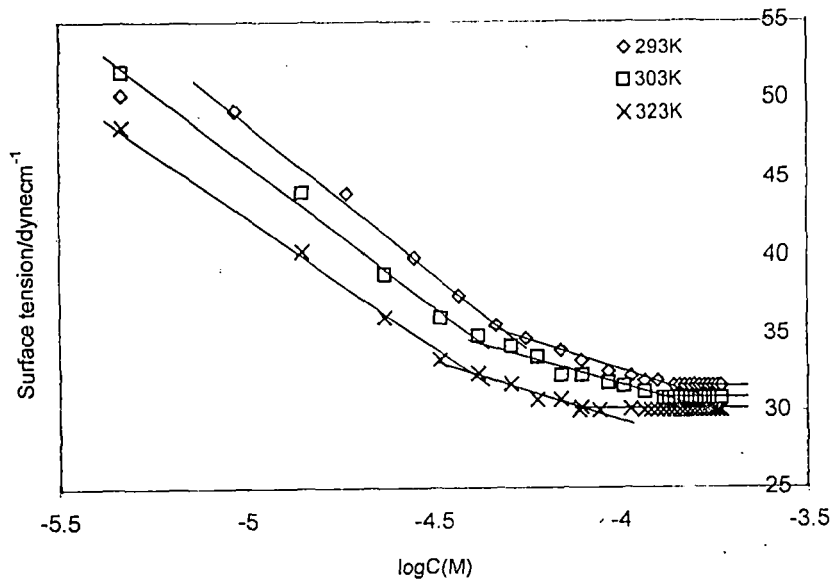


Figure:7.4:Surface tension vs.  $-\log C$  plot for Tx-100 in presence of 0.009% LPAM at different temperatures.

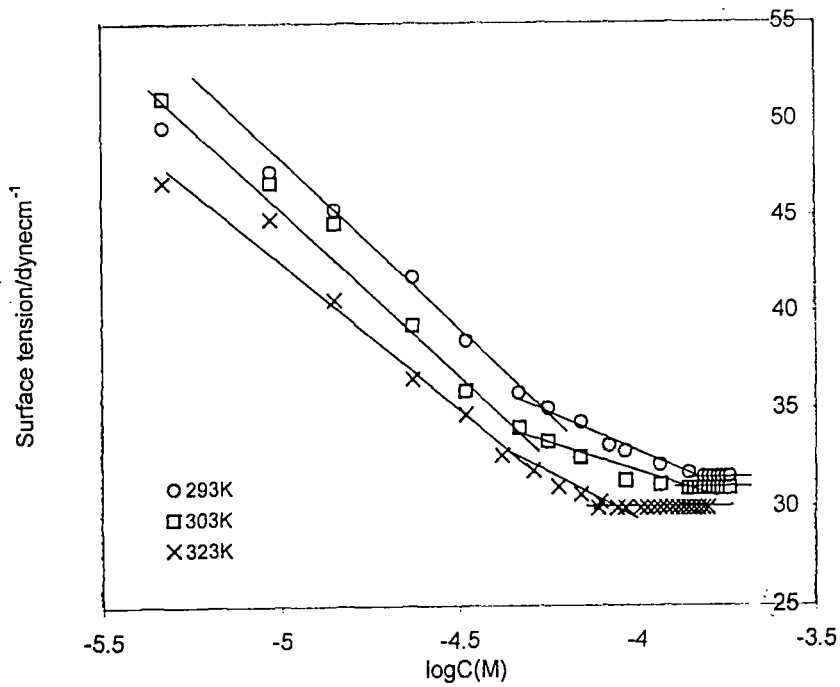


Figure:7.5:Surface tension vs.  $-\log C$  plot for Tx-100 in presence of 0.05% HPAM at different temperatures.

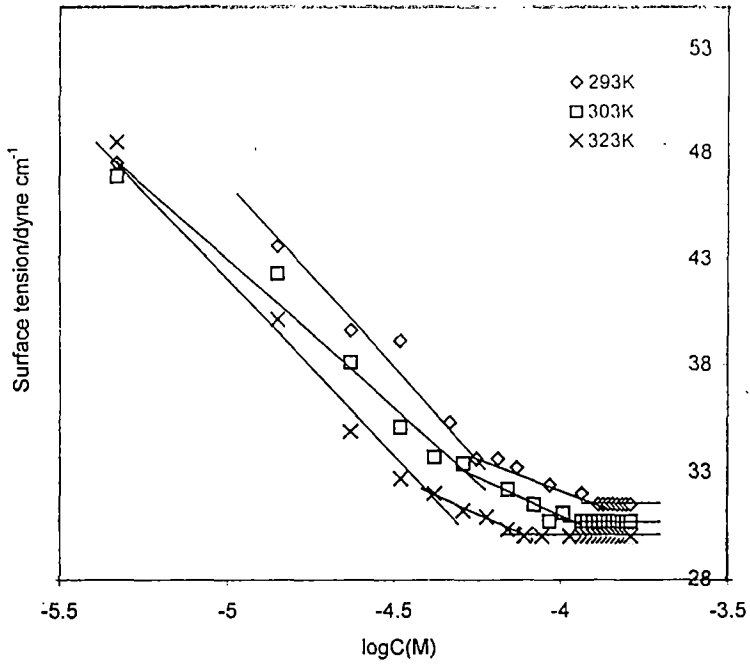


Figure :7.6: Surface tension vs.  $-\log C$  plot for Tx-100 in presence of 0.009 %NPAM at different temperatures.

interface is thus saturated with polymer-surfactant and also normal micelle formation starts even before polymer gets saturated with surfactant.<sup>37</sup> The CAC values of TX-100 in presence of the polymers at four different temperatures are shown in Table 7.12. CAC values are found to decrease with an increase in temperature except in a few at low concentration of the polymer. This trend of variation of CAC values with temperature is similar for all the polymers and is almost independent of the polymer concentration. It is interesting to note that as the carboxyl content of the polymer increases from LPAM (8.2mol %) to HPAM (72 mol %) CAC values also increases. At high polymer concentration and at low temperature, NPAM having higher molecular weight than LPAM and HPAM, yield CAC values, which are higher than that of hydrolyzed PAM's. There are two possible driving forces for polymer surfactant interaction (1) the tendency of polymer to be adsorbed at the micelle - water interface and (2) specific attraction between polymer segments and surfactant heads.<sup>39</sup> For most of the nonionic polymers, specific interaction with ionic or nonionic surfactant heads are usually weak, so that the dominant factor promoting polymer-surfactant complexation is the propensity of the polymer to be adsorbed at a micelle - water interface. Naturally, the trend of change of CAC with polymer concentration for the hydrolyzed (LPAM and HPAM) and unhydrolyzed PAM (NPAM) will be different. Moreover, the molecular weight and the concentration of the polymers influence significantly the polarity along the polymer chain in association with surfactant; high molecular weights polymers always having lower in the polarity, leading to low CAC's, whereas concentration give rise to a somewhat unexpected change. The PSP values for all the above systems at various temperatures are presented in Table7. 14.

**Table 7.12 Critical aggregation Concentration (CAC) X10<sup>5</sup>M of TritonX-100 in presence of different concentrations of anionic and nonionic polyacrylamide at various temperatures (°C).**

Polymer↓ Temp.→	0.0025% PAM				0.009% PAM				0.05% PAM			
	20	30	40	50	20	30	40	50	20	30	40	50
NPAM	4.0	5.0	4.2	4.2	5.5	4.6	4.6	4.8	6.0	5.3	4.7	4.2
LPAM	4.5	4.5	4.2	4.5	4.5	4.0	4.1	3.9	5.1	4.3	4.4	4.6
HPAM	5.6	4.6	4.8	4.8	5.0	4.8	4.7	4.0	5.6	4.5	4.5	4.8

**Table 7.13 Free energy( $\Delta G_{ps}^0$  in  $\text{kJmol}^{-1}$ ) due to polymer surfactant interaction in presence of different concentrations of polymer at various temperatures( $^{\circ}\text{C}$ ).**

Polymer↓	Polymer concentration (%)											
	0.0025				0.009				0.05			
Temp.→	20	30	40	50	20	30	40	50	20	30	40	50
NPAM	4.39	3.89	4.26	4.04	3.62	4.11	4.02	3.68	3.41	3.75	3.97	4.04
LPAM	4.11	4.16	4.26	3.85	4.11	4.46	4.32	4.23	3.80	4.28	4.14	3.79
HPAM	3.57	4.11	3.91	3.68	3.85	4.00	3.96	4.17	3.57	4.16	4.08	3.68

**Table 7.14 Polymer Saturation Point (PSP, mM) of Tx-100 in presence of different concentrations of anionic and nonionic polyacrylamide at various temperatures( $^{\circ}\text{C}$ ).**

Polymer↓	Polymer concentration (%)											
	0.0025				0.009				0.05			
Temp.→	20	30	40	50	20	30	40	50	20	30	40	50
NPAM	0.106	0.103	0.102	0.088	0.114	0.105	0.100	0.077	0.112	0.105	0.092	0.068
LPAM	0.120	0.114	0.105	0.072	0.127	0.119	0.107	0.077	0.129	0.124	0.109	0.081
HPAM	0.111	0.118	0.122	0.093	0.116	0.122	0.128	0.096	0.114	0.132	0.133	0.097

It is seen that for NPAM and LPAM, PSP decreases with the increase in temperature but completely opposite trend is observed for HPAM (upto  $40^{\circ}\text{C}$ ). Lower values of PSP than cmc indicate that polymer facilitates micelle formation even before it gets saturated. Generally, cmc of a nonionic surfactant decreases with an increase in temperature due to changes in water structure and water surfactant interaction. In presence of NPAM and LPAM (8.2 mol% charge), the overall variation of PSP is determined by various interactions in the polymer-TX 100-water system. In this respect, the behavior of LPAM is somewhat similar to that of NPAM. However, for

HPAM (72 mol% Charge) the polyelectrolyte nature of the polymer is responsible for higher PSP values. Moreover, as the polymer concentration increases more binding

**Table 7.15 Thermodynamic Parameters ( $\Delta G^0_{PSP}[1]$  ,  $\Delta H^0_{PSP}[2]$  and  $\Delta S^0_{PSP}[3]$  in  $\text{kJ.mol}^{-1}$  , $\text{kJ.mol}^{-1}$  and  $\text{J.mol}^{-1}.\text{K}^{-1}$ respectively) associated with polymer saturation point at various temperatures ( $^{\circ}\text{C}$ ) in presence of different concentrations of Tx-100.**

Temp.	Polymer concentration (%)									
		0.0025			0.009			0.05		
	Polymer	[-1]	[2]	[3]	[-1]	[2]	[3]	[-1]	[2]	[3]
20	NPAM	32.08	1.35	105	31.90	4.71	93	31.94	6.92	85
	LPAM	31.78	4.78	92	31.64	6.14	87	31.60	5.99	87
	HPAM	31.97	-3.35	120	31.86	-3.50	120	31.90	-5.49	127
30	NPAM	33.25	1.45	114	33.20	5.04	126	33.20	7.40	134
	LPAM	32.99	5.11	125	32.88	6.56	130	32.78	6.41	129
	HPAM	32.90	-3.58	96	32.86	-3.74	96	32.62	-5.88	88
40	NPAM	34.37	1.55	115	34.42	5.37	127	34.63	7.90	136
	LPAM	34.29	5.46	127	34.25	7.00	131	34.19	6.84	131
	HPAM	33.90	-3.83	96	32.82	-3.99	92	33.68	-6.27	87

sites are available for the surfactant to interact, hence PSP values goes on increasing. It is surprising to note that at  $50^{\circ}\text{C}$  temperature PSP values are minimum for all the polymers in the whole range of concentration.

The free energy of micellization ( $\Delta G^0_m$ ) in the absence of polymer and the free energy of aggregation ( $\Delta G^0_{agg}$ ) in the presence of polymer for a nonionic surfactant can be calculated using the following equations,<sup>40</sup>

$$\Delta G^0_m = RT \ln \text{cmc}$$

2

and the corresponding quantity at CAC is

$$\Delta G_{agg}^0 = RT \ln CAC \quad 3$$

Now,

$$\Delta G_{agg}^0 = \Delta G_m^0 + \Delta G_{ps}^0 \quad 4$$

Therefore,

$$\Delta G_{PS}^0 = \Delta G_{agg}^0 - \Delta G_m^0 = RT \ln(CAC/cm_c) \quad 5$$

This quantity ( $\Delta G_{PS}^0$ ) is a measure of the strength of interaction between the surfactant and the polymer.  $\Delta G_{PS}^0$  values of the present systems are tabulated in table 7.13. The difference in the nature of interaction between the polymers with the surfactant is apparent from the values of  $\Delta G_{PS}^0$ . These values are more negative for NPAM than that of LPAM or HPAM. Here again the effect of chain length (molecular weight) on the binding pattern of surfactant on the polymer is noticed. Similar results were also observed in the cases of SDS and TTAB in presence of polyacrylic acid and hydrophobically modified polyacrylic acid.<sup>40</sup> Thermodynamic parameters for micelle formation are computed using the following relations

$$\Delta G_{PSP}^0 = RT \ln PSP \quad 6$$

$$\Delta G_{PSP}^0 = \Delta H_{PSP}^0 - T \Delta S_{PSP}^0 \quad 7$$

Table 7.15 shows the values of standard free energy ( $\Delta G_{PSP}^0$ ), enthalpy ( $\Delta H_{PSP}^0$ ) and entropy ( $\Delta S_{PSP}^0$ ) changes at 20<sup>o</sup>, 30<sup>o</sup>, 40<sup>o</sup> and 50<sup>o</sup>C. The free energy becomes more negative with the increase in temperature. This indicates that the formation of the polymer-saturated micelle is relatively more spontaneous. The micellization in the presence of NPAM and LPAM is endothermic whereas in presence of HPAM it is exothermic. At higher concentrations of polymer, the entropy change value decreases from uncharged to high carboxyl content polyacrylamide. This indicates that the polyelectrolyte nature of LPAM and HPAM yield higher values of thermodynamic parameters. In the case of nonionic surfactant, the entropy gain made by the destruction of structured water shell is commonly credited as the driving force for the process. Moreover, with an increase in temperature the entropic gain is greater than the enthalpic gain and hence the free energy becomes more negative. As the temperature increases dehydration of oxyethylene group occurs and there are more numbers of nonpolar conformation available which provide an entropic driving force for the conformational changes to occur.

### 7.3 REFERENCES

1. S. Saito, T. Taniguchi, *Colloid Interface Sci.*, **44**, 114(1973).
2. M.M. Breuer, I.D. Robb. *Chem. Ind.*, **13**, 531(1972).
3. E.D. Goddard, *Colloid Surf.* **19**, 255, 301(1986).
4. M.J. Schwuger and H. Lauge, Proc. 5<sup>th</sup> Int. Congr. Surface Activity, **2**, 955 (1968).
5. S. Saito, Z. Koll, *Polymer*, **10**, 226(1968).
6. M.D.F. Vesilescu, Anghel, M. Almgren, P. Hansson and S. Saito. *Langmuir*, **13**, 6951 (1997).
7. D.F. Anghel, S. Saito, A. Vescu and A. Baran, *Colloids Surf. A*, **90**, 89 (1994).
8. M.N. Jones, *Coll. Interface Sci.*, **23**, 36(1967).
9. K. Shirahama, *Colloid Polym. Sci.*, **252**, 978 (1974).
10. F.M. Witte, J.B.F.N. Engberts, *Colloids Surf.*, **36**, 417(1989).
11. J. Sabbadin, *Eur. Polym. J.*, **21**, 165(1985).
12. P.L. Dubin, J.H. Gruber, J. Xia, and H. Zhang, *J. Colloid Interface Sci.*, **148**, 35 (1992).
13. H. Lange H. *Kolloid Z.Z. Polym.*, **243**, 101(1971).
14. Lu, J. Thomas R.K. Penfold, *J. Adv. Colloid Interface Sci.*, **84**, 143(2000).
15. J. Brackman, Van Os, M.N. Engberts J. B.F.N. *Langmuir*, **4**, 1266 (1988).
16. F.M. Winnik, *Langmuir*, **6**, 522(1990).
17. C. Maloney and K. Liuber, *J. Colloid Interface Sci.*, **164**, 463(1994).
18. D.F. Anghel, S. Saito, A. Baran and A. Iovescu, *Langmuir*, **14**, 5342 (1998).
19. V. Baranovsky, S. Shenkov, I. Rashkov and C. Borisov, *Eur. Polym. J.*, **28**, 475 (1992).
20. A.S. Cartalas, I. Iliopoulos, R. Auderbart and U. Olsson, *Langmuir*, **10**, 1421 (1994)

21. Iliopoulos, I; Wang, T.K. Auderbert, R, *Langmuir*, **7**, 617 (1991).
22. B. Magny, I. Iliopoulos, R. Auderbart, L.Piculell and B. Lindman, *Prog, Colloid Polym. Sci.*, **89**,118 (1992).
23. S. Biggs and F. Candau, *Langmuir*, **8**, 838 (1992).
24. R. Tanaka, J. Meadows, P.A. Williams and G.O. Phillips, *Macromolecules*, **25**, 1304 (1992).
25. Erlend Hoff, Bo Nystorm, Bjorn Lindman, *Langmuir*, **17**,28 (2001).
26. C. Holmberg and L.O. Sundelf, *Langmuir*, **12**, 883 (1996).
27. C. Holmberg, S. Nilsson, S.K. Singh and L.O. Sundelof, *J. Phys Chem*, **90**, 871 (1992).
28. H. Diamant and D. Andelma, *Europhys Lett.*, **48**, 170 (1999).
29. H. Diamant and D. Andelma , *Macromolecules*, **33**,8050(2000).
30. T.Aubry, M. Moan, J.F. Argiller and A. Audibert *Macromolecules*, **31**, 9072 (1998).
31. K. Ilindel and B. Cabane, *Langmuir*, **14**, 6361 (1998).
32. K. Shirahama and K. Tsuji, *J. Biochem (Tokyo)* **75**,3009 (1974).
33. H. Kurata, W.H. Stockmayer and A. Roig, *J Chem. Phys*, **33**(1),151(1960).
34. T.G. Lopez, L.M. Fernandez and G.R. Allende, *British Polym.J*,**20**,39 (1988).
35. A. Rangaraj, V. Vangani and A.K. Rakshit ,*J Appl Polym Sci.*, **66**,45(1997).
36. V. Vangani and A.K. Rakshit, *J Appl Polym Sci*, **60**,1005 (1996).
37. A. Rangaraj and A.K. Rakshit, *J. Surface Sci. Technol*, **16**, 246 (2000).
38. M.J. Schwuger ,*J. Colloid Interface Sci.*,**43**,491 (1973).
39. Y.J. Nikas and B. Blankschtein, *Langmuir*, 1994, **10**, 3512(1994).
40. Y. Wang, B. Han, H. Yan, J.C.T. Kwak, *Langmuir*, **10**, 3455(1994).

**CHAPTER 8**  
**SUMMARY AND CONCLUSION**

## SUMMARY AND CONCLUSION

An introduction covering various aspects of the present research scheme on aqueous polymerization of acrylamide and solution properties of polyacrylamide have been presented in chapter 1 (page 1-15). Usual redox polymerization of acrylamide in aqueous medium yields polymer having not so high molecular weight primarily because of fast termination process via transfer of electron to the oxidant of the redox couple (e.g. metal ions at higher oxidation state) from the growing polymer chain. It has been shown that if the polymerization reaction could be initiated in the interlayer spaces of a mineral phyllosilicate viz., montmorillonite by redox couple involving the trapped metal ions, one may expect a controlled linear termination process because the growing polymer chain may not be able to transfer the electrons to these metal ions in the constrained spaces. This technique may particularly be useful for obtaining very high molecular weight polyacrylamide (PAM). On the other hand, to understand the role of charged groups on factors that govern the efficiency of PAM in its various uses in solution phase especially in the salt rich waters, complete molecular characterization is required. In the case of charged PAM the relative dissociation of the ionic groups and the distribution and alignment of the charged dipoles along the chain are expected to play a decisive role on the final state of conformation of the polymer chain. In view of the above, attempt has been made to increase the chain length of polyacrylamide by loading the potential electron acceptor (metal ions) into the interlayer space of hitherto unexplored phyllosilicate in the above application viz., vermiculite, prior to the reaction. A brief review covering all these aspects viz., polymers of acrylamide, structure of the clay mineral vermiculite, clay-organic interaction, clay-catalyzed polymerization and polymer-solvent interaction have been presented.

Chapter 2 (page 16 -20) describes the scope and object of the present investigation. In recent years, scientists and engineers working on environmental and industrial problems have renewed their interest in water-soluble synthetic polymers because of their very broad range of application. The critical limitation of polyelectrolytes including those derived from hydrolyzed homo-polyacrylamide is the loss of viscosity in presence of mono and /or multivalent electrolytes. Very high molecular weight polyacrylamide has been found to be exceptionally effective

flocculants. It has already been mentioned that if the polymerization is carried out in a constrained space such that the growing polymer chain cannot transfer the electron efficiently to the oxidant of the redox couple an enhanced chain growth results. On the other hand, many present and possible industrial applications of high molecular weight polymer arise from unusual properties they induce to their solutions. The study of their solution property is a prerequisite for the development of this modern domain. The characterization of very high molecular weight polymers raises a number of problems. Therefore, systematic studies arising from the coupling of different experimental techniques are required for the elucidation of diverse theoretical and experimental aspects. In recent years the study of polyelectrolytes has seen a revival stimulated by the use of newly available experimental techniques and the introduction of new theoretical concepts. It is noteworthy that solutions of polyelectrolyte exhibit a behavior that may differ considerably from that of either uncharged macromolecules or low-molar-mass electrolytes.

The experimental technique for the study of polymerization including the methods of preparation and purification of different vermiculite samples viz., hydrogen vermiculite, ferric vermiculite and ceric vermiculite are presented in chapter 3 (page 21 -25). In addition to the above, different experimental techniques viz., viscometry, potentiometry, conductometry and tentiometry (surface tension measurement) for the study of solution properties of ionic and nonionic polyacrylamide are described.

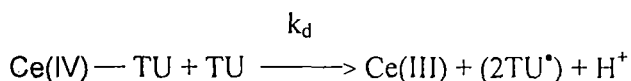
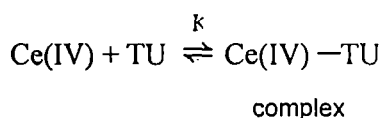
In chapter 4 (page 26 -61), results of the study on the catalytic activity of clay mineral in the present aqueous polymerization process of water-soluble polymers and to prepare polymers having high molecular weight with high rate of formation under ordinary condition are presented. Vermiculite microenvironment has shown a dramatic effect on the polymerization of acrylamide by Ce (IV)/TU combination in aqueous medium via the slow termination due to inability of a growing polymer chain to transfer to the oxidant trapped inside the layered space. A detail study concerning the kinetic and mechanistic aspects has been made for the aqueous polymerization of acrylamide with ceric vermiculite/thiourea initiating system. Kinetic, spectroscopic and other analytical data have been taken into consideration to determine the pathways involved in the reaction. The molecular weights of the polymer are moderately high and ranged from  $2.39 \times 10^5$  to  $1.62 \times 10^6$ . The initial rate of polymerization,  $R_p$ 's observed are ranged between  $(0.79-5.88) \times 10^{-4} \text{ mol.L}^{-1}.\text{s}^{-1}$

depending on various reaction parameters. The plot of the logarithms of empirical rate constant  $R_p$  against the reciprocal of the absolute temperature yields the value of activation energy of the reaction as 29.29 kJ/mol. The  $^{13}\text{C}$  spectra showed methylene, methane and carbonyl carbons of head-to-tail polymer of acrylamide. It seems apparent from the  $^{13}\text{C}$  spectra that Bernoulli statistics are followed and stereo regularity has not been observed. However, the polymer trapped inside the interlayer spaces of vermiculite, which could not be extracted by washing with water may have such possibility of showing stereoregularity. Attempts are being made to extract these polymers in mild condition for further study. The rate of reaction follows the second order kinetics with respect to the monomer concentration, which is deviated from the homogeneous solution phase reaction condition. The significant changes due to the occurrences of the reaction on the vermiculite surface indicate that mechanism of polymerization is greatly affected by mineral microenvironment. The order of polymerization is found to be 0.5 with respect to metal ion oxidant. The relationship of polymerization rate with TU concentration was obtained from the slope of logarithm  $R_p$  versus logarithm  $[\text{TU}]$  plot and from the plot of the  $R_p$  vs.  $[\text{TU}]$ ,  $[\text{TU}]$  exponent of 0.85 was found. This value is also different from that of homogeneous polymerization reaction in which second order kinetics with respect to TU is followed. Ce (IV)-TU couple is an effective initiator for the aqueous polymerization of acrylamide. The polymers formed by this initiating system should carry with TU at the terminal. To rationalize the above findings and to predict the possible mechanism of the above polymerization reactions following assumptions are made:

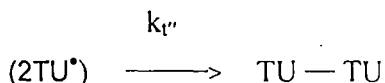
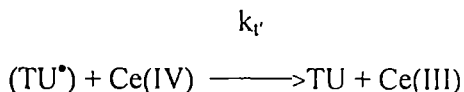
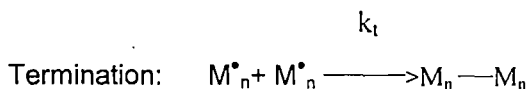
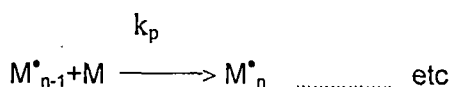
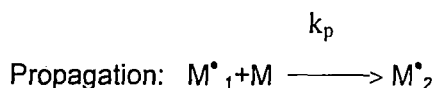
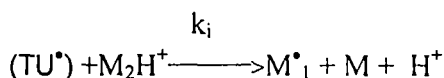
1. Intercalated TU reacts with Ce (IV) ions of the vermiculite layered spaces to form reactive isothiocarbamido primary radical via an intermediate complex. The decomposition of the complex is the rate-determining step.
2. In the constrained interlayer space of vermiculite the monomer molecules remains as pair either through hemi salt formation where two amide molecules share a proton by means of symmetrical hydrogen bond or /and through weak coordination to the exchanged cations.
3. Cage effect is prominent in the vermiculite phase reactions in which the solvent molecules in the constrained space form a potential barrier such that the reactive isothiocarbamido radical cannot diffuse out from the wall of the barrier and favors their recombination.

4. Polymerization locus is the interlayer space of vermiculite. The linear termination of growing polymer chain by Ce (IV) ions is restricted due to the presence of metal ions in the layered space. Initiation, propagation and termination of the polymerization may be shown as follows:

Initiation:



where Ce(III) is ferric ions in vermiculite and (TU\*) is caged TU radicals.



Applying steady state condition for different intermediate species, the rate equation under the present condition has been found to be

$$R_p = k_p (k_d k_i K K^1 / k_t' k_t'')^{1/2} K_{TU}^a (K_m^a)^{1/2} (L_0^a)^3 [Ce(IV)]^{1/2} [TU]_s [M]_s^2$$

(where  $L_0^a$ ,  $K_m^a$ ,  $K_{TU}^a$  are total active sites in unit mass of the mineral and selectivity coefficients of M and TU on vermiculite respectively).

Section B of chapter 4 (page 42-50) deals with the studies on copolymerization of AM with N-t-BAM. Microstructures and reactivity ratios of the copolymers are also determined. Observed data indicate that the copolymerization follow the conventional copolymerization kinetics under a prerequisite that the reactivity of a polymer radical is only determined by the terminal monomer unit. Values of  $r_1$  and  $r_2$  have been found to be 0.43 and 0.32 respectively for Fineman-Ross method and 0.62 and 0.26 for Kelen-Tüdös method. On reversing the indices of the monomer the values of the reactivity ratios changes from 0.43 to 1.56 ( $r_1$ ) and 0.32 to 0.44 ( $r_2$ ). For the AM-N-t BAM copolymers mean sequence length of AM vary between 18.61 and 2.83 at molar ratio of 94.79/5.21 to 81.99/18.01 respectively. For those molar ratio compositions, the values of mean sequence length of N-t-BAM were 1.01 and 1.075 respectively.

In section C of chapter 4 (page 51-54) a general discussion of the foregoing study is presented. The experimental results on the adsorption of AM and TU onto vermiculite also discussed. Low charge vermiculite may have interlayer expansion characteristic, which bear closer resemblance to those of high charge montmorillonite than to those shown by other vermiculite of high charge. The isotherm for Ce (IV) ion adsorption onto vermiculite exhibit L-type nature, which suggests strong sorbate-sorbent interaction. The maximum saturation corresponds to 0.97 meq/g of the mineral. Unlike AM, TU leads to the monolayer formation only and maximum capacity is found to be 1.52 mmol/g, which is consistent with that of the monolayer of the AM.

In the section A (page 62- 76) of chapter 5, the results of the investigation on unperturbed dimension, interaction parameter and related aspects of unhydrolyzed polyacrylamide in water-DMF mixtures have been described. In the previous chapter (chapter 4), we have reported the technique by which the molecular weight of PAM may be increased by trapping the initiator component in the interlayer space of vermiculite. This method has been adopted to prepare polymers of high molecular weights for the solution property studies as presented in this section of the present chapter. The increase in molecular dimension from monomer to oligomer, from

oligomer to usual length polymer and from later one to pleistomer is accompanied by the appearance of new properties. The intrinsic viscosities of the polymer have been measured for different fractions of the polymer and also in different compositions (water/ DMF) of the cosolvent mixture. From the relation between  $[\eta]$  and  $M$ , the unperturbed dimension and molecular expansion factor have been measured. The Huggins constant value in each case was also determined in order to have ideas on the influence of cosolvent system on the aggregation of the polymer. While DMF is a poor solvent for PAM, water – DMF mixture acts as a cosolvent in certain proportions. It is observed that there is a maximum in  $[\eta]$  vs.  $\phi_{\text{DMF}}$  plot at the solvent composition  $\phi_{\text{DMF}} = 0.2$  for PAM type C (low molecular weight) at all the studied temperatures. For PAM type-B (medium molecular weight) at  $50^\circ\text{C}$  and for PAM type-A (high molecular weight) at  $30^\circ\text{C}$  there is a maxima at  $\phi_{\text{DMF}} = 0.3$  and there is a minimum at  $50^\circ\text{C}$  for type-A and at  $40^\circ\text{C}$  for type-B at  $\phi_{\text{DMF}} = 0.2$ . Small values of  $K_H$  indicate better cosolvency at this solvent composition and temperature. Very high values of  $K_H$  for PAM type-B are the indication of strong aggregation for polymer molecules at all temperatures studied. The changes in molecular dimension of unhydrolyzed PAM in water-DMF system are manifested in the varied molecular expansion parameters as a result of interaction with two-component liquid. Values of  $[\eta]$  and  $V_E$  show that higher the molecular weight of the polymer smaller is the concentration of DMF required for developing cosolvency effect. Solutions of all three polymers of different molecular weights generate two antagonistic effects with the increase in temperature. As a result, there has been no visible effect of temperature on  $[\eta]$ . Temperature coefficient ( $K'$ ) values of unperturbed dimension indicate polymer molecules to possess a low energy configuration up to  $\phi_{\text{DMF}} = 0.3$  and a high energy more compact configuration thereafter. Unperturbed dimension ( $K_\theta$ ), actual end to end distance ( $\alpha_n K_\theta$ ), characteristic ratio ( $C_\alpha$ ) and the steric factor ( $\sigma$ ) assume their highest values at  $\phi_{\text{DMF}} = 0.4$  and are decreased with temperature. But  $\alpha_n$ , which represents the long-range interaction, assumes its lowest value at this solvent composition and increases with temperature. Shape factor values of unhydrolyzed PAM molecules are very close to 2.5 and are not affected by solvent composition, molecular weight and the temperature of the study indicating a near spherical configuration.

In the section B (page 77 - 88) of chapter 5, the results of the investigation on unperturbed dimension, interaction parameter and related aspects of hydrolyzed polyacrylamide in water-DMF mixtures have been described. The intrinsic viscosities  $[\eta]$ 's of anionic and nonionic polyacrylamide (PAM) were measured in water-dimethyl formamide mixtures at various temperatures. Non-polyelectrolyte behavior of low carboxyl content polyacrylamide (LPAM) was observed in mixed solvent system. The plots of  $[\eta]$  vs. solvent composition ( $\phi_{DMF}$ ) in mixed solvents passes through a minimum for high carboxyl content (HPAM) and LPAM but through a maximum for nonionic PAM (NPAM). Observed minima may be attributed to the loss of polymer sites available to interact with solvent via H-bonding interaction between neighboring amide and acid groups. The observed maximum for NPAM is possibly due to the most powerful cosolvent effect. Existence of two antagonistic effects is indicated in  $[\eta]$  values of NPAM at various temperatures. Huggins constant ( $K_H$ ) values also show a significant variation of cosolvency as a function of solvent composition. Activation parameters of viscous flow were calculated using Frenkel-Eyring equation. The volume related parameter and the shape factor were also computed. Shape factor data indicate that polymer molecules are more or less rigid spheres and are not affected by temperature and composition of solvent.

Chapter 6 (page 95- 109) reports the results of physicochemical studies on dilute solution properties of high carboxyl content (HPAM) and low carboxyl content polyacrylamide (LPAM) in aqueous solution as a function of concentration, pH, added salt and the temperature. From the reported results it is clear that the conformational properties of carboxyl content polyacrylamide, which is generally used in secondary oil recovery, are strongly dependent on pH and the concentration of added salt. These polymer solutions exhibit that the viscosity decreases with increasing concentration of added salt and increases with pH. Because polyacrylamide are generally used in neutral media, it is of interest to choose hydrolyzed samples that have much higher viscosities than unhydrolyzed polyacrylamide due to the presence of ionic charges. Under salt free conditions the use of highly hydrolyzed samples is preferable because the chains would be more extended. The results on viscosity experiments of LPAM suggest that chain expansion due to intramolecular electrostatic repulsion may not necessarily be essential to cause a marked increase in viscosity at low polymer concentration, since intramolecular repulsion is small for LPAM. This is contradictory to one of the most fundamental concepts in

polyelectrolyte solution. Although the results seem to be clear, there is still a possibility that some polymer chains have larger number of ionic groups in random ionomers, which would lead to some chain expansion due to mutual repulsion of like charges and an increase in viscosity results.

To gain insight into the factors that control the viscosity behavior of dilute solution of nonionic and anionic polyacrylamide under various conditions of temperature and surfactant addition, some experiments are performed and the results of those experiments are presented in chapter 7 (page 110-126). Previously, it was argued that nonionic surfactant could bind cooperatively with ionic polymers only. But present investigation indicates that nonionic polymers also can bind cooperatively with nonionic surfactant. At higher surfactant concentrations, (0.01 and 0.1 %), it is seen that  $[\eta]$  rises at all the experimental temperatures and the conformational expansion as observed is most probably a result of enhanced excluded volume effect due to improved thermodynamic condition. The results of the investigation suggest that the shape of polymer molecules is other than spherical in presence of nonionic surfactant. In this context it may be noted that the shape of the above polymers molecules are spherical in aqueous and aqueous-organic mixtures in the presence or in absence of salt. It is also found that on the initial addition of surfactants the end-to-end distance decreases but further addition of surfactant results in the increase in the end-to-end distance. Three regions of surfactant concentration representing the distinct stages of surfactant-polymer interactions in aqueous solution are observed in the plot of surface tension vs. concentration of nonionic surfactant. In the first region, which is located at lower concentration region of surfactant, the surface tension decreases gradually till the first break point comes. Before the first break point surfactant molecules bind cooperatively to polymers. Generally, critical micellization concentration (cmc) of a nonionic surfactant decreases with an increase in temperature due to changes in water structure and water surfactant interaction. In presence NPAM and LPAM (8.2 mol% charge) overall variation of polymer saturation point (PSP) is determined by various interactions in polymer-TX-100-water system. Here, behavior of LPAM is somewhat similar to that of NPAM. However, for HPAM (72 mol% charge) the polyelectrolyte nature of the polymer is responsible for higher PSP values. Moreover, as the polymer concentration increases more binding sites are available for the surfactant to interact,

hence PSP values go on increasing. It is surprising to note that at 50°C temperature PSP values are minimum for all the polymers in the whole range of concentration.

## List of Publications:

1. MOLECULAR DIMENSION AND INTERACTION PARAMETERS OF POLYACRYLAMIDE IN WATER-N, N-DIMETHYLFORMAMIDE MIXTURES.

G. Bit, B. Debnath and S.K. Saha.

*Journal of Macromolecular Science, Part A : Pure and Applied Chemistry*, **42**, 965 (2005).

2. DILUTE SOLUTION BEHAVIOUR OF PROGRESSIVELY HYDROLYZED POLYACRYLAMIDE IN WATER-N, N DIMETHYLFORMAMIDE MIXTURES.

G. Bit, B. Debnath and S.K. Saha.

*European Polymer Journal*, **42**,544(2006)

3. DILUTE SOLUTION BEHAVIOUR OF PROGRESSIVELY HYDROLYZED POLYACRYLAMIDE IN AQUEOUS SOLUTION.

G. Bit, M. Jha, B. Debnath and S.K.Saha.

*European Polymer Journal* (Submitted).

4. SOLUTION PROPERTIES OF POLYMER-NONIONIC SURFACTANT MIXED SYSTEM.

G. Bit, B. Debnath, A. Chakraborty and S.K.Saha.

*Journal of Macromolecular Science, Part A: Pure and Applied Chemistry* (Submitted).

